2009

Fibrin Formation and Dissolution in the Progression of Amyloid-Beta Pathology in Alzheimer's Disease

Justin Paul

FIBRIN FORMATION AND DISSOLUTION IN THE PROGRESSION OF AMYLOID-BETA PATHOLOGY IN ALZHEIMER'S DISEASE

A Thesis Presented to the Faculty of

The Rockefeller University

in Partial Fulfillment of the Requirements for

the degree of Doctor of Philosophy

by

Justin Paul

June 2009

FIBRIN FORMATION AND DISSOLUTION IN THE PROGRESSION OF AMYLOID-BETA PATHOLOGY IN ALZHEIMER'S DISEASE

Justin Paul, Ph.D.

The Rockefeller University 2009

Alzheimer's disease (AD) is a neurodegenerative disorder that leads to profound cognitive decline and eventually death. There are no effective long-term treatments or preventative measures available, and as the incidence and prevalence of the disease are increasing, new insights and tractable therapeutic targets are sorely needed. Genetic evidence indicates that a major cause of AD is the production of the amyloid-β (Aβ) peptide, which is proteolytically derived from the amyloid-β precursor protein. The Aβ peptide can oligomerize and be deposited as extracellular plaques in the brain and blood vessels, but the mechanism of how it leads to neuronal death is not known. There is increasing evidence of a vascular contribution in AD: patients suffer from brain hypoperfusion, the cerebral vasculature is damaged, and abnormal hemostasis is present. Circulatory deficiencies could therefore play an important role in the pathogenesis of this disease.

We found an increase in blood brain barrier (BBB) permeability and neurovascular damage in AD mice, and showed that fibrin deposition potentiates these processes. We then found that Aβ binds to fibrinogen and alters fibrin clot

formation. Clots formed in the presence of Aβ have an abnormal structure and are resistant to degradation by fibrinolytic enzymes. We also found that ApoE isoforms differentially affect the structure of the fibrin clot formed in the presence of Aβ, which is consistent with the known genetic interaction between AD and the ApoE genotype. These results suggest that in the presence of Aβ, dysfunctional fibrin clots alter thrombosis and hemostasis and exacerbate the BBB damage and neuroinflammation, thus promoting the disease process in AD.

I wish to dedicate my thesis to

my wife and my family

who have been one with me in mind, body and spirit

ACKNOWLEDGEMENTS

I wish to thank my advisor, Dr. Sidney Strickland, for his outstanding mentorship and support. I thank Dr. Jerry Melchor for pioneering the Alzheimer's disease project and my studies are a consequence of his work and initial guidance and Dr. Marketa Jirouskova for pointing out creative ways of approaching common questions in coagulation science. I thank Dr. Allison North as her help in imaging methodology and analysis forms the foundation of my research. I thank the committee members Dr. Jan Breslow, Dr. Barry Coller, and Dr. Costantino Iadecola who have taught me how to think critically of my work and made valuable suggestions for my studies. I also thank Dr. Jay Degen for taking time to act as my external thesis committee member. I thank the members of the Strickland lab for constructive comments during lab meetings, helpful troubleshooting tips, and warm friendship throughout my thesis research.

TABLE OF CONTENTS

LIST OF FIGURES

CHAPTER 1: INTRODUCTION

1.1 Alzheimer's Disease

Alzheimer's disease (AD) is a neurodegenerative disorder characterized by progressive loss of cognitive function and subsequent death. It is the leading cause of dementia in the US (Cummings and Cole, 2002), affecting 5.2 million people and up to 13% of Americans over 65 (Hebert et al., 2003). Due to an aging population, it is estimated that by 2050 the number of individuals affected by this disease will triple if no treatments or preventative measures are introduced.

In AD, the dementia is characterized by a deficit in learning and memory along with a number of language disturbances (aphasia) and visuospatial dysfunction leading to disorientation. In addition to dementia, individuals with AD often suffer from depression, sleep disturbance, wandering, restlessness, and fits of physical aggression (Finkel, 2003). Death is on average six years after the diagnosis, but cases have been documented as long as 20 years (Morrison and Siu, 2000). The most common cause of death is pneumonia, which is likely a result of the increased immobility and swallowing disorders in later stages of the disease. The natural course of this disease often necessitates exhaustive supervision, which can account for the high financial costs associated with the disease and emotional burden of caregivers.

Post-mortem, the AD brain contains an abundance of extracellular neuritic plaques and intracellular neurofibrillary tangles, which are pathologic hallmarks

and required for diagnosis (Glenner and Wong, 1984; Cummings and Cole, 2002). The tangles are paired helical filaments aggregated inside neurons resulting from abnormal phophorylation of the microtubule-associated protein tau (Ballatore et al., 2007). Dystrophic neurons surround the plaques, which consist of a central core of fibrils made up of amyloid-β (Aβ) peptide (Selkoe, 1998). Though plaques and tangles form the diagnostic criteria, other histological pathologies are present and could provide insight into the mechanism for AD. These include neurovascular pathology as Aβ deposits in the blood vessel walls to form cerebral amyloid angiopathy (CAA) (Vinters, 1987; Fischer et al., 1990; Ellis et al., 1996), and neuroinflammation as microglia and astrocytes are found in neuritic plaques (Akiyama et al., 2000).

However, Alzheimer's pathology is not limited to neurons as one of the earlier manifestations of the disease is abnormal cerebral vasculature. This neurovascular pathology may accelerate other Aβ-mediated pathologies or affect neuronal damage directly (Vinters et al., 1996; Farkas and Luiten, 2001; de la Torre, 2004).

1.2 Aβ hypothesis

One of the most striking features of Alzheimer's neuropathology is the presence and accumulation of the Aβ peptide into neuritic plaques, and research on the Aβ peptide has led to several milestones in Alzheimer's research. The first is the discovery of mutations in the genes for AβPP and presenilin, which co-segregate with heritable forms of AD with early onset. These mutations result in elevated

levels of Aβ production and production of the more fibrillogenic Aβ species (Tanzi et al., 1996).

Aβ is derived from the amyloid-β precursor protein (AβPP) through two proteolytic events (Figure 1). First, this type I transmembrane protein is cleaved at the N-terminus of Aß by β-secretase (Vassar et al., 1999), followed by γ-secretase cleavage at the carboxyl terminus. These two cleavages result in the secretion of soluble Aβ peptide and the production of a membrane-bound C-terminal fragment, referred to as the APP intracellular domain (AICD) (Passer et al., 2000; Kimberly et al., 2003). A non-amyloidogenic pathway exists, but it is the β-secretase pathway that generates soluble Aβ. One particular 42 amino acid form due to its two additional hydrophobic residues aggregates rapidly to form amyloid fibrils (Jarrett et al., 1993). Soluble multimer formation can cause considerable neuronal damage before multimers acquire a β-pleated sheet conformation leading to fibril formation and deposition in plaques (Lambert et al., 1998; Walsh and Selkoe, 2004; Cleary et al., 2005).

Studies detailing Aβ action have converged on the Aβ hypothesis, which states that increased Aβ generation is responsible for the senile plaques and dementia observed in AD patients (Hardy and Selkoe, 2002). This hypothesis is supported by the existence of rare early onset familial AD (EOFAD). These forms involve mutations within AßPP and the β-secretase pathway enzymes.

Using these mutations, transgenic mice have been genetically engineered to express AβPP and presenilin genes with these human mutations; these mice show AD like pathology and cognitive deficits (Games et al., 1995; Duff et al.,

1996; Hsiao et al., 1996; Chishti et al., 2001). Clearance of Aβ in these mice by immunization attenuates the aggregation and subsequent cognitive pathology (Schenk et al., 1999; Janus et al., 2000; DeMattos et al., 2001; Dodart et al., 2002). Removing BACE1 from transgenic Tg2576 mice also reduced the Aβ load and rescued memory dysfunction (Ohno et al., 2004).

Many of the AD hallmarks are present in the transgenic mice. The PDAPP mouse model overexpressing human AßPP driven by the platelet-derived growth factor promoter shows age-dependent deposition of Aβ, inflammation, and cognitive deficiencies, with prominent pathology seen at about nine to ten months (Games et al., 1995). Other AD mouse models include the Tg2576 mouse (Hsiao et al., 1996) and the TgCRND8 mouse, carrying a double mutant form of APP695 (KM670/671NL+V717F) under the control of the PrP gene promoter on a mixed background (C57XC3H/C57) (Chishti et al., 2001). Aβ deposits are evident in TgCRND8 mice at 3 months of age, with dense core plaques and neuritic pathology presenting at 5 months. Behavioral pathology is present at 3 months using the reference memory version of the Morris water maze. Though the mice differ in age of onset and extent of pathology, the major drawback of the model is that these transgenic mice overexpressing AβPP do not replicate all of the pathology apparent in AD brains.

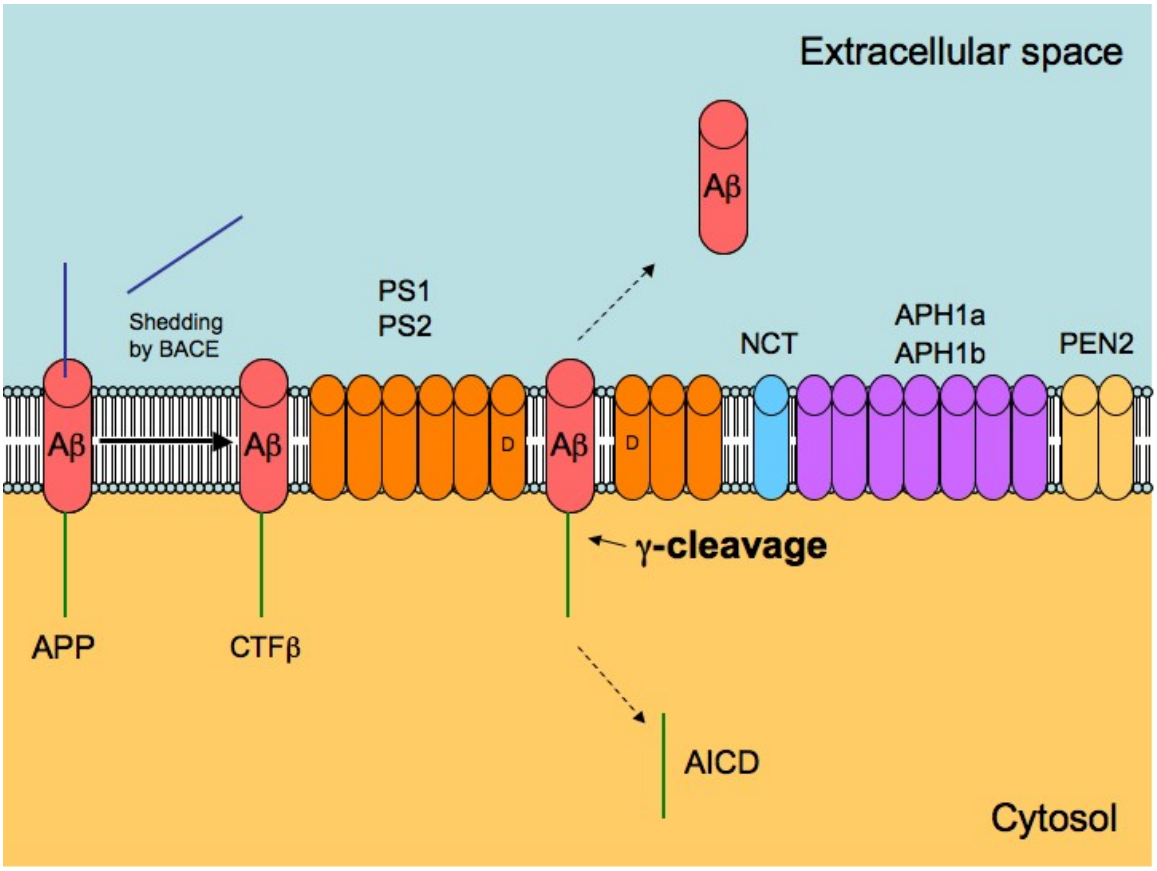

Figure 1. Amyloidogenic processing of β-amyloid precursor protein (APP) by β-site APP-cleaving enzyme (BACE) and the γ-secretase complex. First, full-length APP (left) is processed by BACE, and the large ectodomain is secreted. The remaining membrane retained stub (CTFβ) binds to a docking site on the surface of the γ-secretase complex and is then transferred to the active site that includes transmembrane domains 6 and 7 of presenilin-1 (PS1) or PS2. PS1 and PS2 are both activated by presumed autoproteolytic cleavages. The core complex including presenilin and three other essential γ-secretase components, APH1a (or APH1b), PEN2 and nicastrin (NCT) is required for γ-secretase activity. The two intramembrane aspartate residues in the presenilins (marked with a D) are a crucial part of the protease. The γ-secretase cleavage occurs in the middle of the membrane and liberates amyloid β-protein (Aβ) and the APP intracellular domain (AICD), whose function is unclear. Intramembrane proteolysis by γ-secretase is variable and can occur at least after amino acids 38, 40 and 42. These sites of cleavage are highly relevant for the subsequent aggregation propensity of Aβ. Adapted from Haass and Selkoe, *Nature Reviews: Molecular Cell Biology* 2007.

1.3 Vascular hypothesis

Blood flow to any organ is essential for proper function, but the brain is especially susceptible because there are no long term energy stores and no alternative to the metabolism of oxygen and glucose (Farkas and Luiten, 2001).. In AD, there is significant evidence that patients suffer from inadequate perfusion.

First, Aβ may affect the blood directly as can augment blood platelet aggregation *in vitro*, which would increase thrombosis (Kowalska and Badellino, 1994; Wolozin et al., 1998). This result is supported by the observed protective effect of anti-platelet therapy against AD disease progression (Lim et al., 2000; Zhou et al., 2003). In fact, hypercoagulation in AD is suggested by elevated levels of molecules reflecting abnormal hemostasis such as fibrin degradation products, von Willebrand factor, and plasminogen activator inhibitor (PAI-1) in the blood of AD patients (Mari et al., 1996). In contrast to normal aging individuals, AD patients have elevated levels of fibrin degradation products in the blood suggesting fibrin is formed and degraded more than normal (Gupta et al., 2005). Indeed, markers of thrombosis are independent predictors of dementia in the elderly (Barber et al., 2004), and cardiovascular disease is associated with more rapid cognitive decline in AD patients (Mielke et al., 2007).

Second the cerebral vasculature is damaged early in AD (de la Torre, 2004) and can cause dementia independent of AD (Breteler, 2000). Consistent with this, studies of AD mice show endothelial cells are dysfunctional early, which reduces their response to vasodilators (Niwa et al., 2002b) and impairs critical regulation of blood flow (Niwa et al., 2002a; Iadecola and Gorelick, 2003). Blood

vessels laden with Aβ have also been shown to be directly toxic to cultured neurons (Grammas et al., 2000). Epidemiology links AD to cardiac disease (Breteler et al., 1998) and atherosclerosis correlates with disease pathology in sporadic AD (Roher et al., 2003).

Third, the AD mouse brain is particularly susceptible to injury as middle cerebral artery occlusion produced 30-40% larger infarcts than wild type littermates (Zhang et al., 1997). Examination of AD brains reveals white matter lesions resembling ischemia (Brun and Englund, 1986). Consistent with the link between AD and stroke (Honig et al., 2003), there is a correlation between reduced cerebral blood flow and severity of dementia (Farkas and Luiten, 2001). But not only the cognitive changes are reflected as this compromised blood flow in can lead to the pathologic synaptic changes characteristic of AD (Wen et al., 2004b; Wen et al., 2004a).

The cerebral microvasculature is highly specialized to protect the homeostasis of the central nervous system (CNS) microenvironment. One of the primary functions of the blood-brain barrier (BBB) is to restrict access to large macromolecules, such as fibrin(-ogen) that are normally in circulation. The BBB is known to be compromised in AD patients and mouse models (Mattila et al., 1994; Farkas and Luiten, 2001; Ujiie et al., 2003; Dickstein et al., 2006), which results in fibrin deposition in extravascular space (Fiala et al., 2002), but the pathological significance is unknown. The blood-brain barrier has been proposed as a target for treatment strategies (Donahue and Johanson, 2008).

1.4 Fibrin

Fibrin is the protein component of a blood clot. The inactive precursor fibrinogen circulates as a 340 kDa dimer, but when cleaved by the serine protease thrombin, fibrinogen dimers polymerize non-covalently to form protofibrils which branch to form an insoluble network of fibrils. This clot network incorporates platelets in order to functionally impede blood flow and plug sites of vascular injury. Fibrin is naturally degraded by plasmin. The serine protease tissue plasminogen activator (tPA) converts plasminogen (plg) to plasmin, another potent serine protease with a variety of substrates.

Fibrinogen is normally excluded from the brain parenchyma by the BBB. Neurovascular damage can allow fibrinogen access to the central nervous system (CNS). Fibrinogen is present in the brains of AD patients (Fiala et al., 2002) but the pathologic significance is not known.

Fibrin deposition increases in the context of deficiency in the tissue plasminogen activator/plasmin(ogen) (tPA/plg) protease cascade (Tabrizi et al., 1999). Plasminogen-deficient mice accumulate extravascular fibrin and have impaired wound healing and high mortality (Bugge et al., 1995), both of which are corrected in mice deficient for both plasminogen and fibrinogen (Bugge et al., 1996). Reduction of fibrinogen can also be achieved with administration of ancrod, a serine protease derived from the venom of the Malayan pit viper *Agkistrodon rhodostoma.* Ancrod prevents fibrin polymerization, allowing degradation by the liver and removal from the circulation (Bell et al., 1978; Burkhart et al., 1992). Ancrod administration has been used to alleviate fibrin(-

ogen) mediated pathology in the peripheral nervous system (Busso et al., 1998; Akassoglou et al., 2000).

The hippocampus, a region of the brain known for its role in learning and memory, can express tPA. But the activation of plg is regulated by serine protease inhibitors (serpins) such as plasminogen activator inhibitor-1 (PAI-1). In mice, PAI-1 is up-regulated in the presence of Aβ (Melchor et al., 2003), which agrees with the clinically observed elevation of PAI-1 levels in the cerebrospinal fluid (CSF) (Sutton et al., 1994).

Therefore, in the brains of AD patients and mouse models of the disease, clearance of fibrin by the tPA/plasmin system is expected to be reduced as tPA activity is diminished (Ledesma et al., 2000; Melchor et al., 2003). Because inflammation is universal in AβPP transgenic mice and can be observed as early as 13 weeks of age, (Dudal et al., 2004), early extravasation of fibrinogen might initiate or exacerbate the observed neuroinflammation. An exaggerated fibrin-induced inflammatory process could inflate the damage to the vasculature thus promoting this process of disease progression. With increased permeability of the BBB and diminished activity of fibrinolysis pathway components, the AD brain presents a milieu that tends to accumulate fibrin.

BBB damage and neurovascular pathology exist in AD tissues in the CNS and may exacerbate and accelerate an Aβ-mediated disease process. Though the leaky blood-brain barrier could be initally caused by Aβ (Thomas et al., 1996), the opened BBB and potential fibrin(-ogen) deposition in the extravascular space may aggravate tissue damage and impede regeneration (Adams et al., 2004).

1.5 Apolipoprotein E (ApoE)

Apolipoprotein E (ApoE) is a 299 amino acid protein (34 kDa) that belongs to a family of soluble apolipoproteins. Apolipoprotein (Apo) E has a strong epidemiological link to Alzheimer's disease (AD)(Corder et al., 1993). There are three human isoforms of this protein: ApoE2, E3, and E4. Individuals carrying the ApoE4 allele have a higher risk of developing AD. However, it is likely that ApoE4 is not acting directly through Aβ as ApoE4 is does not increase plaque deposition (Altamura et al., 2007).

In the brain, it is primarily expressed in astrocytes and microglia and, in addition to its known lipid transport and removal function, it is also involved in synaptogenesis (Mauch et al., 2001), neuronal plasticity, and membrane remodeling and repair (reviewed in (Holtzman and Fagan, 1998)). ApoE has three common isoforms (ApoE2, ApoE3, and ApoE4) that are products of three alleles e2, e3, and e4, where e3 is the most common in the human population. These proteins have two functional domains - the receptor binding domain and the lipid-binding domain. The three isoforms only differ in two amino acids in the receptor binding domain at positions 112 and 158. However, these alterations not only affect the receptor binding affinity but also influence the tertiary structure and the charge distribution of the whole protein, greatly affecting the interaction between the two domains by altering the isoforms' folding ability and stability (reviewed in (Hatters et al., 2006)). This difference in two amino acids modulates the functional and structural properties of the ApoE isoforms, which affects their

role in pathological conditions (reviewed in (Strittmatter and Bova Hill, 2002; Hatters et al., 2006)).

Inheritance of the different ApoE alleles influences the risk of developing AD (Strittmatter and Roses, 1995). Individuals with the e4 allele develop the disease earlier and present higher amounts of Aβ plaques than individuals with the e3 allele. Therefore, the presence of this allele is considered a risk factor for developing AD (Corder et al., 1993). Conversely, the presence of the e2 allele may be protective (Corder et al., 1994). This different influence between ApoE isoforms in developing AD could be mediated through their effects on Aβ binding and metabolism. It has been shown that ApoE interacts (Naslund et al., 1995) and colocalizes with Aβ in senile plaques (Wisniewski et al., 1997) and CAA vessels (Navarro et al., 2003).

The physical interaction between ApoE and Aβ is mediated by Aβ residues 12-28 (Munson et al., 2000) and ApoE residues 244-272 (Strittmatter and Bova Hill, 2002). Although this region is the same in all ApoE isoforms, Aβ/ApoE binding is isoform specific (LaDu et al., 1994; Aleshkov et al., 1997). Different *in vivo* approaches have demonstrated that the presence of ApoE influences Aβ fibrillogenesis in an allele-dependent manner (ApoE4>>ApoE3>ApoE2), acting as a pathological chaperone, and ApoE can also affect the clearance of Aβ from the interstitial space in an isoform dependent way (ApoE2=ApoE3>ApoE4) (reviewed in (Bales et al., 2002)). Therefore, ApoE is playing a dual role in Aβ metabolism. The ultimate success of Aβ clearance *versus* deposition may be decided, among other factors, by the ApoE genotype.

To study the influence of the different human ApoE isoforms on Aβ burden, mice were generated in which the murine ApoE gene was replaced by the different human ApoE isoforms. These mice also have been crossed with different AD models. The expression of the human ApoE4 isoform in AD mice produced greater Aβ deposition as well as higher Aβ fibrillar staining than mice expressing human ApoE3 or ApoE2, confirming the important isoform-specific function of ApoE in humans (Holtzman et al., 2000; Fagan et al., 2002).

CAA (Aβ deposits in the vessels) may develop through improper clearance of Aβ as it is normally eliminated along the perivascular pathway. This process declines with age due to changes in the elasticity of brain arteries (Weller et al., 2002). This decreased elimination of Aβ is one of the main causes of AD. In the case of familial AD, mutations in AβPP and Presenilin 1 and 2 genes have been shown to increase the production of Aβ that may overwhelm the Aβ elimination process, but these only represent a small percentage of all AD cases. In sporadic AD, where there is no strong evidence of Aβ overproduction, other factors such ApoE genotype may play a very important role (Weller et al., 2008). It is known that the inheritance of the e4 allele is strongly associated with the severity of CAA, while parenchymal Aβ accumulation seems to be independent of ApoE genotype (Chalmers et al., 2003). Also, the expression of human ApoE4 isoform in the AD mouse provokes an enhancement in the Aβ CAA deposits *over* plaques deposition (Fryer et al., 2005). However, the exact reason why this risk is greater with the e4 allele than with the e2 allele is not yet known.

1.6 Conclusion

AD represents a disease of unknown origin. The lack of a defined pathological mechanism has impeded development of drugs for this condition, and at present there are only five drugs approved which have minor effects on disease progression (Doraiswamy, 2006). Therefore, new approaches are needed urgently. A large body of research, including some from our lab, implicates blood circulation as a contributing factor in AD. We seek to examine in detail the effects of Aβ on blood clots and the consequences of these effects on the progression of AD.

CHAPTER 2: MATERIALS AND METHODS

2.1 Animals

The AD transgenic mice used, which develop Aβ-associated pathology, include the Tg2576 (Hsiao et al., 1996) TgCRND8 (Chishti et al., 2001), and PDAPP (Games et al., 1995). The Tg2576 mice (APP695; K670N, M671L driven by the hPrP promoter) are on a C57B6/SJL mixed strain background and develop cognitive deficits by nine months of age. The TgCRND8 mice (APP695; K670N, M671L, V717F driven by the hPrP promoter) are on a mixed background (C57XC3H/C57) and exhibit defects in memory as early as three months of age (provided by Drs. Azhar Chishti and David Westaway, Center for Research in Neurodegenerative Disorders, University of Toronto, CA). The PDAPP mice (APP695, 751, 770; V717F driven by the PDGFβ promoter) used in this study were backcrossed to C57Bl/6 mice and display memory defects by 8 months (provided by Drs. Ronald B. Demattos and Stephen M. Paul, Eli Lilly Research Laboratories, Indianapolis, IN). Mice deficient for plasminogen (Bugge et al., 1995) and fibrinogen (Suh et al., 1995; Degen et al., 2001), both backcrossed onto the C57Bl/6 background, were used for crosses with TgCRND8 and PDAPP mice. Littermates were used in all experiments whenever transgenic mice were compared to non-transgenic (wild-type) mice. Where multiple crosses or strains are presented in a single figure, non-transgenic littermates from each cross were averaged and presented as one bar for clarity and brevity. Mice were maintained

in the Rockefeller University Laboratory Animal Research Center (LARC) and treated in accordance with protocols approved by LARC.

TgCRND8 transgenic mice (referred to as AD mice throughout) develop Aβ-associated pathology. These AD mice (APP695; K670N, M671L, and V717F driven by the human prion protein promoter) are on a mixed background (C57XC3H/C57) and exhibit defects in memory as early as three months-of-age (provided by A. Chishti and D. Westaway, University of Toronto, Canada). Non-transgenic (wild type) littermates were used in all experiments where indicated. Mice were maintained in The Rockefeller University Laboratory Animal Research Center and treated in accordance with IACUC-approved protocols.

2.2 Evans blue extravasation assay

A solution of 2% Evans blue/PBS was injected (4 ml/kg) via the tail vein. Six hours post-injection, the mice were anesthetized and blood drawn by cardiac puncture followed by transcardial perfusion with 0.9% saline-heparin (5U/ml) to remove intravascular dye. One brain hemisphere was frozen for sectioning and microscopy studies while the other hemisphere was weighed and homogenized in 400 µl of dimethylformamide (DMF) to solubilize the Evans blue. To extract the dye, samples were centrifuged, the supernatant was collected, and analyzed for absorbance at 620 nm. The plasma was diluted 1:100 in DMF and analyzed exactly as the brain homogenate. Evans blue units of extravasation were calculated as the A620 of brain homogenate divided by the A620 of plasma.

2.3 Evans Blue Fluorescence Profiling

To visualize the extent of the blood-brain barrier damage, mice were injected via tail vein with Evans blue dye. After six-hours, mice were anesthetized and perfused with a solution containing large-fragment 2,000 kDa FITC-conjugated dextran dissolved in PBS to outline the intraluminal space (Morris et al., 1999). Evans blue fluorescence from 50 μm coronal sections was visualized with a laser scanning confocal imaging system (Zeiss LSM 510 confocal system fitted on an Axiovert 200 inverted microscope, Bio-Imaging Resource Center at The Rockefeller University). Optical slices were processed by Axiovision confocal imaging software and reconstructed images evaluated for Evans blue dye present outside the fluorescein delineated intraluminal space. For views of the entire brain hemisphere, a composite of stitched 10X images (8x8) was produced during acquisition with a motorized stage.

2.4 ELISA (brain or plasma)

Brains were perfused, weighed and homogenized in 0.1M Tris pH 7.2/0.2 % Triton X-100 with 5 mM EDTA, 100 mM tranexamic acid, and protease inhibitor cocktail (Roche). Protein concentrations were measured by Lowry assay (Bio-Rad). Quantification of fibrinogen was performed using a hamster anti-mouse fibrinogen capturing antibody, 7E9, provided by Dr. Marketa Jirouskova, The Rockefeller University (Jirouskova et al., 2001) and HRP-conjugated rabbit anti-human fibrinogen detecting antibody (Dako Cytomation, Carpinteria, CA). Aβ

levels were measured by ELISA according to manufacturer's protocol (Biosource International, Camarillo, California).

2.5 Immunostaining and semi-quantitative analysis

To localize the leakage of Evans blue dye, one brain hemisphere was sectioned and fixed with ice-cold ethanol. To evaluate fibrin(ogen) extravasation and deposition, sections from Evans blue dye-treated animals were processed for fibrin(ogen) immunoreactivity with a FITC-conjugated anti-fibrinogen antibody (Dako Cytomation). Microglial staining was performed with a biotin-conjugated anti-CD11b antibody (1:100) (BD PharMingen, San Diego, CA) visualized with FITC- or Rhodamine-conjugated avidin (1:500). To analyze microvasculature rat anti-PECAM-1 antibody (BD PharMingen) was used (1:50) and visualized with a FITC-conjugated goat anti-rat (1:1000). Aβ was detected with a rabbit anti-pan-Aβ antibody (1:100) (Biosource/QCB, Camarillo, CA). Apoptotic cells were stained with a rabbit anti-active-caspase-3 antibody (1:200) (Cell Signaling Technology, Inc., Danvers, MA)

Coronal sections (from bregma -1.5 to -2.0 mm) were processed and stained for the markers listed above. A composite (3x3) of 10X images was stitched together to include hippocampus and cortex during acquisition using a laser scanning confocal imaging system equipped with a motorized stage (Zeiss LSM 510 confocal system fitted on an Axiovert 200 inverted microscope, Bio-Imaging Resource Center at The Rockefeller University). Composite images were converted to 1-bit images using ImageJ (National Institutes of Mental

Health, http://rsb.info.nih.gov/ij/). Using this bit-depth, regions including either hippocampus, cortex or both were selected by hand as shown in Figures 3 and 4 and quantified for percent immunofluorescence.

2.6 Fluoro-Jade B staining

Fluoro-Jade B staining was performed according to the protocol by Schmued and Hopkins (2000) and viewed under fluorescence microscopy (Schmued and Hopkins, 2000). Briefly, sections were immersed sequentially in 1% NaOH/80% alcohol for 2 min, 70% alcohol for 2 min, water for 2 min, 0.06% potassium permanganate for 10 min, water for 2 min, and 0.0004% Fluoro-Jade B in 1% acetic acid for 20 min, and then rinsed in water three times. The sections were then dried, immersed in Histoclear and mounted with neutral DPX polystyrene medium. The sections were viewed under blue-green excitation light with a fluorescent microscope.

2.7 Ancrod/Tranexamic acid treatments

To explore whether removal of fibrinogen from the circulation can affect the progression of Aβ pathology, we treated transgenic mice with Viprinex (ancrod) (provided by Dr. David E. Levy, Neurobiological Technologies, Inc). Mini osmotic pumps were subcutaneously implanted to deliver four units/day of ancrod activity over four weeks with replacement at two weeks while a control group received saline (DURECT Corp, Cupertino, CA). To measure the fibrinogen depletion

effect of ancrod, plasma samples were obtained weekly by tail prick and fibrinogen quantified by ELISA.

Deficiency in fibrinolysis was accomplished pharmacologically by implantation of a mini osmotic pump for delivery of tranexamic acid. Because the drug is also orally active, this dosage was supplemented with tranexamic acid dissolved in drinking water at 20 mg/ml. The total daily dose was estimated to be 100 mg/day.

2.8 Turbidity and pure fibrin and plasma lysis times

Clots were formed by mixing purified human fibrinogen (30 μM; Calbiochem) with human thrombin (40 nM or 2 U/ml; Sigma) in the presence of Aβ peptides (5 nM - 5 mM; Anaspec) or vehicle control. Calcium chloride was adjusted to 20 mM. Absorbance was measured for 10 minutes at 405 nm. For formation/degradation curves, clots were formed under the same conditions with tPA (140 nM; Genentech) and purified human plasminogen (1 μM; Sigma).

Clots were also formed with citrated normal human plasma (New York Blood Center), which was centrifuged at 10,000 x g for 15 min (to obtain platelet-deficient plasma) and added to Aβ peptides (5 nM - 5 μM; Anaspec), tPA (140 nM; Genentech) and human thrombin (40 nM or 2 U/ml; Sigma). Calcium chloride was adjusted to 20 mM.

To check for FXIIIa (transglutaminase) activity and clotting efficiency, purified fibrin clots were formed in parallel as described above. After 10 minutes of clot formation, clots were centrifuged 14,000 x g for 10 minutes, and the supernatant collected for protein quantification by the Lowry method. Clots were solubilized

in reducing buffer and analyzed under reducing conditions by SDS-PAGE. Tranglutaminase-dependent formation of gamma-gamma dimers was detected as a 94 kD band.

To control for enzyme activity, plasmin (50 ug/ml; Sigma) or thrombin (2 U/ml; Sigma) was incubated with Aβ42 for 10 minutes and added to Pefachrome PL or Pefachrome TH, respectively. Absorbance at 405 nm was measured for 5 minutes.

Amyloid solutions were tested for congophilicity using Congo Red dye. Aβ 5 μM was incubated with 1 mM Congo Red for 20 min. Absorbance spectrum was recorded from 400 to 600 nm.

2.9 Ex vivo lysis time and immunoprecipitation

Mice were sacrificed, and brains were dissected, weighed, and homogenized in PBS. Although the fibrin exudates in the AD mouse brain alter the composition of the brain matter, protein concentrations were not altered when corrected for wet tissue weight. Homogenized brain tissue (10 μg) from AD mice and their wild type littermates was added to recalcified citrated human plasma.

To deplete extracts of Aβ, 4G8 monoclonal IgG antibody (1-5 μg/ml), which recognizes residues 17-24 of Aβ peptide in monomeric and oligomeric form, or irrelevant (anti-NeuN) IgG monoclonal antibody (5 μg/ml) was added to extracts and incubated overnight at 4°C. Antibodies were precipitated using GammaBind-Plus Sepharose beads (GE Healthcare), which were collected by centrifugation at 500 x g for 1 minute. The supernatant was added to recalcified citrated human plasma as above. Beads were resuspended in 2x sample buffer and mixed

gently before bound material was removed. Beads were boiled at 100°C for 5 min to dissociate the immunocomplexes. The beads were then collected by centrifugation and the supernatant mixed with Congo Red as before to determine depletion of fibrillar Aβ.

2.10 Electron microscopy

Fibrin clots were formed from purified fibrinogen on glass coverslips. After 20 minutes, clots were washed with sodium cacodylate buffer and fixed with 2% glutaraldehyde. Clots were dehydrated, critical point dried, and sputter-coated with gold palladium. Images were obtained using a LEO 1550 scanning electron microscope.

To visualize amyloid fibrils present in congophilic solutions, we used a standard negative staining protocol. Samples were adsorbed onto formvar and carbon coated grids (glow discharged for 1 min before use). The grids were transferred onto drops of ddH2O and stained with 2% Uranyl Acetate for 1 min. Excess stain was removed with wet filter paper and samples were allowed to air dry. Scanning was performed using FEI Tecnai D1201 Transmission Electron Microscope at 80KV and pictures were taken with Gatan 895 Ultrascan Digital camera.

2.11 Confocal image analysis and lysis front retreat rates

Clots were formed as described above on a glass-bottomed dish with Alexa-488-fibrinogen (50 ug/ml; Molecular Probes). Images were obtained with an inverted

Zeiss Axiovert 200 microscope with Zeiss Plan-Neofluar 63x/1.3 NA oil immersion objective (Carl Zeiss, Mannheim, Germany), acquired with LSM 510 v. 3.2 confocal software (Zeiss), and analyzed with MetaMorph software (Universal Imaging). Some clots contained Congo Red (1 mM) or biotinylated Aβ at the same concentrations with AlexaFluor-568-conjugated streptavidin (10 μg/ml; Molecular Probes).

For lysis experiments, tPA was injected into the center of the pre-formed clot (20 minutes after mixing), and time-lapse image stacks were recorded for five minutes as the lysis front retreated from the center. Images were obtained at 15 second intervals using an inverted Zeiss Axiovert 200 microscope, acquired with LSM 510 v. 3.2 confocal software, and analyzed with MetaMorph software. Initial and final images were overlayed, and the distance between lysis fronts was divided by the five minute collection period. Three to four random lysis fronts were identified in four separate experiments.

ApoE isoforms (120 nM; Sigma) were also added to plasma and pure fibrin reaction mixtures. Images were acquired as described above, and cluster density was measured in four randomly selected 146 μm x 146 μm fields after 90 minutes. Images were thresholded, and the Integrated Morphometry Analysis function of MetaMorph was used to quantify the percent image area of objects classified by minimum area, shape factor, and fiber breadth. Data is presented as mean cluster density +/- SEM.

An additional morphometric method was used as a control and produced identical results. The thresholded image was used to generate a Euclidean distance map, where the intensity value indicates the Euclidean distance, measured in pixels, to the nearest white pixel in the original binary image

(MetaMorph). The new image is displayed with a pseudocolor look-up table (LUT) that illustrates the change in intensity values within the image. This scheme presents thin fibers as low intensity and dense aggregates as high intensity. The Euclidean distance map is therefore used to quantify the areas only of high intensity.

2.12 Stereotactic fibrin injections

To examine the clearance of deposited fibrin *in vivo*, AD and wild type mice were stereotactically injected with a solution containing purified fibrinogen and Evans blue, which was used to outline the injection site. Mice were anesthetized with 500 mg/kg avertin and 0.04 mg/kg atropine and placed in the stereotactic injection device. A 2% Evans blue and fibrinogen (1:1) solution (500 nl) was injected into the hippocampus (Bregma -2.0mm/1.8mm/1.2mm) of each mouse. After one day, mice were perfused, and 20 µm-thick coronal brain sections were prepared for immunofluorescence using a FITC-conjugated antibody for fibrin(ogen) (Dakocytomation). During acquisition (LSM 510 v. 3.2 confocal software) using an inverted Zeiss Axiovert 200 microscope equipped with a motorized stage, a composite (3x4) of 10X images was stitched together to include the hippocampus and cortex. Thresholded area percentage from 3-4 samples from each mouse was recorded using Metamorph.

To determine the clotting of injected fibrinogen, we checked for D-Dimer. One day after stereotaxic injection of fibrin, brains weighing between 0.15 and 0.20 g were dissected and homogenized. Tissue suspensions were centrifuged at 14,000 x g for 10 min at 4°C. Protein concentrations were determined by the Lowry method. For Western blot analysis of D-dimer content, 40 µg of

supernatant protein was resolved by SDS–PAGE with purified fibrinogen (Sigma) as protein standards. Gels were transferred overnight, and membranes were stained with a polyclonal HRP-conjugated antibody to fibrinogen (1:1000; Dakocytomation) for 2 hours at room temperature and developed by enhanced chemiluminescence.

2.13 Examination of thrombosis in Cerebral Amyloid Angiopathy (CAA)

To examine thrombosis in the presence of amyloid deposition in blood vessels, coronal brain sections from non-injected AD mice were stained with FITC-conjugated fibrin(ogen) antibody (1:1000; Dakocytomation) and costained with Congo Red to detect CAA.

Immunofluorescence images were acquired using an inverted Zeiss Axiovert 200 microscope equipped with a motorized stage to produce a composite of 10X images including the hippocampus and cortex. Total amyloidosis was obtained using Metamorph software as thresholded area percentage from 4 TgCRND8 mice. CAA was identified in each image by hand and subtracted from the total amyloidosis to obtain plaque area percentage as shown in Figure 38.
Post-mortem sections of human AD brains were obtained from the University of Pennsylvania Alzheimer's Disease Core Center. Sections were deparaffinized blocked with albumin and stained using a monoclonal antibody that specifically recognizes the fibrin II polymer and not fibrinogen, mouse anti-human fibrin II β-chain monoclonal antibody (clone NYBT2G1, 1:1000) from Accurate Chemical. Sections were co-stained with Thioflavin S.

2.14 Automated Activated Partial Thromboplastin time

AD and wild type mouse plasma was obtained by cardiac puncture at time of sacrifice. Blood was centrifuged at 4000 x g for five minutes, and plasma was collected and added to a reaction mix according to manufacturer's protocol (Biomerieux). Absorbance at 405 nm was measured over a five minute period. Western blot analysis was performed to determine plasma fibrinogen concentration. Plasma (1 µL) was resolved using SDS–PAGE under reducing conditions. Gels were transferred, and membranes were treated as described above.

2.15 Intravital imaging of thrombosis

This procedure details the surgical preparation of a mouse for direct observation of pial microcirculation in experimental animals for 60 minutes before sacrifice by overdose of anesthetic. We used TgCRND8 transgenic mice with wild type littermates of varying age from 13 to 40 weeks weighing 15 to 35 g.

All animals were anesthetized by IP injection of 500 mg/kg avertin and 0.04 mg/kg atropine supplemented as necessary and placed in a stereotaxic device. A 4-mm circular craniotomy was prepared over the parietal cortex using 5-10 circular brush strokes with a fine dental drill bit. The dura mater was peeled away and dental acrylic secured a 10 mm plastic ring around the window, which was filled with saline to protect the brain surface and prevent drying. Each mouse received a 0.3-ml bolus of a 5% (w/v) solution of 2 MDa fluorescein-conjugated dextran in PBS, injected into the tail vein to label the blood plasma.

Perfusion of the brain surface with increasing doses of ferric chloride irritates the wall of the vessel and subsequently triggers a clotting cascade that leads to an

occlusion. We recorded thrombosis using real-time video acquisition with a video camera fitted to an upright Zeiss Axiovert 200 epi-fluorescence microscope (Metavue software). 2-4 mice were used in each group and up to 10 vessels with a diameter greater than 20 micrometers were thrombosed per mouse. After imaging, the mice were sacrificed by overdose of avertin.

This hands-on training is supplemented by online video protocol, which is archived in the Journal of Vizualized Experiments: "A Craniotomy Surgery Procedure for Chronic Brain Imaging" by Ricardo Mostany and Carlos Portera-Cailliau, Department of Neurology, University of California, Los Angeles.

This video can be found online at http://www.jove.com/index/Details.stp?ID=680

After treatment with 10 % ferric chloride, the cranial window was perfused with recombinant tPA (140 nM; Genentech) to activate fibrinolysis. Clot formation and dissolution was observed using time-stamped image stacks. Clot size was traced by hand using Metamorph software to calculate the area of the dark zone representing the clot, which had an average pixel intensity below 1500.

2.16 Behavioral analysis

Behavioral pathology was evaluated using the Y-Maze, a hippocampal learning and memory task that analyzes spontaneous exploration of novelty. The Y-Maze consists of three plexiglass arms and a floor covered with bedding. Experiments were performed in a sound-attenuated room under soft illumination, and visual clues were placed on the walls of the testing room. Each trial consisted of two five-minute periods, separated by a two minute intertrial interval in which the mouse was placed in its home cage. During the first five-minute period, one of

the three arms was blocked by an opaque plexiglass insert; this arm acts as the novel arm in the subsequent five-minute testing period. For the second five-minute period, the plexiglass insert was removed to reveal the novel arm. The entire experiment was recorded for analysis. The first two minutes of the testing period were analyzed, and time spent in the novel arm was averaged and compared between groups. More time spent in the novel arm compared to the other two arms indicates that the mouse remembers this arm is novel and the other arms are not.

2.17 Statistical analysis

All numerical values presented in graphs are mean +/- SEM. Statistical significance was determined using the student's t-test comparing control to experimental groups.

CHAPTER 3: FIBRIN AGGRAVATES PATHOLOGY

3.1 Fibrin is deposited through a disrupted neurovasculature in transgenic mouse models of Alzheimer's Disease

When the blood-brain barrier is compromised, macromolecules in circulation can accumulate in the brain parenchyma (Yepes et al., 2003). Because Evans blue dye binds to albumin in the blood, extravasation of the dye serves as a marker for blood-brain barrier permeability and neurovascular damage. We compared Alzheimer's mouse models Tg2576, PDAPP and TgCRND8 to non-transgenic littermates for defects in the neurovasculature. Because these mice bear AβPP with different familial AD mutations and are driven by different promoters, they exhibit differing ages of onset of Aβ-associated pathology. Therefore, we compared extravasation of Evans blue dye in mice at six months and 12 months of age.

As shown in Figure 2-3, brains of all three Alzheimer's mouse models were significantly more permeable to the dye. Non-transgenic littermates showed increased blood-brain barrier permeability as age increased. However, in all three Alzheimer's mouse models, the brain was significantly more permeable to the dye at these ages. These data are consistent with previously observed microvascular damage in the Tg2576 mouse (Dickstein et al., 2006), although the TgCRND8 mice show earlier onset.

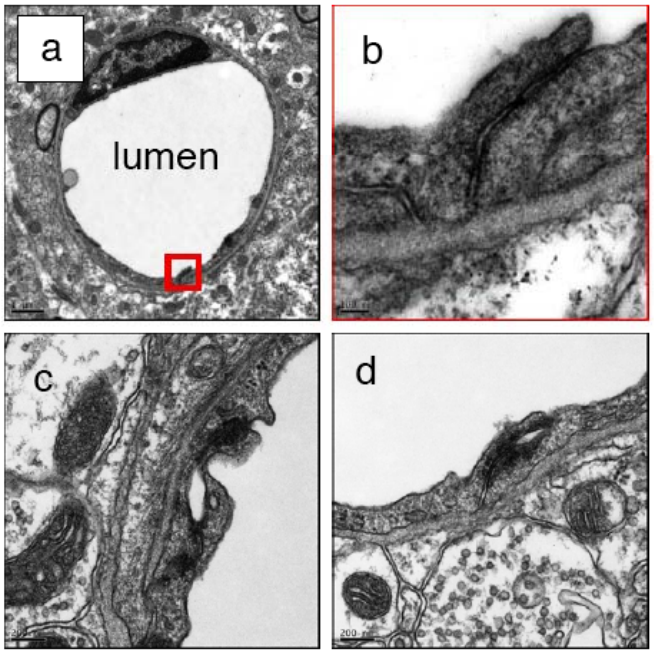

Figure 2. Alzheimer's mice blood vessels are damaged and the blood-brain barrier is defective. (A) Normal endothelial cell from a 6-month wild type mouse. (B) Endothelial cell tight junction shown in (A) shown at high magnification. (C-D) Two representative images of disrupted and leaky tight junctions in a six-month-old TgCRND8 mouse.

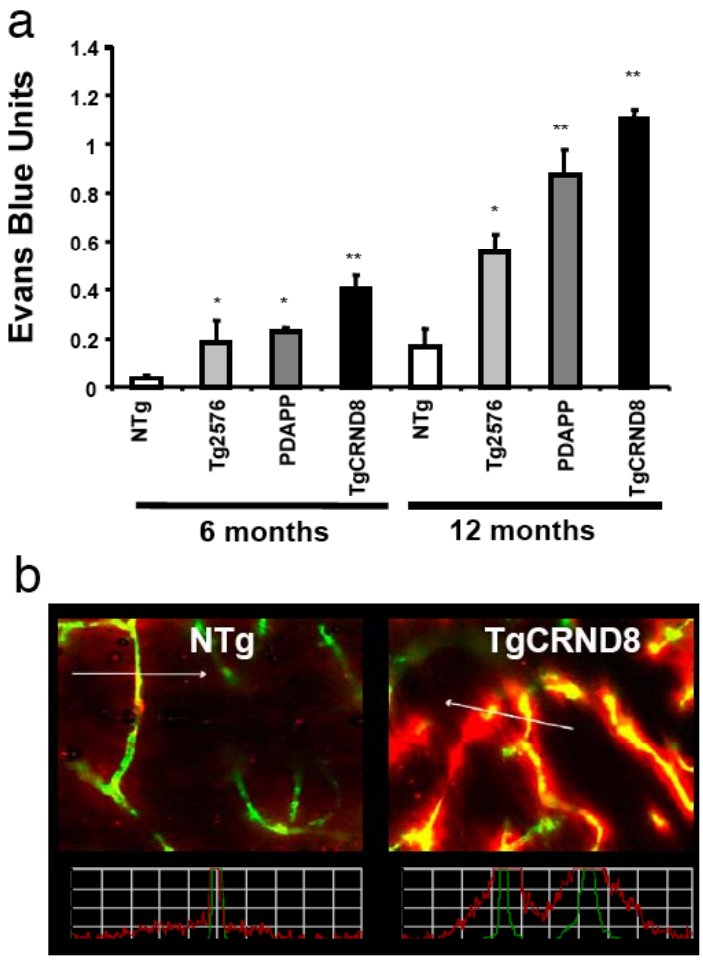

Figure 3. Blood–brain barrier permeability and neurovascular damage is increased in three mouse models of AD. (A) Evans blue assay indicates increased blood–brain barrier permeability in the Tg2576, PDAPP, and TgCRND8 transgenic mice compared with nontransgenic (NTg) littermates. Data are given as Evans blue extravasation calculated from A620 of perfused brain homogenates and normalized to plasma Evans blue levels. For 6-mo mice, n = 9 for NTg (three each from Tg2576, PDAPP, and TgCRND8 litters), n = 3 for Tg2576, n = 6 for PDAPP, and n = 7 for TgCRND8; for 12-mo mice, n = 9 for NTg (three each from Tg2576, PDAPP, and TgCRND8 litters), n = 4 for Tg2576, n = 4 for PDAPP, and n = 4 for TgCRND8. Error bars represent the mean ± SEM. *, $P < 0.05$; **, $P < 0.001$, relative to nontransgenic littermates. (B) Laser-scanning micrograph of microvasculature in hippocampus of 6-mo TgCRND8 mouse and NTg littermate injected with Evans blue (red) 6 h before and perfused at the time of killing with 2,000-kD dextran (green). Fluorescence intensity across a cross section (indicated by white arrow; 100 μm) of a capillary is scanned for the distribution of each fluorochrome.

To visually observe extravascular deposition of Evans blue, mice treated with Evans blue for six hours were perfused with fluorescent dextran at time of sacrifice. This 2,000 KDa dextran is impermeable to both healthy and damaged blood vessels, and therefore serves as an outline of intravascular space. The non-transgenic littermate blood-brain barrier retained both dyes within the blood vessel as shown in the left panel of Figure 3B. The damaged TgCRND8 blood vessel in the right panel showed diffuse accumulation of Evans blue around the contained dextran. As shown underneath each micrograph, the distribution of each fluorochrome can be analyzed for fluorescence intensity across a cross section of a capillary, which reveals Evans blue with a broader distribution than the dextran in the AD mouse (Benchenane et al., 2005). Together with the quantitative extravasation assay, these comprehensive estimates indicated increased blood-brain barrier permeability in the TgCRND8 mouse.

To gain insight into blood vessel health, mice brain sections were stained for platelet/endothelial cell adhesion molecule-1 (PECAM-1). Images of perfused and stained microvasculature were obtained from the cortex of TgCRND8 mice and non-transgenic littermates at six months of age (Fig. 10). Healthy endothelial cells constitutively express this surface marker (Baldwin et al., 1994), but sections of TgCRND8 brains showed diminished signal intensity and vessels appeared tortuous and fragmented.

Because the AD mouse blood-brain barrier was permeable to albumin-bound Evans blue dye, we hypothesized that fibrinogen could gain access to the brain's extravascular space. Given this, and because tPA activity is reduced in

the AD mouse brain (Melchor et al., 2003), we reasoned that fibrin could deposit and accumulate over the lifespan of the mouse. Perfused TgCRND8 brains contained elevated levels of fibrin(ogen) as determined by ELISA. Three to nine-month old mice showed that Aβ accumulated in an age-dependent manner, and fibrin(ogen) levels correlated with soluble Aβ1-40 and Aβ1-42 levels as measured by ELISA from the same tissue homogenates (Fig. 4).

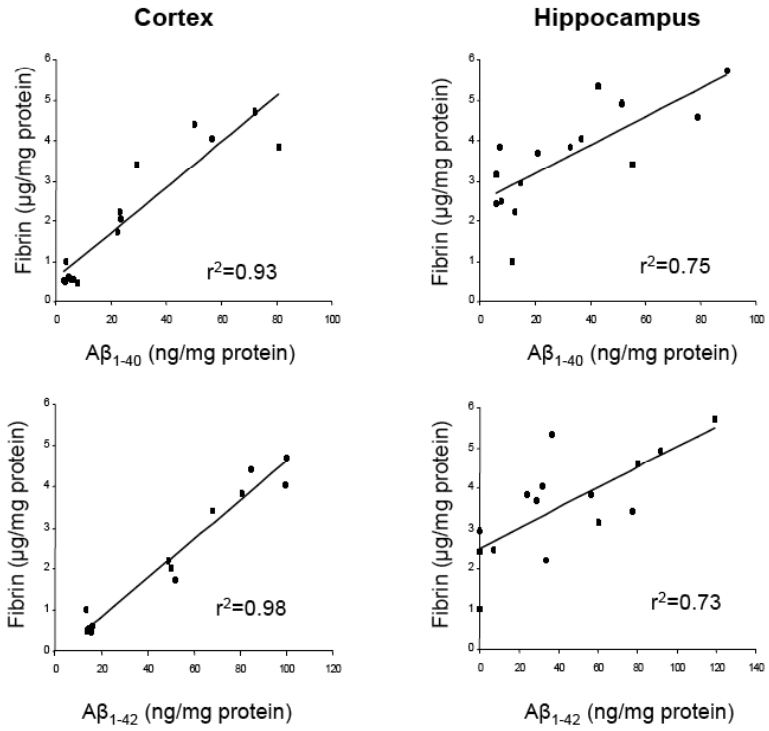

Figure 4. Fibrinogen accumulates through the damaged neurovasculature. (A) Fibrin(ogen) deposition parallels age-dependent Aß accumulation. TgCRND8 cortex and hippocampus were isolated, and homogenates were assayed each for fibrinogen and Aß1-40 by ELISA. Each point represents one TgCRND8 mouse. Correlation coefficients are indicated. (B) The same cortex and hippocampus homogenates were assayed each for fibrinogen and Aß1-42 by ELISA.

3.2 Neuroinflammation and microvascular injury are diminished by pharmacologic depletion of fibrinogen

Since fibrin is a pro-inflammatory molecule and could aggravate pathology upon exiting the vasculature (Akassoglou et al., 2000; Adams et al., 2004), we asked if fibrinogen depletion might reduce the inflammation in AβPP transgenic mice. TgCRND8 mice are appropriate because of the early onset of neurovascular dysfunction and neuroinflammation, as seen by microgliosis at 13 weeks (Dudal et al., 2004). We therefore reduced circulating fibrinogen levels using a recombinant form of the Malayan pit viper protease ancrod. Ancrod is a thrombin-like protease that cleaves fibrin and prevents its polymerization, allowing degradation by the liver and removal from circulation (Bell et al., 1978; Burkhart et al., 1992). TgCRND8 mice were treated with either ancrod or saline for four weeks prior to sacrifice at six months of age. Fibrinogen levels were reduced by 50-75% in circulation by ancrod. Accordingly, sections of perfused brains after ancrod treatment showed diminished fibrin immunoreactivity (Fig. 5).

Perfused sections of transgenic brains from each treatment group were stained with CD11b, an integrin receptor present on microglia, and inflammatory foci were visualized. The total area of inflammatory foci can be quantified within the regions of interest as shown in Figure 6. Areas of inflammation were compared between ancrod and saline. Ancrod treatment reduced the area of inflammation by ~64% (Fig. 6, $p=0.00001$). In saline-treated mice, microglia were identified by their amoeboid morphology. As shown in Figure 7, these aggregated microglia formed inflammatory foci, and appeared to concentrate

around plaques with reduced number after fibrinogen-depletion. Because ancrod is a protease and could be acting directly on Aβ levels, we quantified levels of plasma Aβ1-40, and cortical Aβ, neither of which were significantly different in ancrod-treated mice (Fig. 6), indicating that depletion of fibrinogen rather than deposited Aβ is responsible for the reduced microgliosis.

As inflammation can contribute to blood-brain barrier permeability, we assayed ancrod-treated mice for Evans blue extravasation and found a reduction when compared to saline-treated mice (Fig. 8). This attenuation of vascular damage prompted analysis of the microvasculature from both cortex and hippocampus. Identical areas of the brain (Fig. 9) were quantified for vascular density as percent image area (Fig. 9), and indicated that ancrod treatment partially prevents blood vessel loss.

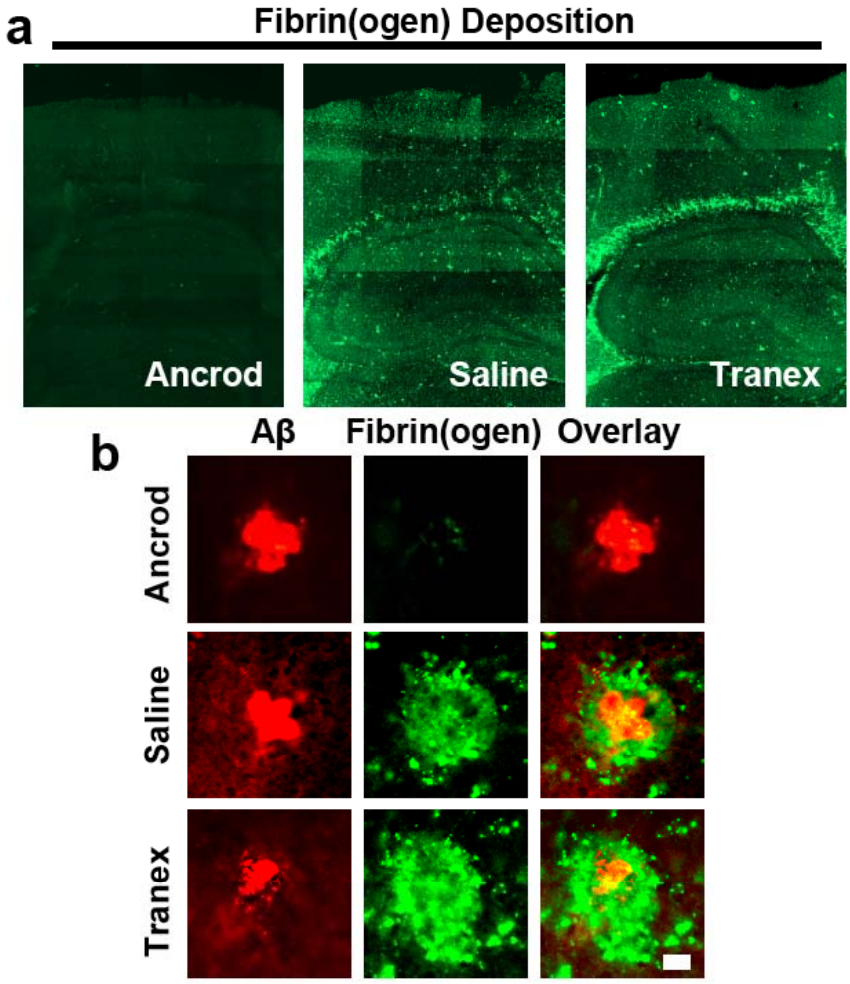

Figure 5. Fibrin(ogen) deposition and vascular damage are modified by manipulation of fibrinogen levels and fibrinolysis. (A) Representative images of perfused brains from each treatment group stained for fibrin(ogen). Images were tiled together using a motorized stage on a confocal microscope. (B) High-magnification images of fibrin(ogen) deposition (green) with Aß plaques (red). Bar, 20 µm.

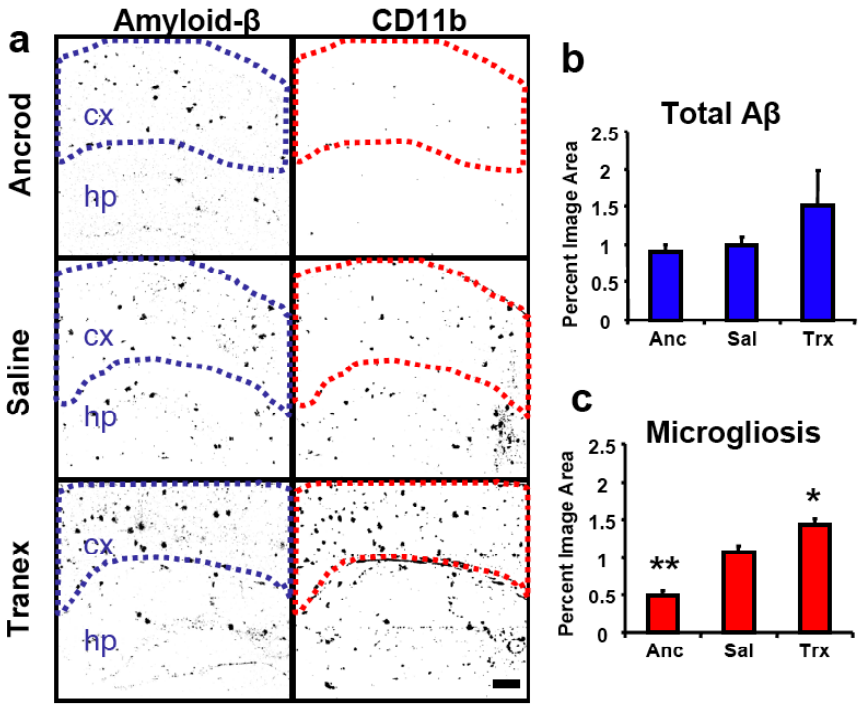

Figure 6. Fibrinogen depletion and inhibition of fibrinolysis in the 6-mo TgCRND8 mouse have opposite effects on neuroinflammation. (A) Representative immunofluorescent images of brains colabeled for Aß (left) and CD11b, a marker for activated microglia, either resident in the brain or peripherally derived (right). Regions of interest are outlined to demark the cortical region quantified in each image. Images show increased density of inflammatory foci in the cortex of plasmin-inhibited transgenic mice, whereas fibrinogen-depleted transgenics show decreased density relative to age-matched saline-treated TgCRND8 mice. Bar, 200 µm. (B) Analysis of total Aß staining within marked regions of interest in the cortex; the differences were not significant ($P > 0.05$). (C) Analysis of CD11b staining shows increased inflammation density in the cortex of plasmin-inhibited transgenic mice, whereas fibrinogen-depleted transgenics show a decrease. Error bars present the mean ± SEM of four images for each of five ancrod-, four tranex-, and two saline-treated mice. *, $P < 0.05$; **, $P < 0.001$, relative to saline-treated mice.

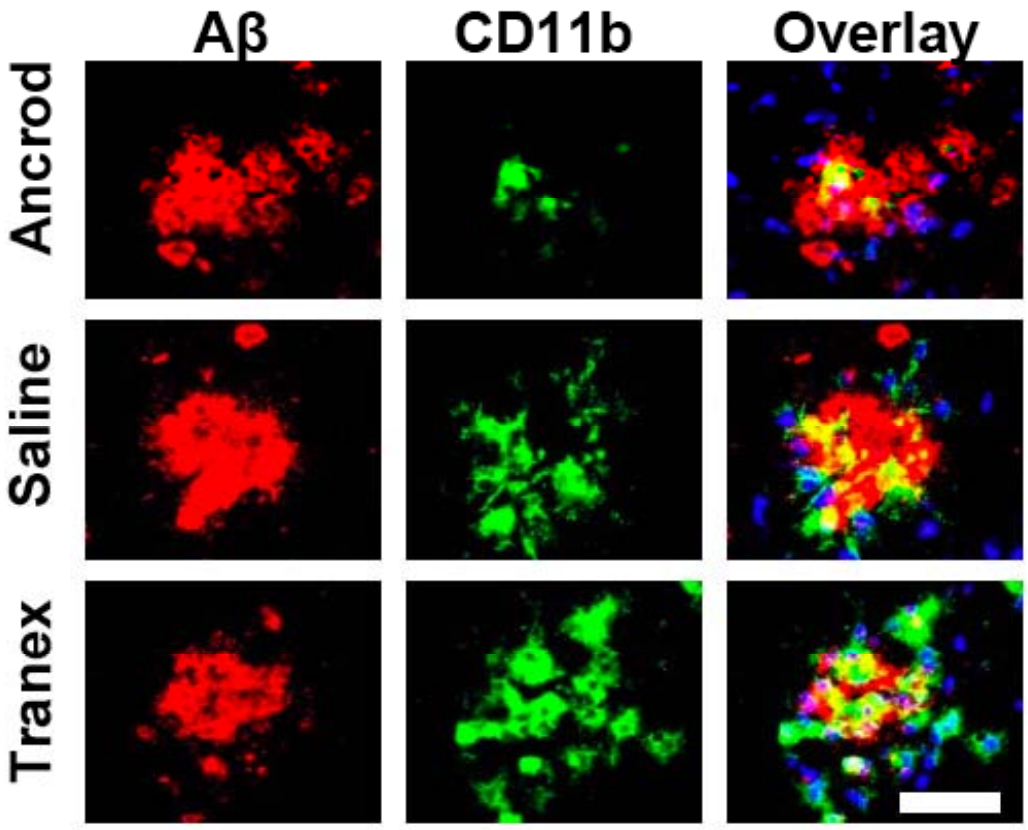

Figure 7. Fibrinogen depletion and inhibition of fibrinolysis in the 6-mo TgCRND8 mouse have opposite effects on inflammatory foci. High-magnification images of microglia (green) and Aß plaques (red) in each treatment group. Bar, 50 μm.

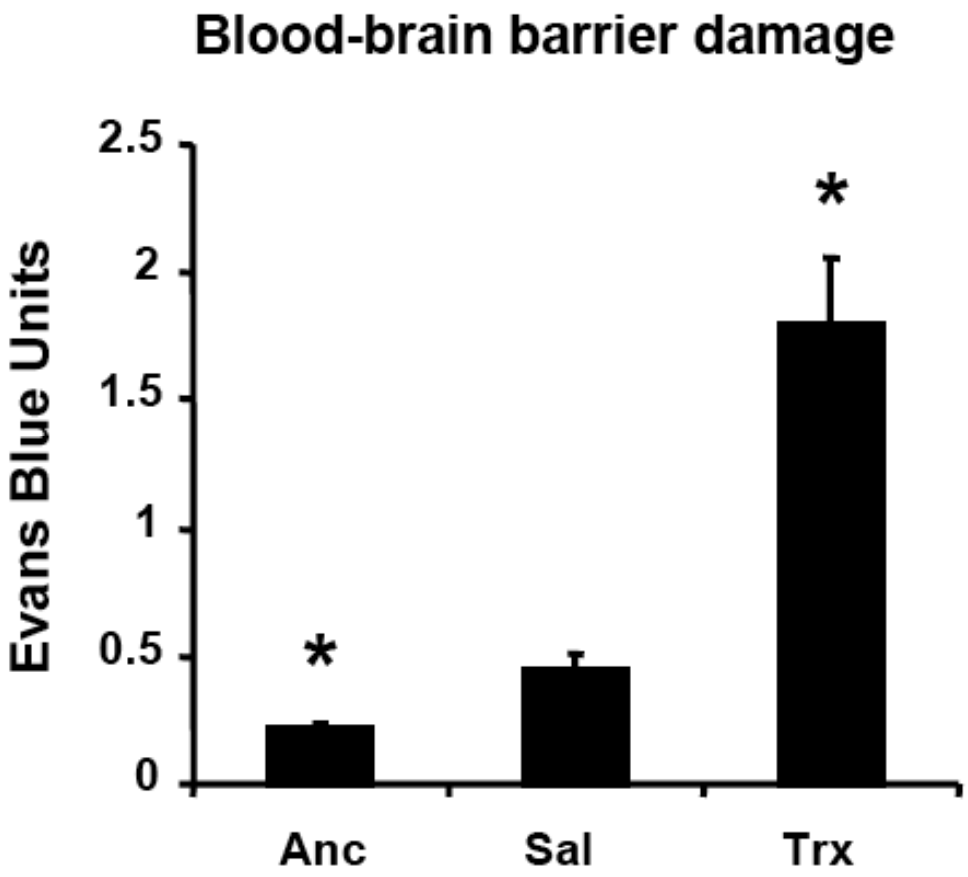

Figure 8. Fibrin(ogen) deposition and vascular damage are modified by manipulation of fibrinogen levels and fibrinolysis. Evans blue extravasation from ancrod-, saline-, and tranexamic acid–treated 6-mo TgCRND8 mice. Data are represented as mean ± SEM of each treatment group, where n = 3 for each group. *, $P < 0.05$, relative to saline-treated mice. Fibrinogen depletion with ancrod reduces vascular damage, whereas plasmin inhibition enhances permeability.

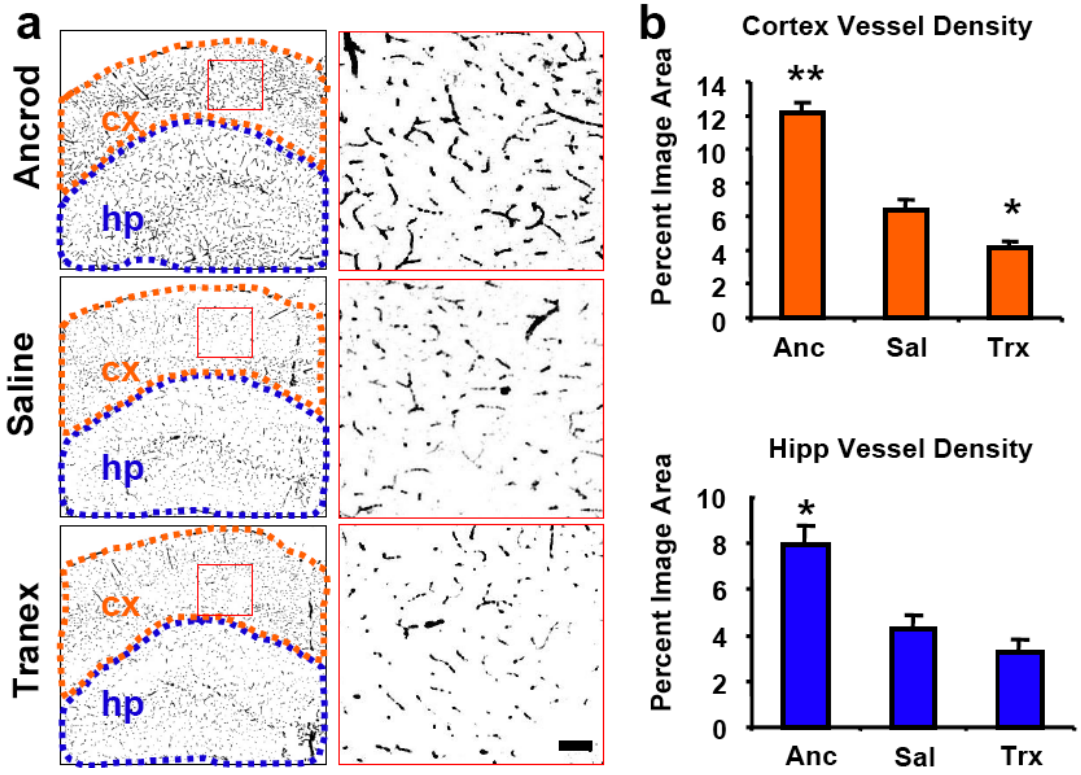

Figure 9. Fibrinogen depletion and inhibition of fibrinolysis in the TgCRND8 mouse have opposite effects on neurovascular damage. (A) Neurovasculature in ancrod-, saline-, and tranexamic acid–treated TgCRND8 mice. Images of brains labeled for PECAM-1 (black) are shown with higher magnification images of the regions shown in red to the right. Regions defining cortex (orange) and hippocampus (blue) were used for quantification of vascular density. The images show decreased vascular density in the cortex (cx) and hippocampus (hp) of plasmin-inhibited transgenic mice, whereas fibrinogen-depleted transgenics show increased vascular density over age-matched saline-treated TgCRND8 mice at 6 mo. (B) Semiquantitative analysis of PECAM-1 staining in the cortex and hippocampus shows decreased vascular density in plasmin-inhibited transgenic mice, whereas fibrinogen-depleted transgenics show an increase. Bars represent the percentage of image area reported as the mean ± SEM of four images of the cortex and hippocampus of four mice in each treatment group. *, $P < 0.05$; **, $P < 0.001$, relative to saline-treated mice.

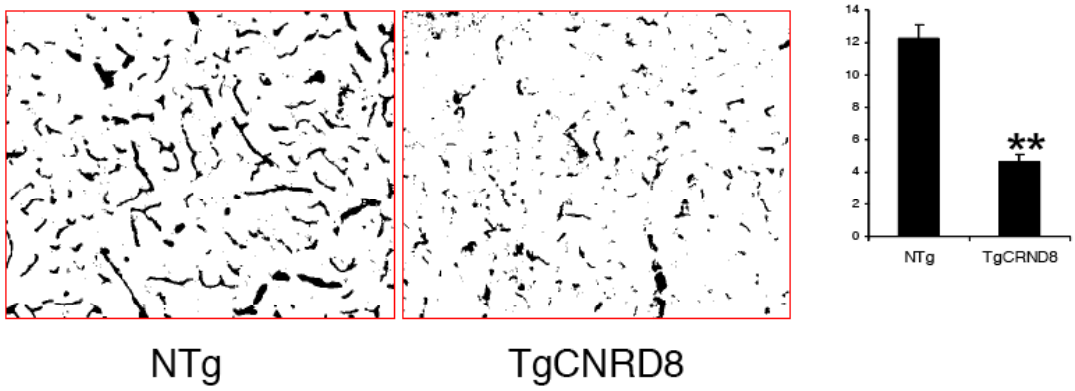

Figure 10. Representative examples of immunofluorescent images of brains labeled for PECAM-1 in TgCRND8 and nontransgenic (NTg) littermates, quantified by percentage of image area. **, P < 0.001 relative to NTg littermates.

3.3 Neurovascular pathology is promoted by pharmacologic inhibition of fibrinolysis

To complement fibrinogen depletion experiments, we tested whether absence of plasmin-mediated clearance of fibrin accelerates pathology. We treated TgCRND8 mice with a plasmin inhibitor, tranexamic acid, for four weeks prior to sacrifice at six months of age alongside littermates treated with saline or ancrod. Inflammatory foci were again visualized using microglia staining with CD11b (Fig. 6). Plasmin inhibition by tranexamic acid treatment significantly increased microgliosis in treated mice as compared to control mice ($p=0.014$, Fig. 6).

We also reasoned that the inhibition of plasmin-mediated clearance of fibrin and subsequent inflammation could aggravate neurovascular damage in TgCRND8 mice. We observed that administration of tranexamic acid increases damage to the blood-brain barrier (Fig. 8). Decreased blood-brain barrier integrity after four-week tranexamic acid treatment prompted analysis of the microvasculature. Tranexamic acid-treated TgCRND8 mice showed a reduction in microvascular density and vessels appeared damaged (Fig. 9).

With the increased pathology observed in the tranexamic acid-treated animals, we asked if inflammation and Aβ were sufficient to promote neurodegeneration. Active caspase-3 staining did not reveal apoptotic cells in treatment or control groups. Samples also were negative for neurodegeneration by Fluoro-Jade B staining (unpublished data).

3.4 Neurovascular pathology in the transgenic mouse model is modulated by genetic deficiency in plasminogen or fibrinogen

We crossed transgenic AD mice to mice deficient for fibrinogen (fib-/-) in order to obtain TgCRND8;fib+/- mice bearing only one functional copy of the fibrinogen gene. Additionally, because accumulated fibrin in the extravascular space can cause damage, we asked if a reduction in plasminogen levels on a background of the AβPP transgene could promote neurovascular pathology. Similar to the fibrinogen cross, we generated TgCRND8;plg+/- mice and compared them to TgCRND8 littermates. We examined the N1 generation from mice crossed to TgCRND8 mice because pathology presents at an earlier age than PDAPP and Tg2576. Heterozygosity for plasminogen deficiency in TgCRND8 mice produced a significant increase in Evans blue extravasation (Fig. 11, $p=0.042$). Conversely, TgCRND8;fib+/- mice showed reduced neurovascular pathology at six months ($p=0.003$). Plg+/- and fib+/- controls showed little permeability to the dye, suggesting that a product of the AβPP transgene is necessary for neurovascular pathology. To control for the possible effects of different genetic backgrounds on the production and metabolism of the AβPP transgene, PDAPP mice were backcrossed more than 10 generations onto the C57Bl/6 background before crossing with plg-/- mice, which share the C57 background. The results shown in Figure 12 indicate increased blood-brain barrier pathology in PDAPP;plg+/- mice when compared to PDAPP littermates, consistent with the results shown in Figure 11.

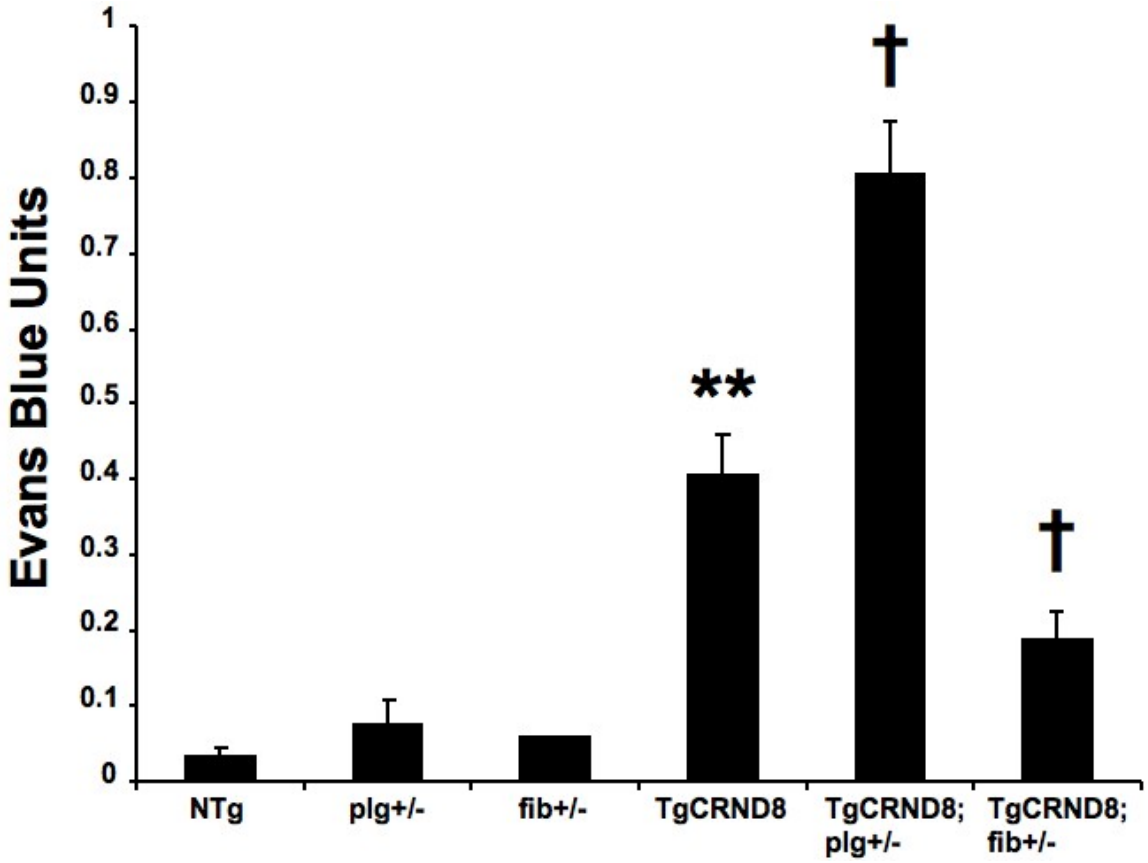

Figure 11. Genetic plasminogen and fibrinogen deficiency modulate defects in the AD mouse blood–brain barrier. 6-mo-old AD mice deficient for plasminogen (TgCRND8;plg+/–) and fibrinogen (TgCRND8;fib+/–) were assayed for Evans blue extravasation alongside TgCRND8 littermates. TgCRND8;plg+/– mice showed increased blood–brain barrier permeability, whereas TgCRND8;fib+/– mice showed a decrease. Data are given as Evans blue extravasation calculated from A620 of perfused brain homogenates and normalized to plasma Evans blue levels. n = 8 for NTg; n = 8 for TgCRND8; and n = 3 for TgCRND8;plg+/–, TgCRND8;fib+/–, fib+/–, and plg+/– mice. Bars represent the mean ± SEM. **, $P < 0.001$, relative to nontransgenics; (dagger) $P < 0.05$, relative to TgCRND8.

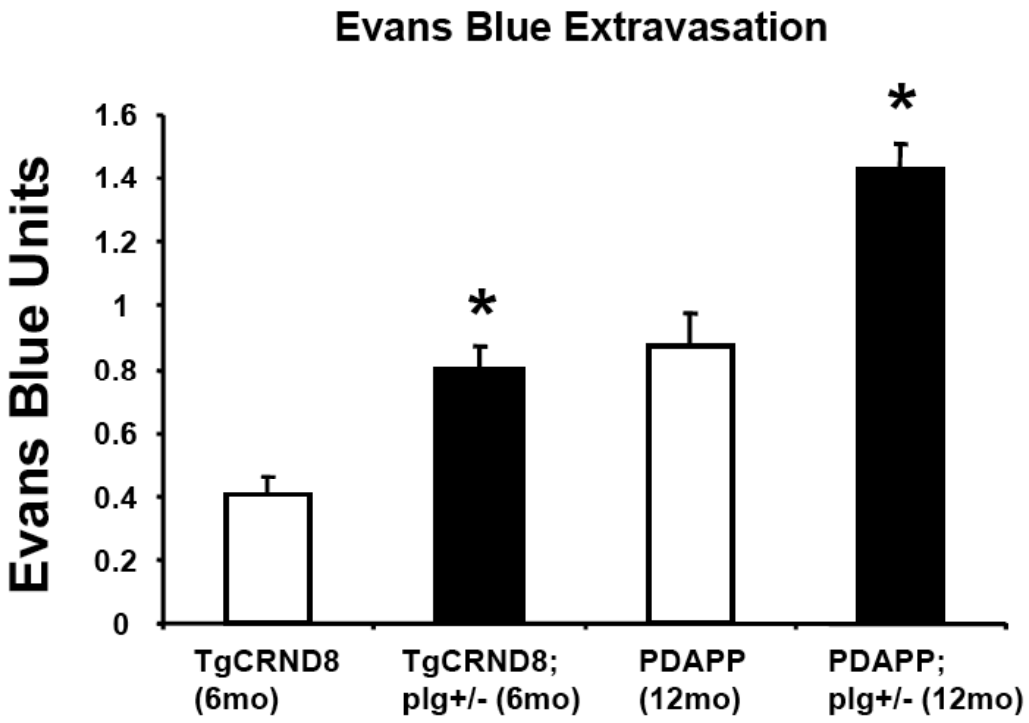

Figure 12. Heterozygous genetic deficiency for plasminogen and early neurovascular damage. PDAPP;plg+/- mice are consistent with changes observed in TgCRND8;plg+/- mice, as indicated by increased Evans blue extravasation at 12 mo of age relative to PDAPP littermates. Data are represented as mean ± SEM, where n = 4 for both PDAPP and PDAPP;plg+/- mice and compared to data from Fig. 5. *, $P < 0.05$ relative to PDAPP littermates.

Because Evans blue dye is fluorescent, the entire hemisphere can be visualized for dye extravasation to determine which areas of the brain are most affected. Images of cerebral hemispheres of each genotype were compared (Fig. 13). The cortex and hippocampus were affected with the highest levels of neurovascular damage consistent with the observation that hippocampus and cortex show the most Aβ deposition. The data indicated that the removal of one copy of the plasminogen gene accelerates the loss of microvascular integrity in TgCRND8 mice, while reduction of one copy of the fibrinogen gene slowed pathogenesis. At 3 months of age, mice homozygous for plasminogen deficiency showed blood-brain barrier damage (Fig. 14), but did not show significant neuroinflammation. Since these mice died early, it cannot be determined if the inflammation would have developed to levels comparable to older AD mice. Nonetheless, this finding indicates presence of Aβ exaggerates fibrin-related neuroinflammation.

3.5 Fibrinogen depletion protects against the deleterious effects of plasmin inhibition

Suppressing plasmin activity with tranexamic acid leads to increased blood-brain barrier breakdown and inflammation, as shown in Figures 6-8. As fibrin and fibrinogen are the primary targets of plasmin proteolysis, this treatment also led to increased fibrin(ogen) deposition (Fig. 5). However, because plasmin is a potent protease that could have many substrates, we investigated whether the vascular damage and inflammation were due to fibrin(ogen) accumulation or some other effect of plasmin inhibition. Therefore, we implanted pumps with

either saline or ancrod in two groups of mice for a pretreatment period of one week. After pretreatment, both fibrinogen-depleted and control groups received tranexamic acid to inhibit plasmin activity for one week. All mice were assayed for blood-brain barrier damage and inflammation as before. As expected, plasmin inhibition increased Evans blue extravasation and microglial staining in the control group. By comparison, the fibrinogen-depleted group showed significantly less pathology (Fig. 15). Levels for fibrinogen-depleted mice were similar to untreated mice (Fig. 3) suggesting that fibrinogen depletion protected mice from the increased vascular damage and inflammation induced by plasmin inhibition. This result indicates that fibrin(ogen) deposition is a critical pathologic consequence of reduced plasmin activity in the brains of AD mice.

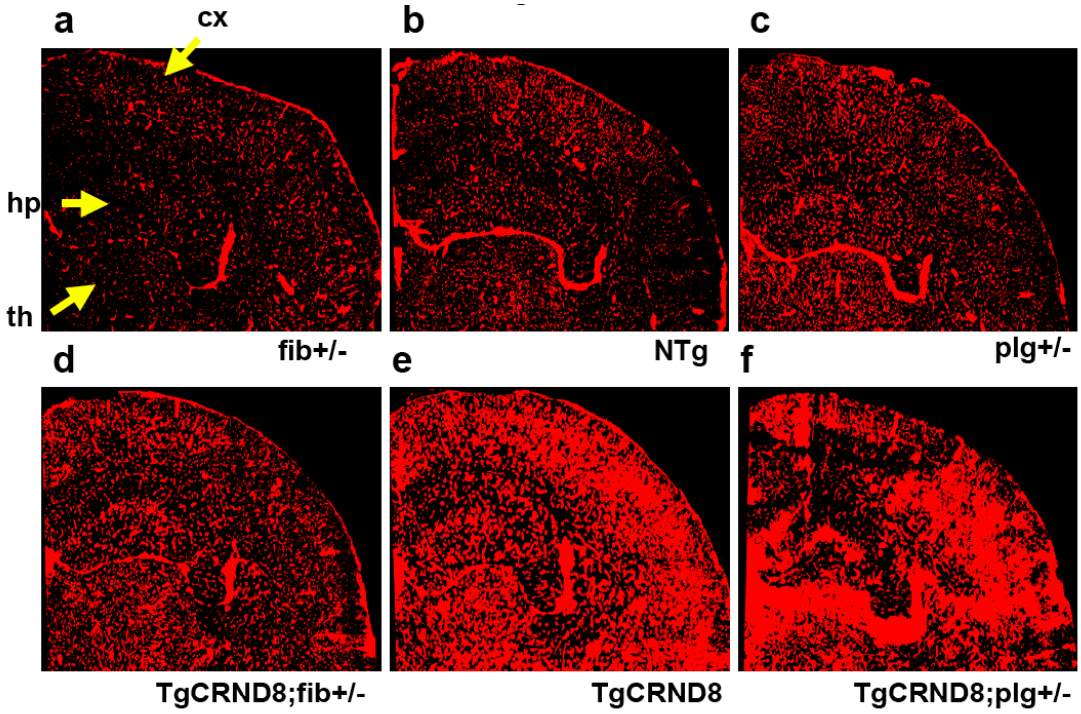

Figure 13. Localization of vascular pathology in AD mice deficient for fibrinogen or fibrinolysis. (A–F) Composite images of cerebral hemispheres of 6-mo-old mice perfused with Evans blue for 6 h. TgCRND8;fib+/– (D) and TgCRND8;plg+/– (F) mice are compared with TgCRND8 mice (E) and fib+/– (A), NTg (B), and plg+/– (C) controls. Pathologic dye accumulation is most apparent in the cortex (cx), hippocampus (hp), and thalamus (th).

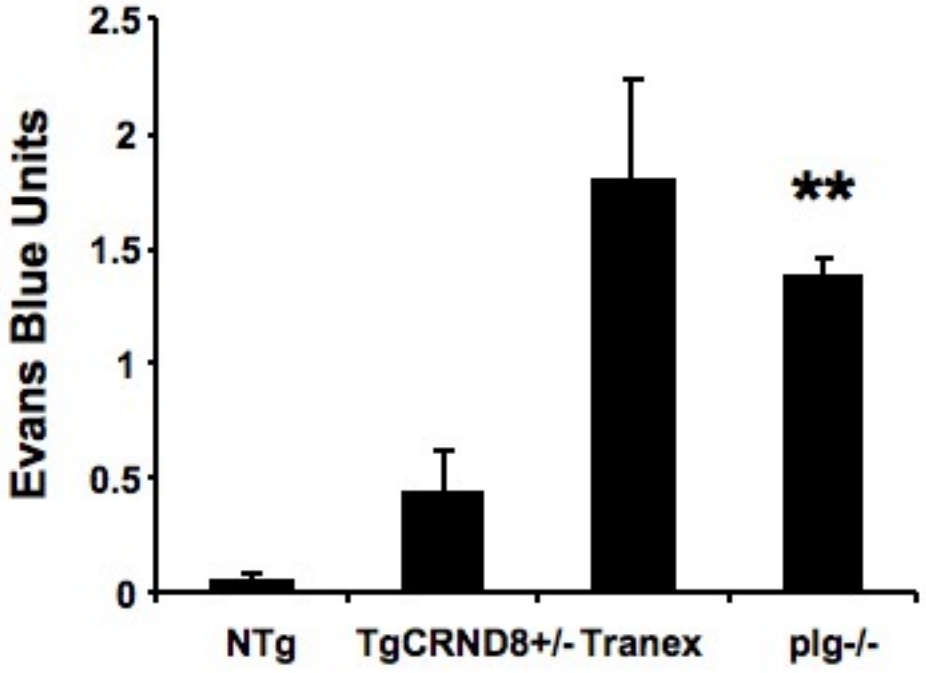

Figure 14. Complete genetic plasminogen deficiency produces early neurovascular damage without neuroinflammation. Plasminogen-null (plg-/-) mice were assayed for Evans blue extravasation at 3 mo of age. Data are represented as mean ± SEM, where n = 4 for plg-/- and compared to data from Fig. 1 A; **, $P < 0.001$ relative to wild types. Plg-/- mice showed increased blood-brain barrier permeability comparable to transgenic mouse treated with a plasmin inhibitor.

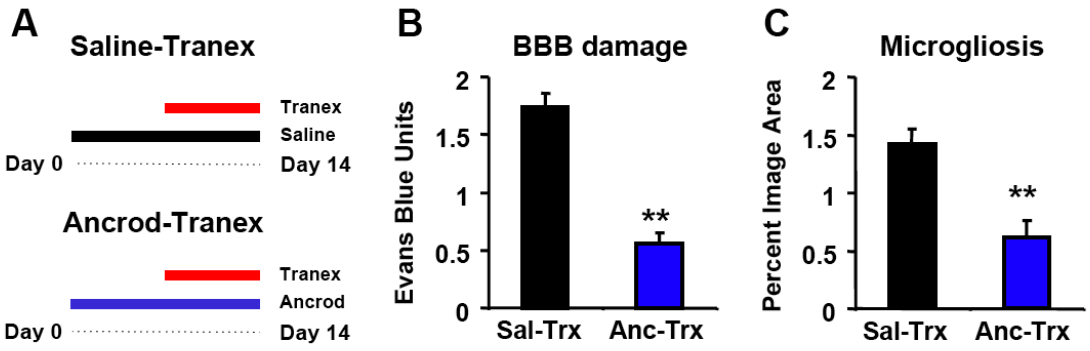

Figure 15. Ancrod treatment protects AD mice from increased pathology induced by tranexamic acid. (A) Two groups of 6-mo TgCRND8 mice were treated as indicated. (B) Evans blue extravasation. (C) Analysis of CD11b staining for microglia, either resident in the brain or peripherally derived. In both cases, pretreatment with ancrod reduced the effect of tranexamic acid. Error bars present the mean ± SEM of four images for each of four ancrod- and four saline-treated mice. **, $P < 0.001$.

CHAPTER 4: Aβ ALTERS FIBRIN CLOTS

4.1 AD mouse brains cannot clear fibrin efficiently

Fibrin(ogen) accumulates in the brains of AD patients (Fiala et al., 2002) and AD mice that are transgenic for human AβPP (Paul et al., 2007). Since one possible reason for the fibrin(ogen) accumulation in mice was a higher level of fibrinogen in the blood, we measured fibrinogen levels in wild type and AD mice and found no difference (Fig 25). Another possibility was increased persistence of fibrin(ogen) in AD mice. Therefore, we determined if these mice had increased stability of fibrinogen injected into the brain. Six-month old AD mice and their wild type littermates were injected with purified human fibrinogen into the hippocampus and sacrificed the following day. Though injected with the same amount of fibrinogen, AD mouse brains contained more exogenous fibrin(ogen) than their wild type littermates (Fig. 16 a-c). Areas of fibrin(ogen) deposition conincided with amyloid deposits (Fig. 16 d-g). Conversion of at least a portion of injected fibrinogen to fibrin was demonstrated by detection of D-dimer in brain homogenates (Fig. 26), indicating that the injected fibrinogen was polymerized and cross-linked by transglutaminase before proteolytic cleavage. Therefore, injected fibrinogen was converted to fibrin in the AD mouse hippocampus, and this fibrin persisted longer in the AD mouse brain compared to wild type.

Persistent fibrin(ogen) could be due to increased formation or decreased clearance (Sutton et al., 1994; Melchor et al., 2003). To examine this effect further, cortical homogenates were prepared from 26-week-old AD mice and wild type littermates, by which time the cortex has high levels of Aβ. These homogenates were added to normal human plasma *in vitro* in the presence of excess thrombin and tPA. As thrombin converts fibrinogen to a fibrin network,

the newly formed fibers scatter light and the solution increases in turbidity. As fibers are formed, they become substrates for tPA-activated plasmin, and the equilibrium shifts from formation to dissolution, reducing the turbidity as the clot is dissolved. Turbidity increased similarly in both groups during the initial clot formation phase (Fig. 17a), suggesting there was no direct effect on thrombin. However, the wild type samples initiated fibrinolysis earlier and dissolved the clot with greater overall efficiency. The AD cortex achieved a greater maximum turbidity and completed dissolution at later time points (Fig. 17b). Using streptokinase, the AD cortex again showed a reduced lysis of fibrin (Fig. 17c-d), indicating that Aβ did not interfere with the tPA /plasminogen or tPA/fibrin interactions. Also, this result showed that increased PAI-1 was not responsible since streptokinase is not inhibited by PAI-1. In contrast to cortical extracts, cerebellar AD mouse brain homogenates, which at this age contain low levels of Aβ (Chishti et al., 2001), had no effect on the degradation of fibrin clots (Fig. 18a-b).

To determine if Aβ was responsible for these effects, we depleted it from cortical homogenates by immunoprecipitation with an anti-Aβ antibody. We found that the Aβ-immunodepleted homogenates no longer bound Congo Red dye while the precipitated solution was congophilic. Fibrin clearance times in the presence of cortical extracts from AD mice brains were substantially reduced after Aβ depletion (Fig. 18c-d). However, depletion of Aβ did not completely restore normal degradation times. This result suggests that the removal was incomplete or that there are additional factors in the AD mouse brain contributing to the formation/dissolution equilibrium. Taken together, these findings suggest that Aβ may be causing alteration of the fibrin clot, which is retarding its clearance.

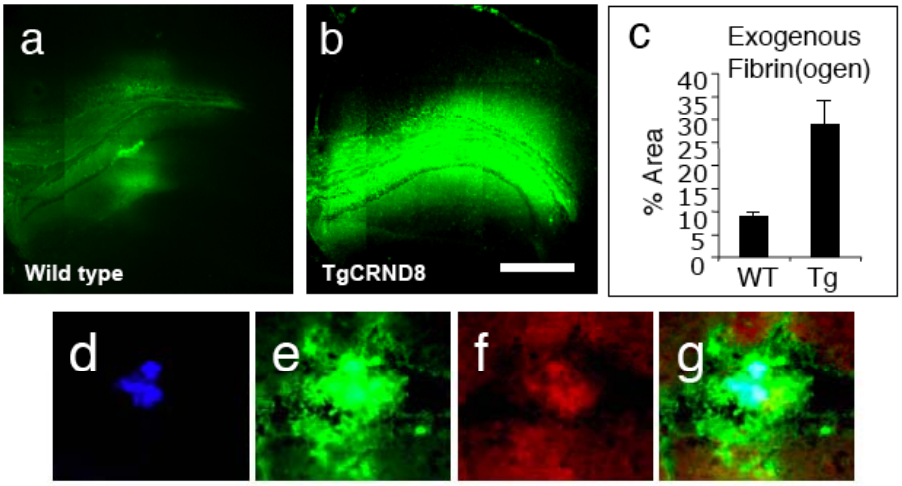

Figure 16: AD mouse brains do not clear fibrin(ogen) efficiently due to increased Aβ load. (a) Immunofluorescent detection of fibrin(ogen) in the hippocampus of a wild type mouse one day following stereotaxic injection with fibrinogen. Scale bar is 1 mm. (b) Detection of fibrin(ogen) in equivalent brain region of an AD mouse one day post-injection. (c) Fibrin(ogen) area units were calculated for mice in each group using the area of fibrin(ogen) staining divided by the area of co-injected Evans blue dye. Fibrin(ogen) colocalizes with amyloid after stereotactice injection (d-g). Sections of AD mouse brains injected with Evans blue (f) and fibrinogen one-day prior to sacrifice were stained for Thioflavin S (d) and polyclonal anti-fibrinogen antibody (e). Amyloid deposits near the site of injection showed fibrin(ogen) staining as shown in the merged image (g).

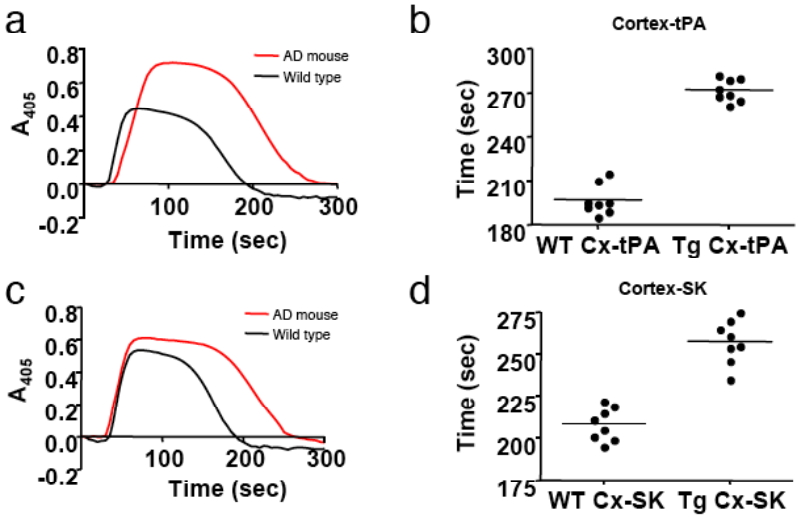

Figure 17: AD mouse brains do not clear fibrin efficiently due to increased Aβ load. (a) Formation and degradation of clots in the presence of brain extracts. Clotting of normal human plasma was initiated with thrombin in the presence of brain extract from the cortex of AD mice (red) or wild type littermates (black) with excess tPA. (b) Total lysis time for ex vivo extract assay in (a) determined from initiation to complete dissolution for wild type and AD mice. (c) Formation/degradation assay in the presence of cortex extracts of AD mice (red) or wild type littermates (black) with streptokinase (SK) added to normal human plasma clots. (d) Total lysis time for wild type and AD mouse brain extracts in (c). All curves are representative assays.

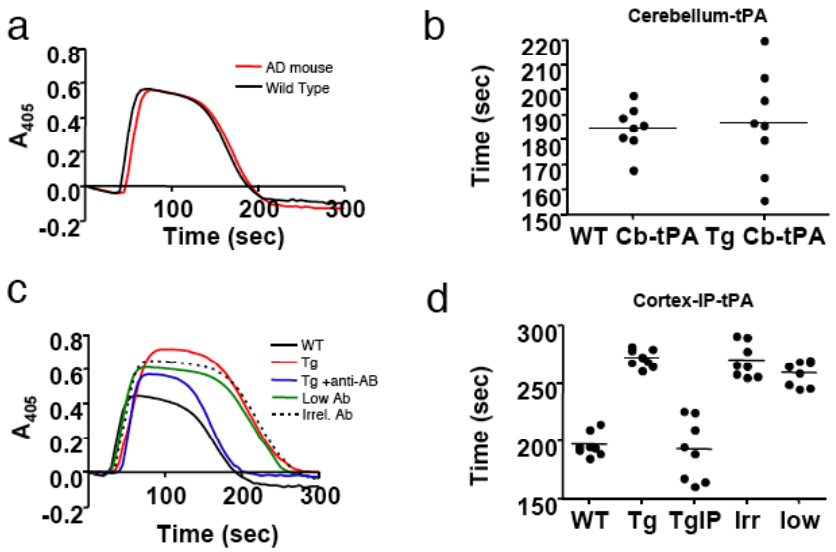

Figure 18: AD mouse brains do not clear fibrin efficiently due to increased Aβ load. (a) Formation/ degradation assay in the presence of cerebellum extracts of AD mice (red) or wild type littermates (black) with tPA added. (b) Total lysis time for wild type and mouse cerebellar extracts with tPA in (a). (c) Formation/degradation curves of AD mouse brain homogenates depleted of Aβ with 5 μg/ml of 4G8 antibody (blue) or 5 μg/ml of irrelevant IgG (black dashed). Other controls included low concentration of 4G8 (green) and no antibody in AD (red) or wild type (black). (d) Total lysis times for immunodepletion experiments in (c). * $p<0.001$, AD mice compared to wild type; control Ab compared to 4G8. All curves are representative assays.

4.2 Purified Aβ impairs fibrinolysis

To further simplify our analysis, we performed clot formation/degradation experiments with purified human fibrinogen and tPA in the presence or absence of various forms of Aβ. In the presence of congophilic Aβ42, the thrombin-catalyzed fibrin clot was formed normally in the initial phase of the curve (Fig. 19a), but its dissolution was delayed (Fig. 19b). One possible explanation for this result is that congophilic Aβ42 may affect the known interaction of tPA and plasminogen (Hoylaerts et al., 1982), reducing the fibrinolytic potential. To examine this possibility, the experiment was repeated using streptokinase rather than tPA since its activation of plasminogen does not require proteolytic cleavage. Clot lysis by streptokinase was also delayed in the presence of Aβ, suggesting a fundamental difference in clot structure in the presence of this peptide (data not shown). It could be that Aβ promoted Factor XIIIa (transglutaminase) activity, since increasing cross-linking could strengthen the fibrin clot and reduce lysis speed. However, there was no difference in gamma-gamma crosslinking (D-Dimer) in the presence or absence of Aβ as determined by analysis of fibrin degradation products (data not shown). Thus, the actions of Aβ42 on clotting are likely due to direct molecular interactions with clotted fibrin or fibrinogen.

Aβ42 has been shown to stimulate tPA activation of plasminogen without increasing proteolytic activity (Kranenburg et al., 2002). This effect would be inconsistent with delayed fibrinolysis. Therefore, the effect of Aβ on fibrinolysis had greater observable impact than the stimulation of plasminogen activation. Also, although tPA activation of plasminogen is enhanced in the presence of Aβ,

there was no direct enhancement of tPA proteolytic activity as determined by colorimetric enzymatic assays. Additionally, there were no effects of congophilic Aβ42 on thrombin or plasmin (Fig. 27).

To test this effect in the presence of all of the components involved in hemostasis, we clotted recalcified human plasma in the presence of tPA (Fig. 19c). Similar to the pure fibrin clots, fibrinolysis was delayed in the presence of congophilic Aβ42 (Fig. 19d). To observe the degradation process alone, we added tPA to a clot previously formed from recalcified platelet-deficient plasma and observed fibrinogen degradation using confocal time-lapse image acquisition (Fig. 20a)(Collet et al., 2000). The lysis front retreated as the clot was degraded by plasmin, and the retreat rate was calculated. In the presence of congophilic Aβ42, lysis was delayed and retreat of the lysis front was slowed (graph in Fig. 20b).

Because Aβ misfolds to form ordered fibrillar aggregates, we determined if protein folding played a role in these results. Congo Red is a dye that recognizes fibrillar amyloid plaques in AD postmortem tissue, due to its sensitivity to the anti-parallel β-pleated sheet conformation. Upon binding, the absorbance spectrum of the dye changes, producing a red shift (Klunk et al., 1999). Purified Aβ did not exhibit a red shift immediately after reconstitution. After mixing the solution overnight at room temperature to promote nucleation and growth of Aβ oligomers (Chauhan et al., 2001), peptides in the solution were enriched in β-sheets and thus became congophilic. We confirmed the presence of fibrils in the congophilic Aβ42 samples used in this study with electron microscopy (Fig. 37). Non-congophilic solutions of Aβ did not produce the effects on lysis time in fibrin clots, while congophilic Aβ solutions affected lysis rates (Fig. 19a-d). Therefore,

oligomerization and β-pleated sheet structure are necessary to observe the effects on fibrin polymerization.

To separate possible effects of Aβ on clot formation and dissolution, we next tested the effect of Aβ on fibrin only during the formation phase. The presence of Aβ42 during thrombin-induced clot formation from pure fibrinogen produced a dose-dependent decrease in the normal rise in turbidity (Fig. 20b). The decreased turbidity could reflect incomplete clotting. However, in both the presence and absence of Aβ, all the fibrinogen was removed from solution and incorporated into the clot (data not shown), indicating complete clotting in both cases. Therefore, the lower turbidity suggested that the fibrin clot formed in the presence of Aβ was structurally abnormal. Structurally altered clots can be resistant to fibrinolysis (Collet et al., 2000; Sugo et al., 2006), which could explain the persistence of fibrin in the presence of Aβ.

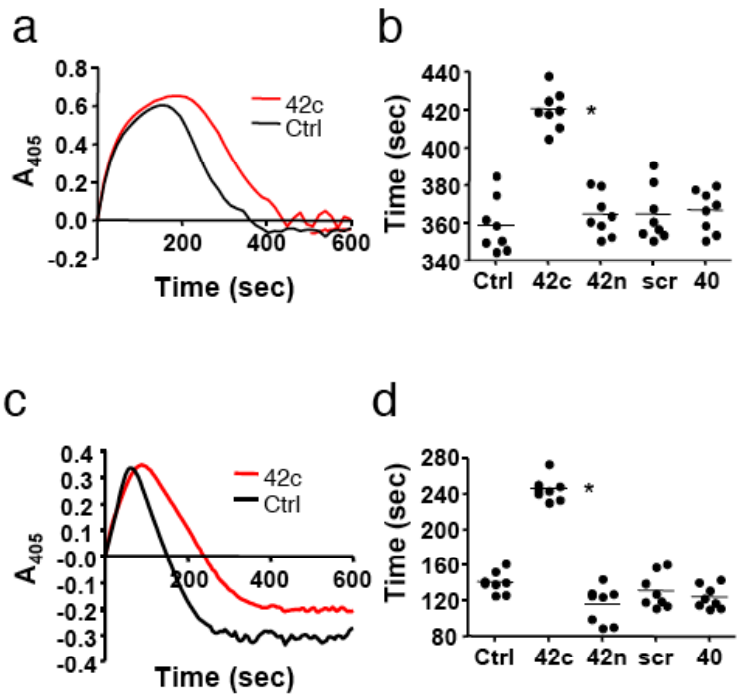

Figure 19: Aβ alters the development of fibrin clot turbidity and slows degradation. (a) Combined fibrin formation/degradation assay. Clotting of purified fibrinogen was initiated with thrombin in the presence of tPA and human plasminogen. Control (vehicle), black; Aβ42 500 nM, red. (b) Formation/degradation time for pure fibrin clots determined from initiation to complete dissolution. Ctrl = control; 42c = congophilic Aβ42 500 nM; 42n = non-congophilic Aβ42 500 nM; scr = scrambled Aβ42 peptide; 40 = Aβ40 500 nM. (c) Human plasma formation/degradation assay. Clotting of plasma was initiated with thrombin in the presence of tPA. Control, black; Aβ42 500 nM, red. (d) Formation/degradation time for human plasma clots determined from initiation to complete dissolution. Ctrl = control; 42c = congophilic Aβ42 500 nM; 42n = non-congophilic Aβ42 500 nM; scr = scrambled Aβ42 peptide ; 40 = Aβ40 500 nM. All curves are representative assays of 5 experiments.

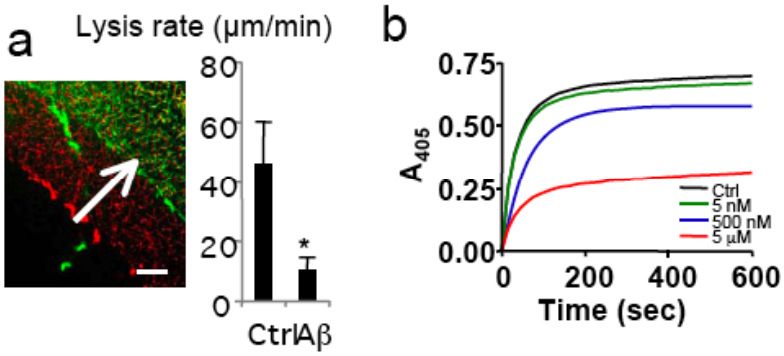

Figure 20: Aβ alters the development of fibrin clot turbidity and slows degradation. (a) Lysis front retreat rate determined from 5 minute time-lapse confocal acquisitions from clots formed from plasma with fluorescent fibrinogen incorporated into the clot. After addition of tPA, red shows the edge of a clot formed in the presence of congophilic Aβ42 at 0 minutes and green shows the edge at 5 minutes. The data for 4 experiments of control (vehicle) and congophilic Aβ42 were quantified as the speed the edge retreated in μm/min. * p <0.001. Scale bar = 36.5 μm. (b) Progress of turbidity upon clot initiation by adding human thrombin to fibrinogen at time 0. Control (vehicle), black; Aβ42 5 nM, green; Aβ42 500 nM, blue; Aβ42 5000 nM, red. All curves are representative assays of 5 experiments.

4.3 Structural deformation of fibrin in the presence of Aβ

This decreased turbidity (Fig. 20b) prompted examination of the clot's structure. We acquired images from native hydrated fibrin using confocal microscopy. Images using a fluorescent fibrinogen conjugate showed that the pure fibrin clots formed in the presence of congophilic Aβ42 are structurally altered with fibrils arranged in a non-homogeneous network. Areas of normal clotting were interrupted by irregular regions of clustering in the Aβ42-influenced fibrin (Fig. 21a-b). Immunostaining of fibrin in the presence of Aβ without using labelled fibrinogen produced identical aggregates (data not shown). Aggregates stained positive with Congo Red (Fig. 21c-d), suggesting they were formed only in the presence of fibrillar forms of Aβ. Neither fibrin fluorescence nor Congo Red-positive Aβ aggregates were observed when thrombin was omitted from the reaction mix (data not shown).

To further investigate this conclusion, we used biotinylated Aβ in the clotting reaction and then stained with fluorophore-conjugated streptavidin. Aβ peptide alone did not produce aggregates since streptavidin-conjugated fluorescence and staining for Aβ was only observed in the aggregates, confirming that the peptide was confined to these areas (data not shown). The size of the aggregates ranged from two to 40 μm in diameter, and the average size and number increased over time (Fig. 22a-b). During lysis of clots, aggregates often detached from the lysis front and dissolved slowly (Supplementary Videos). Degradation-resistant aggregates staining positive for Congo Red remained after surrounding fibrin had been degraded (Fig. 23c-d). Cluster formation and delayed lysis were not detected in control clots or those formed in the presence of non-congophilic or scrambled Aβ42 peptide. Fibrin clots formed in the

presence of Aβ40 did not contain aggregates. Interestingly, the destabilizing Dutch (E22Q) and Arctic (E22G) mutations in Aβ40, which enhance fibrillogenesis, promoted cluster formation similar to Aβ42 (Fig. 22c-d). Adding equal amounts of Aβ42 to collagen did not introduce any irregularities into the network of collagen fibrils (Fig. 28), suggesting that fibrin may be uniquely susceptible to Aβ.

Scanning electron microscopy (SEM) images of purified fibrin also showed aggregate formation in the presence of Aβ (Fig. 23a-b). Because SEM images were obtained from clots that were fixed and post-processed, fibrils appeared tangled and up to 10 times thinner than in normal hydrated clots. Aβ fibrils can aggregate platelets (Kowalska and Badellino, 1994), but these aggregates were formed in Aβ-influenced clots using platelet-deficient plasma and purified fibrinogen (Fig. 28a-b). As purified fibrinogen contains no platelets, the aggregates were not aggregates of platelets in this case.

Given the effects of Aβ on clot structure and given that the genotype of the blood protein ApoE influences the development of AD (Corder et al., 1993), we examined whether the various isoforms of ApoE could influence the fibrin network organization in the presence of Aβ. ApoE2, ApoE3, and ApoE4 had similar effects when added to pure fibrin clots. Alone, each ApoE isoform increased the turbidity of pure fibrin clots, but had minimal effects on clot structure (data not shown). However, when added in combination with Aβ42, clot structures showed isoform-specific differences. Aggregate formation was comparable between Aβ42-influenced clots formed with or without ApoE4 (Fig. 24), and the clots showed similar plasmin lysis where aggregates detached from the lysis front and were difficult to degrade. However, both ApoE2 and ApoE3

showed reduced cluster formation in the presence of Aβ (Fig 24). AD epidemiology suggests the ApoE2 is protective, ApoE3 has an intermediate effect, and the less common ApoE4 has a gene-dosage effect to increase the risk of developing the disease earlier. These data suggest the increased risk could be due to a loss-of-function to stabilize and facilitate normal clot formation in the presence of Aβ.

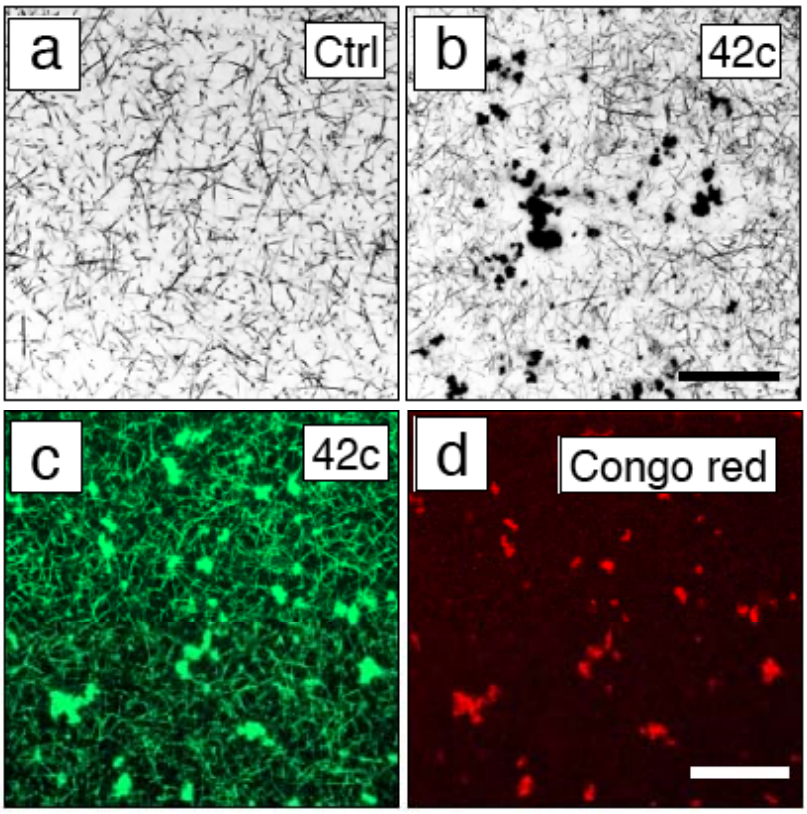

Figure 21: Aβ alters clot structure. (a) Confocal image (inverted gray levels) of control (vehicle) fibrin clot using fluorescent fibrinogen at low magnification. (b) Aβ42-influenced clot (500 nM) at low magnification. Scale bar = 36.5 μm. (c) Image of fluorescent fibrin (pseudocolored green) forming network with aggregates in the presence of Aβ. (d) Image of congo red fluorescence (pseudocolored red) in the same field as in (c).

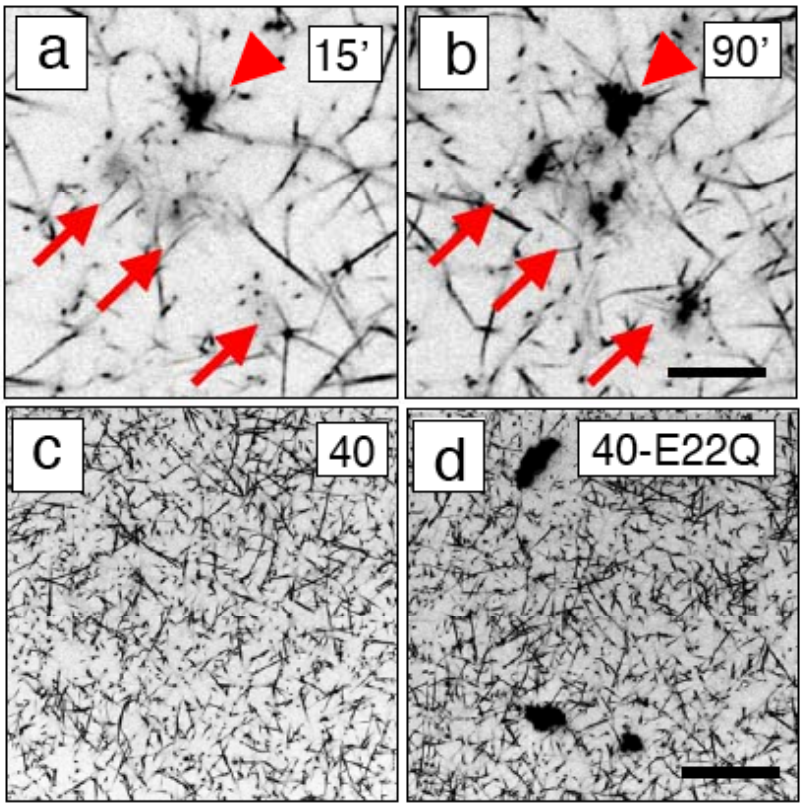

Figure 22: Aβ alters clot structure over time. (a) Confocal image (inverted gray levels) of fibrin clot showing aggregates acquired 15 minutes after addition of thrombin. (b) Confocal image of the fibrin clot shown in (a) showing aggregates after 90 minutes. Scale bar = 8.75 μm. (c) Aβ40-influenced (500 nM) clot at low magnification. (d) Aβ40-Dutch (E22Q)-influenced clot (500 nM) at low magnification. Scale bar = 36.5 μm.

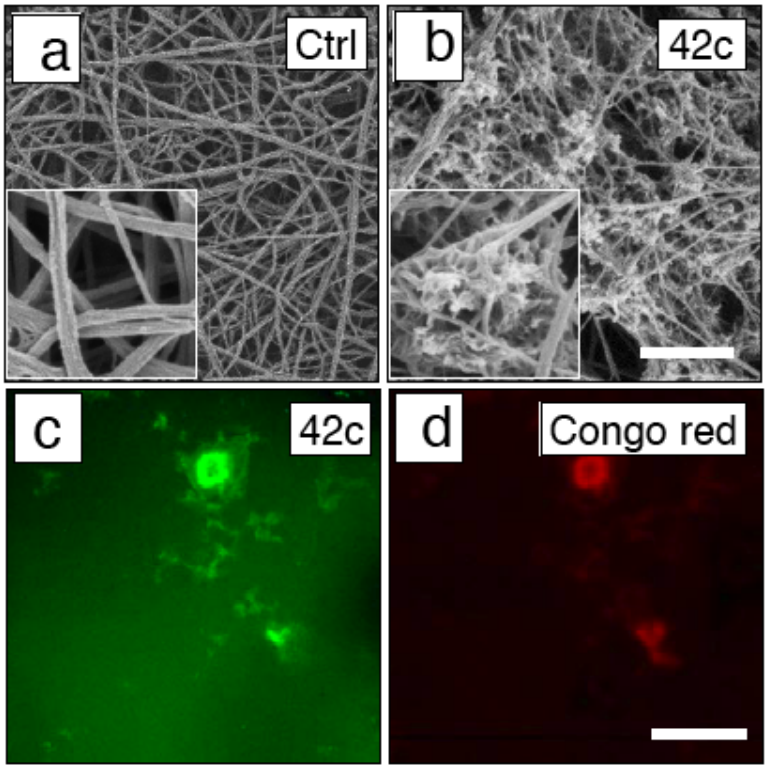

Figure 23: Aβ alters clot structure by SEM. (a) Scanning elecron micrograph (SEM) obtained from control clot formed from pure fibrinogen and thrombin. (b) SEM of fibrin formed in the presence of Aβ42 (500 nM). Scale bar = 1.25 μm, and inset is 1 μm x 1 μm. (c) Confocal image of green-fluorescent fibrin(ogen) aggregated in the presence of congophilic Aβ42 remains after fibrinolysis was completed and surrounding network is dissolved. (d) Congo Red stains the remaining aggregate shown in (c).

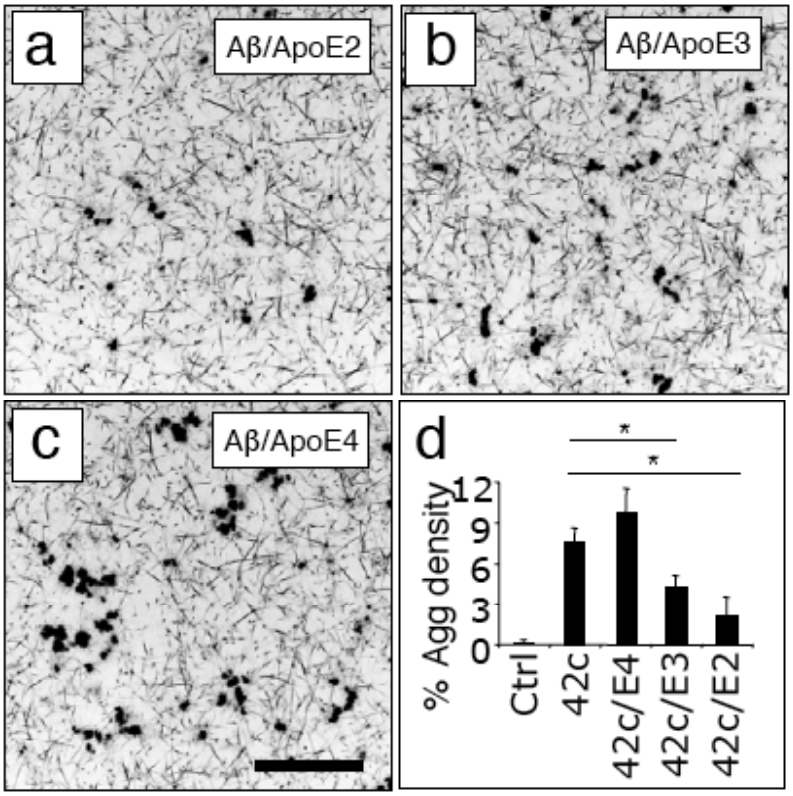

Figure 24: ApoE2 and ApoE3 attenuate the effect of Aβ on blood clot structure. (a-c) Confocal images (inverted gray levels) of fibrin clot showing aggregates formed from platelet-deficient human plasma and thrombin in the presence of fluorescent-conjugated fibrinogen, Aβ42 (500 nM) and (a) excess ApoE2 (50μM), (b) ApoE3 (50 μM), or (c) ApoE4 (50 μM). Scale bar = 36.5 μm. (d) Percent density of aggregates in clots formed after 90 minutes. * indicates p <0.001.

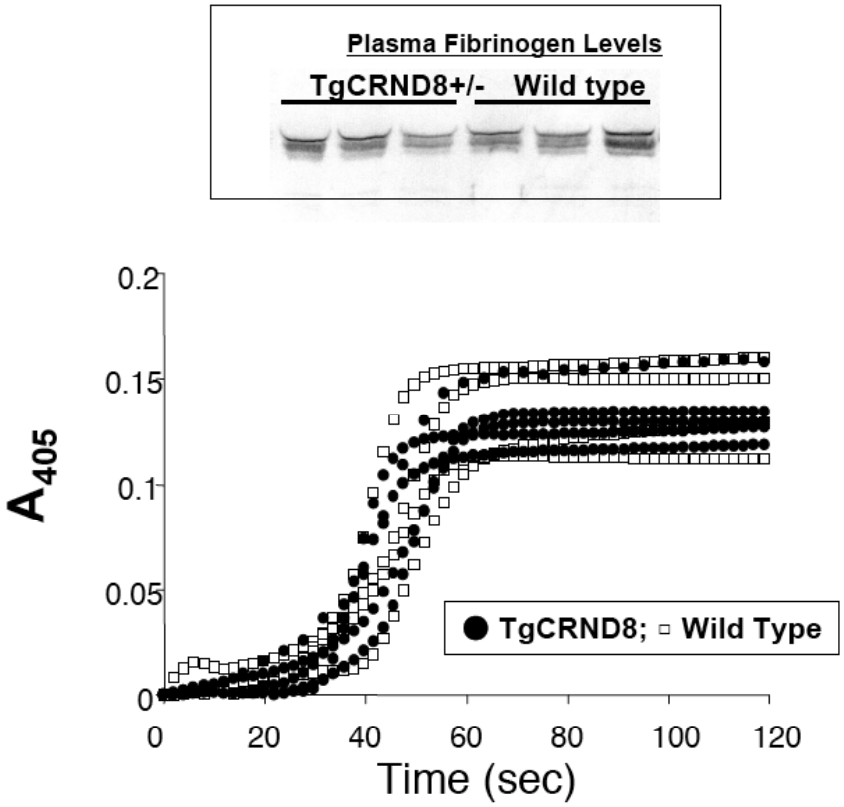

Figure 25. Western blots of plasma samples show that circulating fibrinogen is similar in AD and wild type mice (n=3 per group). Activated partial thromboplastin time curves for AD and wild type mice. AD mouse blood is not hypercoagulable as clotting time and turbidity values are similar.

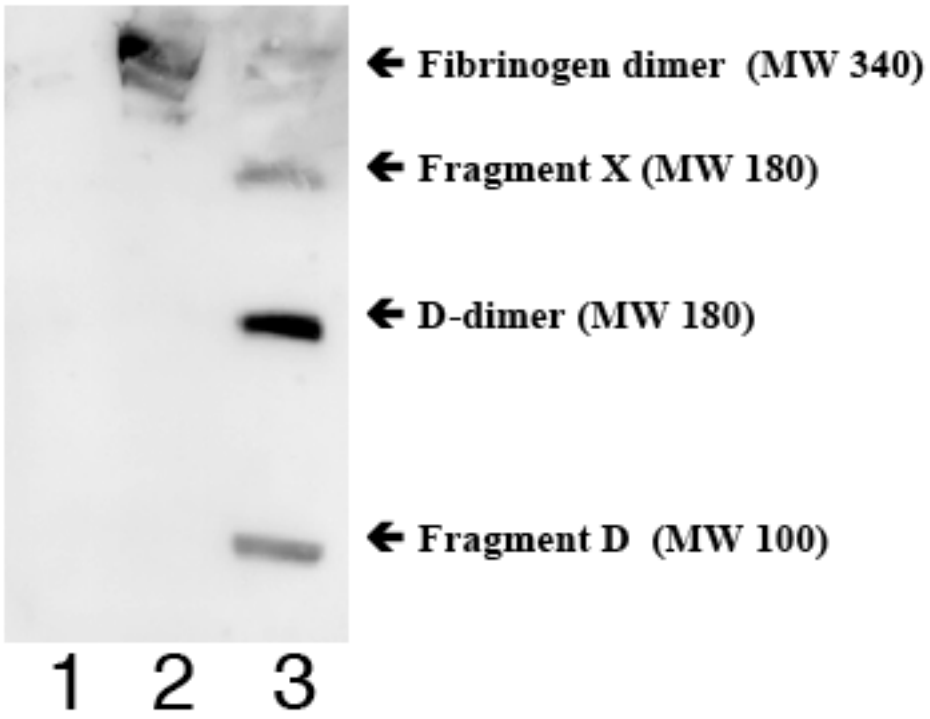

Figure 26: Presence of D-Dimer indicates conversion of fibrinogen to fibrin upon injection into AD mouse brains. Lane 1 represents wild type. Lane 2 represents pure fibrinogen. Lane 3 shows detectable levels of fibrin degradation products are present in the homogenized AD mouse brain after injection with fibrinogen. Without injection, these products are only detectable by ELISA.

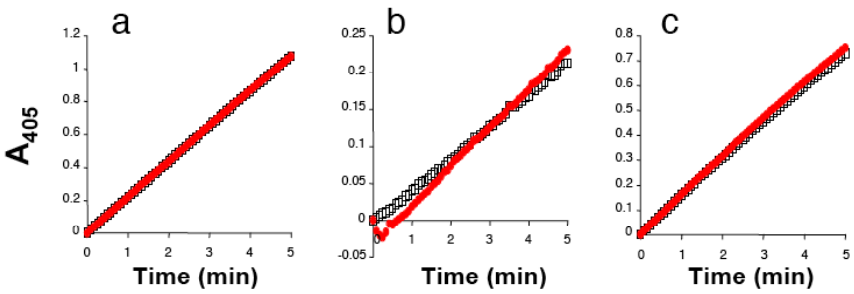

Figure 27: Enzyme activity assays using purified enzymes and colorimetric substrates. Plasmin (a), tPA (b), and thrombin (c) show no difference in activity in the absence (black boxes) or presence of (red circles) Aβ42 (500 nM).

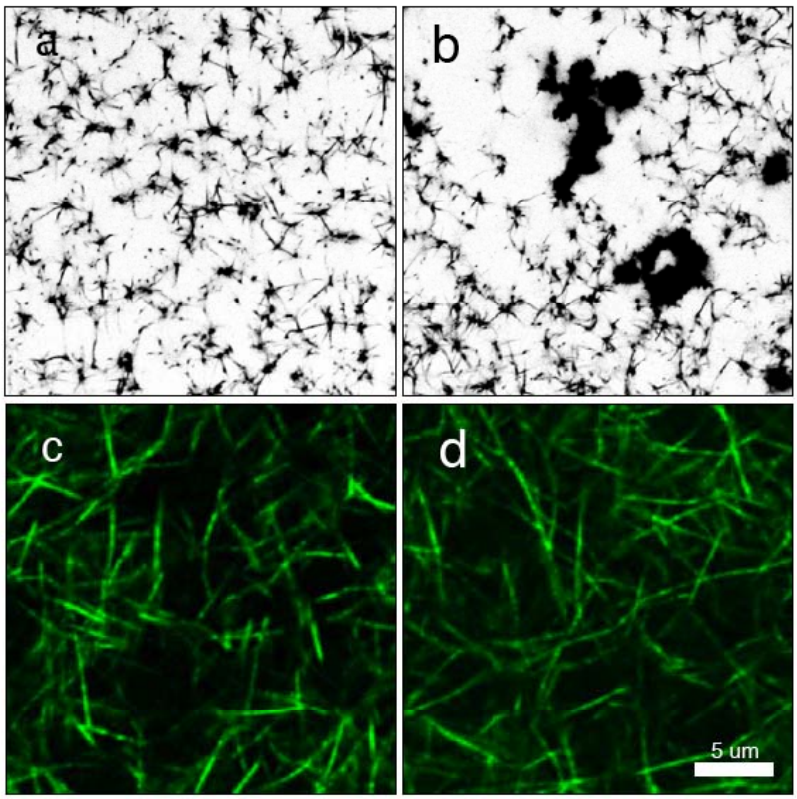

Figure 28: Aβ affects purified fibrin clots. (a) Confocal image acquired 90 minutes after addition of thrombin to pure fibrinogen (inverted gray levels), showing no aggregates are formed in the absence of Aβ. Image is 35 μm x 35 μm. (b) Confocal image of fibrin clot showing aggregates in the presence of Aβ after 90 minutes. (c) Collagen fibrils imaged using gold colloid and reflectance confocal imaging. No aggregates are formed in the absence (c) or presence (d) of Aβ. Image is 35 μm x 35 μm.

4.4 AD mouse and human cerebrovasculature contain fibrin(ogen) deposits

Next, we determined if the classical role of fibrinogen in hemostasis might be challenged within the cerebral vasculature. Blood vessels in the brain serve as an interface for interaction between fibrinogen and Aβ as excess brain-derived Aβ is actively drained through the vasculature (Shibata et al., 2000). We examine fibrin(ogen) deposition at this interface by co-staining perfused AD mouse brains for amyloid and fibrin(ogen). We found fibrin(ogen) deposited in the amyloid-laden vessels of AD mice (Fig. 29), consistent with fibrin deposits resistant to degradation. We counted the number of Congo Red positive vessels (CAA), which stained positive for fibrin(ogen) and found that 85% of amyloid vessels contained fibrin(ogen) deposits. We also counted the number of fibrin(ogen) immunoreactive vessels that also stained positive with Congo Red. Only 9% of apparently thrombosed vessels were positive for amyloid (Fig. 30). Therefore, the AD mouse cerebral vasculature is likely a prothrombotic environment but doesn't require fibrillarized Aβ for this to take place. We also examined the effects of pharmacologic depletion of fibrinogen in AD mice on the distribution of amyloid to plaques or to vessels. We found a decrease in vascular amyloid relative to saline treated groups, while plaque levels remained similar (Fig. 38). Inhibition of plasmin with tranexamic acid produced the opposite effect to increase CAA in treated AD mice.

To determine the clinical significance and further characterize the fibrin(ogen) deposition, we used a monoclonal antibody that recognizes fibrin but not fibrinogen to stain post-mortem brain samples of human AD. We found that Thioflavin colocalized with fibrin immunoreactivity, though there were many instances of fibrin stained blood vessels in the absence of amyloid (Fig. 31).

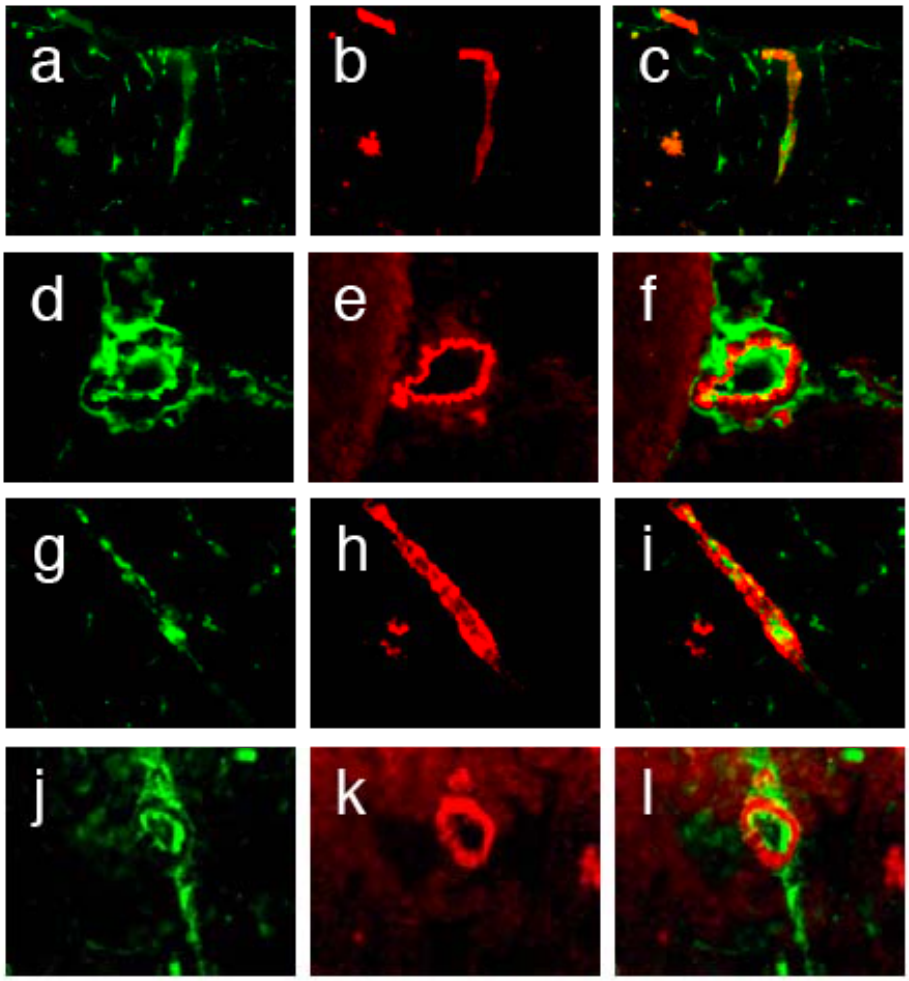

Figure 29. Intravascular Fibrin(ogen) deposition. Fibrin deposits are detected in vessels laden with congophilic Aβ. Perfused AD mice at 52 weeks-of-age have deposits of fibrin(ogen), (green) at sites of cerebral amyloid angiopathy detected by Congo Red fluorescence (red). Scale bar is 50 μm. Fibrin(ogen) deposits are detected in the cortex with longitudinal sections (a-c) as well as transverse sections (d-f). Fibrin(ogen) deposits are detected in the hipocampus with longitudinal sections (g-i) as well as transverse sections (j-l).

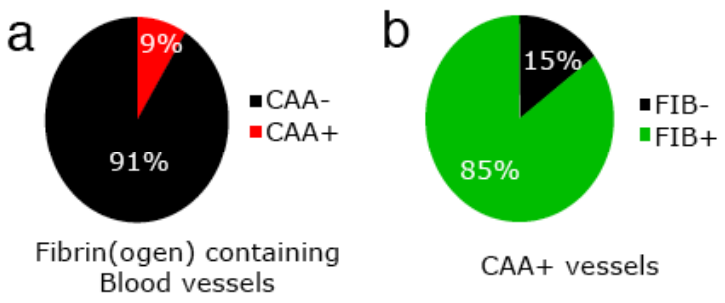

Figure 30. Distribution of intravascular fibrin(ogen) deposits. The distribution of fibrin(ogen) deposits and cerebral amyloid angiopathy in 12-month AD mice was imaged and colocalization quantified. (a) Of all fibrin(ogen) stained vessels identified in the cortex and hippocampus, 9% were positive for Congo Red fluorescence. (b) Of all vessels staining positive for amyloid, 85% contained fibrin(ogen) deposits.

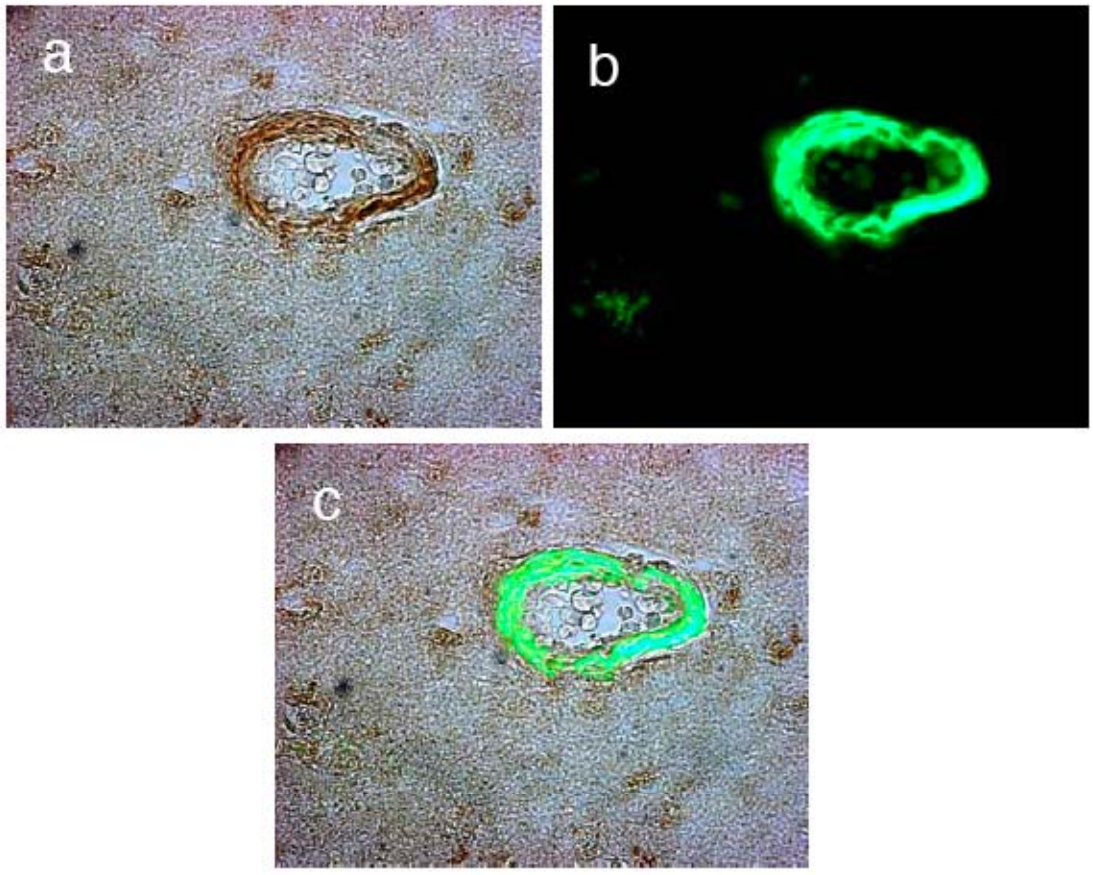

Figure 31. Intravascular fibrin deposition in humans. Post-mortem sections of patients diagnosed with AD were stained with a monoclonal antibody recognizing fibrin but not fibrinogen. Blood vessels in the cortex staining positive with clotted fibrin deposits (a) stained positive for Thioflavin S reflecting amyloidosis (b) as shown in the overlay (c).

4.5 AD mouse cerebral blood hemostasis is dysfunctional

To determine the significance of this fibrin accumulation in the brains of AD mice, we examined the relationship between cognitive performance in the Y-maze and individual characteristics of each mouse such as age, Aβ immunoreactivity, and fibrin deposition. Age showed poor correlation (r^2=0.412) with cognitive decline, while Aβ and fibrin correlated with cognition to a similar degree (r^2=0.688 and 0.730, respectively) (Fig. 36).

As Aβ peptides had strong effects on the turbidity and structure of the clots *in vitro* we wanted to better understand the *in vivo* effects on thrombosis and hemostasis. We devised an intravital system for viewing thrombosis in real time using epi-fluorescence (Fig. 32). AD and wild type mouse brains were exposed by craniotomy and blood flow was recorded using injected fluorescent-conjugated dextran to label blood flow. We then perfused the surface of the brain with the dura peeled back with ferric chloride. Thrombosis was exhibited by the appearance of an enlarging shadow superimposed on normal blood flow. Typically smaller clots appeared on the sides of vessels and grew over time until complete occlusion (Supplemental movies).

We counted the number of visibly occluded large vessels (>20 μm) over time for both AD and wild type mice. AD mice often thrombosed spontaneously even before the addition of ferric chloride, and lower doses were needed to occlude similar sized vessels (Fig. 33). To determine the rates of fibrinolysis, we formed clots with 10% ferric chloride in each mouse and then perfused the brains with tPA. Clot lysis is observed as the shrinking and eventual disappearance of the shadow over the fluorescent labelled blood flow (Supplemental movies). The size of the shadow was measured at one-minute time points. Clots formed in AD

mice remained of similar size for more than 5 minutes, while wild type mouse clots lysed quickly, often dissolving within 30 seconds (Figs. 34 and 35).

These measures suggest the AD mouse brain is an environment conducive to thrombosis. However, these results were not limited to thrombosis since we observed frequent uncontrolled hemorrhage after perfusion of clots with tPA (Supplemental movie). This effect was not observed in wild type littermates. These events can be explained by a weakened vessel wall due to smooth muscle loss and endothelial damage in CAA. The results are consistent with numerous studies linking CAA to intracerebral hemorrhage after treatment with a thrombolytic agent (Ramsay et al., 1990; Pendlebury et al., 1991; Winkler et al., 2002; McCarron and Nicoll, 2004).

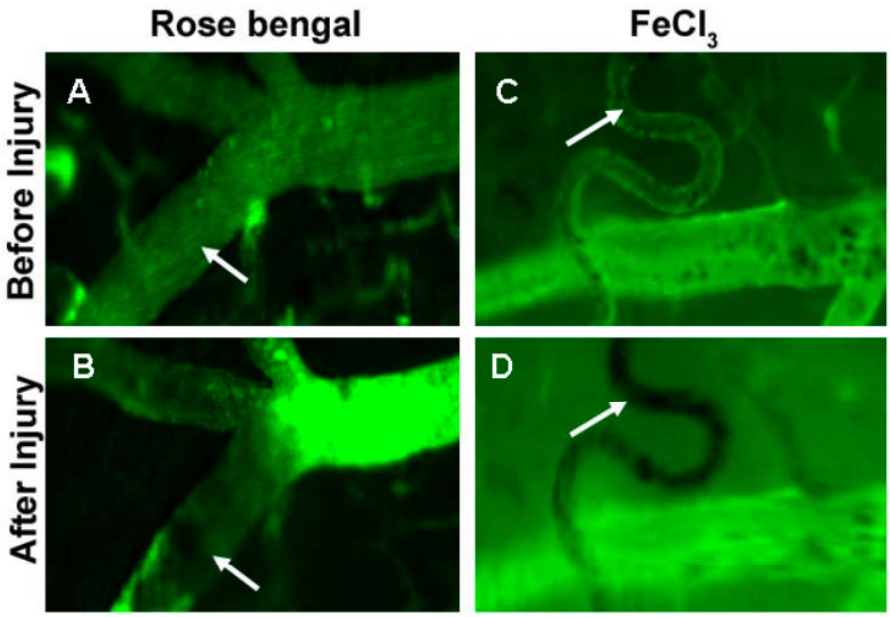

Figure 32. Intravital visualization of thrombus formation in the mouse brain. Fluorescein-labeled dextran was injected, and a cranial window was prepared. Images show vessels before (A,C) and after (B,D) clot formation. Thrombi were formed (B) after injecting Rose Bengal and inducing photo-injury by a multiphoton confocal microscope, or (D) by topical application of $FeCl_3$ and visualizing with a widefield microscope. Arrows indicate where thrombi were formed after the application of the laser (B) or the $FeCl_3$ solution (D).

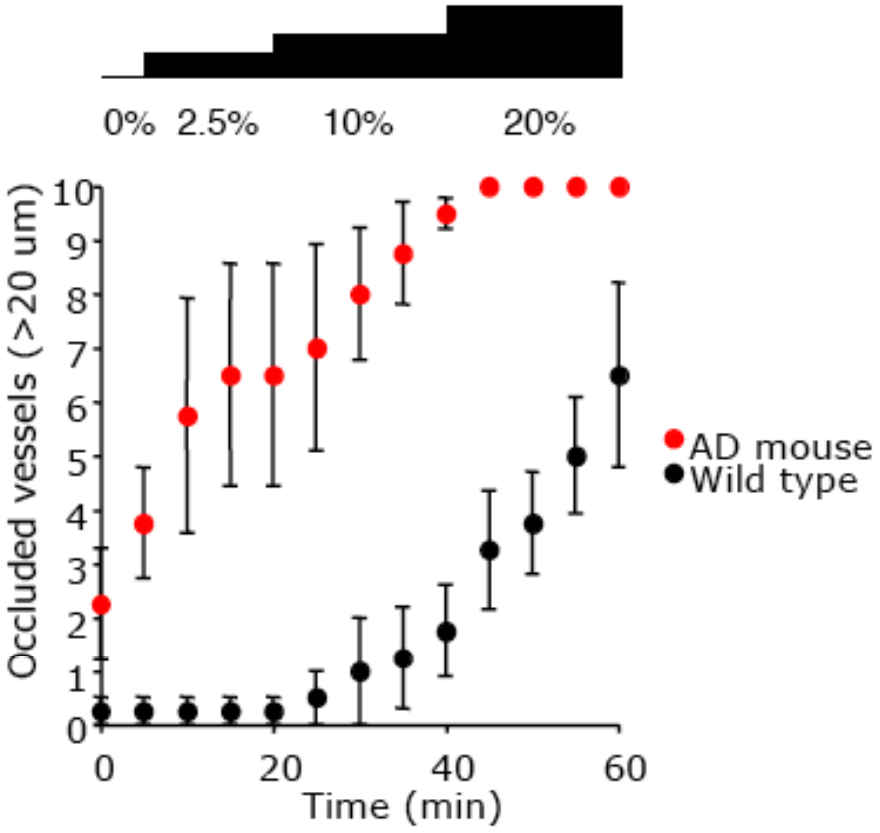

Figure 33. Time to brain blood vessel occlusion in AD and WT mice. Blood flow was observed in blood vessels of size >20 μm after topical application of ferric chloride at incremental doses of 2.5% (first blue dotted line at 5 min), 10% (second blue dotted line at 20 min), and 20% (third blue dotted line at 40 min). The number of occluded vessels was recorded in AD mice (red) and wild type littermates (black) over time and plotted. AD mice show occlusion earlier and with lower doses of ferric chloride.

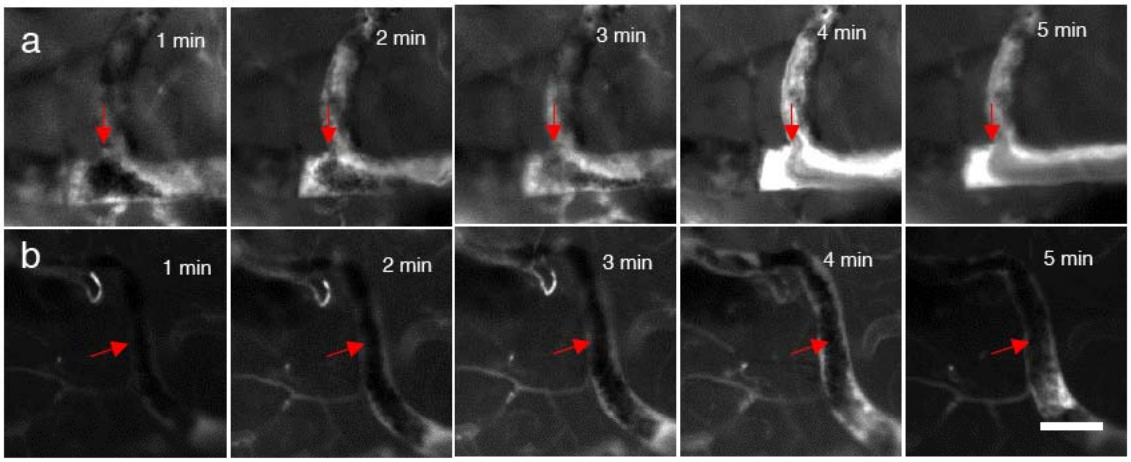

Figure 34. Altered thrombosis and fibrinolysis in AD mice. (a) Fluorescent labeled blood flow is interrupted with dark zones representing clot formation in cerebral arteries (arrows). Scale bar is 50 um. (b) Time series of clot dissolution after tPA treatment of a preformed clot in an AD mouse. (c) Time series of clot dissolution after tPA treatment of a preformed clot in a wild type mouse.

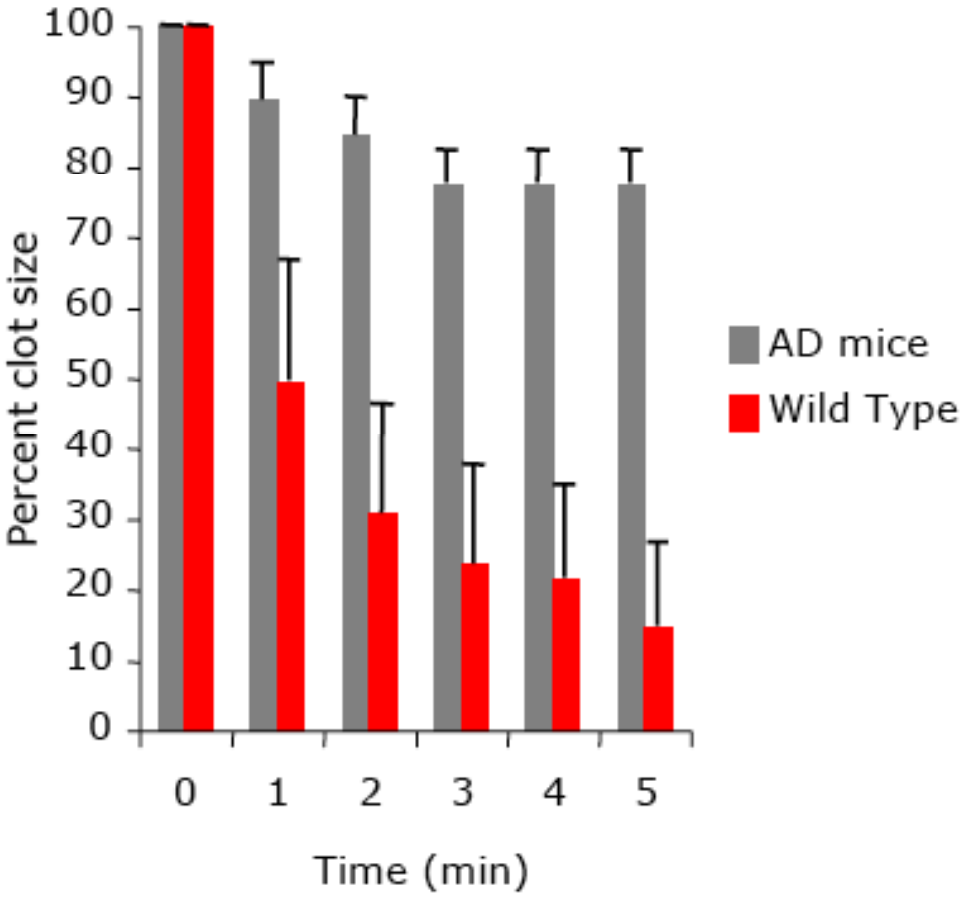

Figure 35. Altered thrombosis and fibrinolysis in AD mice. Clot size determinations over time post tPA treatment of preformed clots in AD and wild type mice. * $p<0.001$, AD mice compared to wild type.

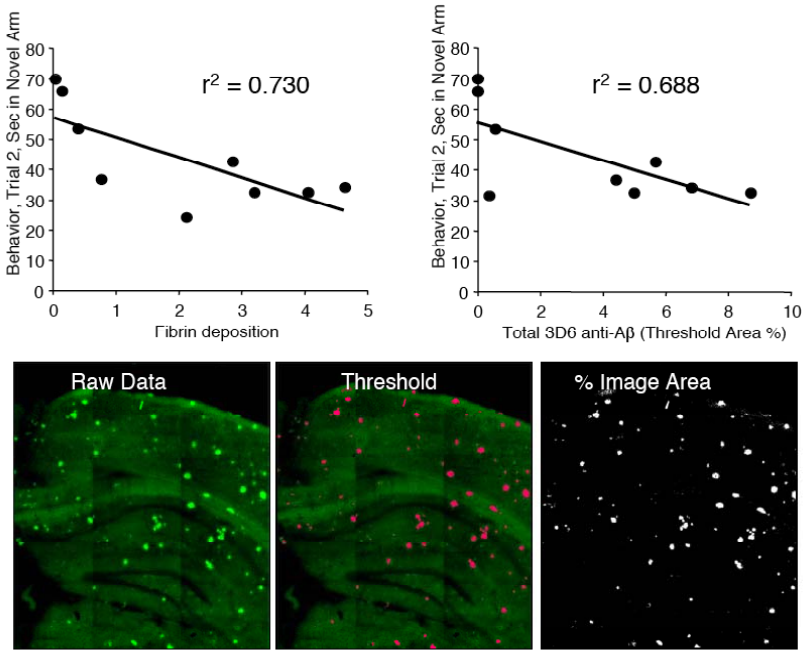

Figure 36: Correlation between behavior and biochemical analyses. Behavior was measured as the percentage of time each mouse spent in the novel arm during the first two minutes of the Y maze memory test. Diffuse Aβ and fibrin were measured using threshold area percentage analysis after immunostaining. Correlations between age, cognitive impairment, diffuse Aβ, and fibrin deposition were made. The strongest correlations to behavioral pathology are found with (a) diffuse Aβ (r^2 = -0.68) and (b) fibrin deposition (r^2 = -0.73), both of which are related to vascular damage. Correlation of histological pathology and behavior did not differ greatly between the hippocampus and cortex in any case. There was low correlation (r^2 = -0.41) between behavioral pathology and age (not shown).

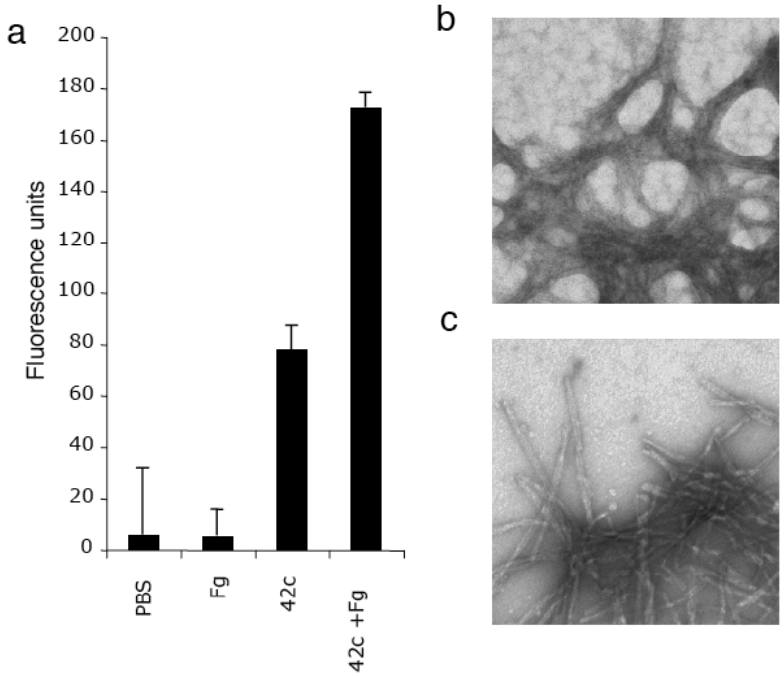

Figure 37. Fibrinogen may influence Aβ aggregation. We incubated pure fibrinogen with pure Aβ42 overnight and mixed with Thioflavin T to examine β-sheet content of the mixture. (a) Though fibrinogen does not form fibrils alone, when mixed with Aβ the observed fibrillization reflected in fluorescence units is doubled. Transmission electron microscopy also reveals denser, more compact fibrils formed when Aβ and fibrinogen are mixed (b) than Aβ alone (c).

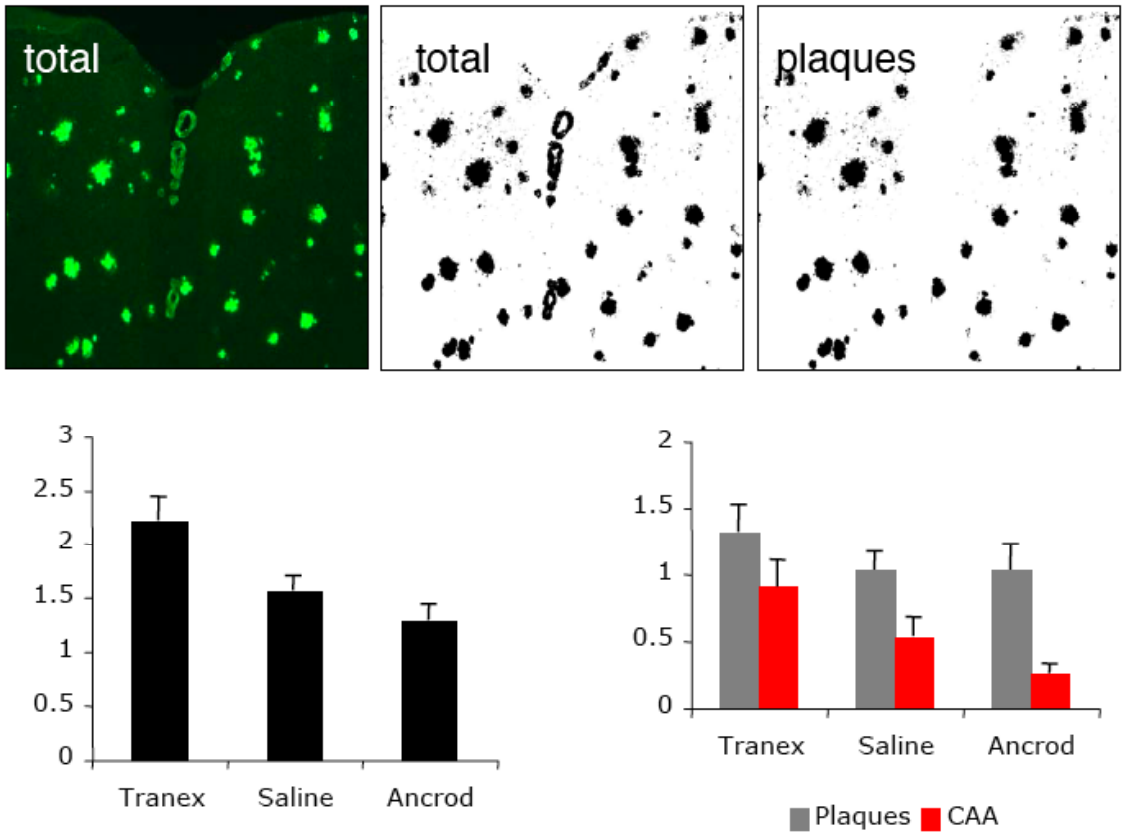

Figure 38. Fibrin levels modulate CAA but not plaques. AD mice were defibrinogenated with ancrod, plasmin inhibited with tranexamic acid, or treated with saline and analyzed for distribution of amyloidosis in the hippocampus and cortex after four weeks of treatment. While all groups showed similar area density of plaques, ancrod-treated showed less CAA and plasmin-inhibited mice showed increased CAA using 4 images from 4 mice in each group. Bars represent mean +/- SEM * $p<0.05$ Students t-test comparing CAA from saline to ancrod and from saline to tranex.

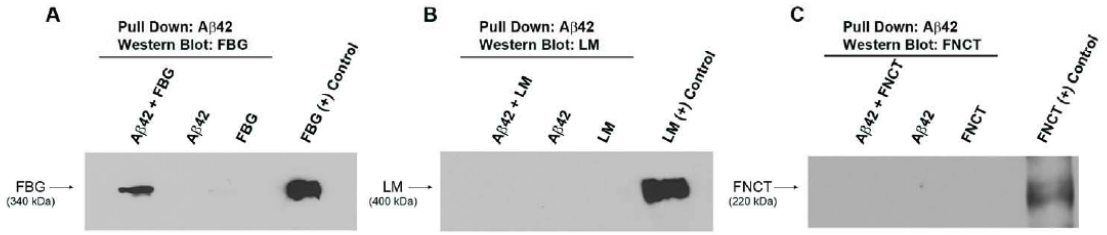

Figure 39. Interaction of Aβ42 and fibrinogen *in vitro*. Biotinylated Aβ42 (Aβ42) was incubated with (A) fibrinogen (FBG), (B) laminin (LM), or (C) fibronectin (FNCT) as described, and pull down assays were carried out using Streptavidin-sepharose. (A) A Western blot was performed in non-reducing conditions using an antibody against fibrinogen. (B,C) In the case of laminin and fibronectin, gels were run in reducing conditions since the reduced forms of both proteins were more easily detected than the non-reduced forms (900 kDa for laminin, 440 kDa for fibronectin). 500 ng of FBG, LM, and FNCT were loaded on each corresponding gel as a positive control ((+) control).

CHAPTER 5: DISCUSSION

5.1 Neurovascular dysfunction in the AβPP transgenic mouse

The Tg2576 mouse has deficits in vascular integrity shown by blood-brain barrier damage (Ujiie et al., 2003; Kumar-Singh et al., 2005), decreased blood flow and increased susceptibility to ischemia (Zhang et al., 1997). In addition, vascular density is reduced in these animals as measured by glucose transporter type 1 GLUT-1 beginning at 12 months (Kouznetsova et al., 2006). Subsequently, it was shown that the blood-brain barrier compromise is rescued in the Tg2576 mouse with passive Aβ1-40 peptide immunization (Dickstein et al., 2006). The present study explores the contribution of fibrin(ogen) to neurovascular damage as part of the amyloid-β disease process and broadens the knowledge of vascular deficits to other AβPP-transgenic mouse models.

The Aβ peptide causes endothelial and smooth muscle cell dysfunction and cell death *in vitro* thus disrupting two major components of the blood-brain barrier (Haass et al., 1992; Thomas et al., 1996; Blanc et al., 1997; Hase et al., 1997; Sutton et al., 1997; Thomas et al., 1997; Melchor and Van Nostrand, 2000; Zlokovic, 2008). Therefore the initial insult to the microvasculature likely arises from increased Aβ levels. Cerebral amyloid angiopathy (CAA) is a hallmark of Alzheimer's disease and it is be important to consider the specific vascular amyloid burden in these mice.

However, the neurovascular damage in the plasminogen-deficient mouse suggests decreased fibrinolysis might promote the damage to blood vessels and

subsequent fibrin deposition. Because neuroinflammation was low in the plasminogen-deficient mouse, fibrin(ogen) deposition alone is not sufficient for observed pathology and Aβ is necessary to initiate the inflammatory process.

5.2 Alzheimer's Disease and the tPA/plasmin fibrinolytic system

TPA/plasmin fibrinolytic activity is regulated by serine protease inhibitors (serpins) such as plasminogen activator inhibitor-1 (PAI-1). In mice, PAI-1 is up-regulated in the presence of Aβ, which agrees with the clinically observed elevation of PAI-1 levels in the cerebrospinal fluid of AD patients (Sutton et al., 1994; Sutton et al., 1997; Melchor et al., 2003), and decreased plasmin activity in the AD brain (Ledesma et al., 2000).

The tPA/plasmin system is down-regulated in AD, in accord with reductions in other naturally occuring Aβ-degrading proteases (Ledesma et al., 2000; Selkoe, 2001; Leissring et al., 2003). The direct consequences of this general lack of protease activity might be the diminished clearance of Aβ peptide (Selkoe, 2001). The present study proposes that decreases in clearance of fibrin(ogen) can also contribute to the progression of Aβ pathology.

It is important to consider the effects of the loss of a single copy of the plasminogen gene. Heterozygosity decreases the fibrinolytic activity to 55% of normal in pooled plasma obtained from wild type mice according to clot lysis assays (Ploplis et al., 1995). We did not attempt to generate TgCRND8;plg-/- mice since plg-/- mice develop several thrombotic complications that could complicate the CNS pathology. Additionally plg-/- mice exhibit early mortality,

which would preclude comparison at later ages. TgCRND8;fib-/- mice are also difficult to generate due to breeding restrictions and limited survival (Degen et al., 2001).

These genetic constraints are addressed with the experiments using pharmacologic reduction of fibrinolysis and fibrinogen depletion by ancrod. The convergence of the results of both genetic and pharmacologic approaches forms solid evidence that manipulation of fibrin levels in Alzheimer's mouse models modulates inflammation and vascular integrity.

5.3 Fibrinogen and inflammation

Fibrinogen has several active roles in normal and abnormal physiology including cellular responses in clotting and inflammation that are mediated by fibrinogen receptors. Of interest in the present study are the integrin receptors expressed on leukocytes, monocytes, and macrophage/microglia. Three notable inflammatory integrins are α5β1, αvβ3, and αMβ2 (Mac-1 or CD11b/CD18) (Ugarova and Yakubenko, 2001). Binding of the fibrinogen dimer to microglial αMβ2/CD11b elicits activation of the NF-κB pathway causing increased expression of cytokine genes (Perez et al., 1999; Flick et al., 2004).

The involvement of inflammation has been studied in Alzheimer's disease. Clinical and epidemiological data concerning anti-inflammatory medications are provocative and require further studies to determine their potential in controlling disease progression (McGeer et al., 1996; Koistinaho and Koistinaho, 2005). The present study suggests that fibrin may be an upstream effector of

neuroinflammation and the damaging effect of decreased fibrinolysis on the neurovasculature is intriguing. Fibrin-induced microgliosis could be toxic to endothelial cells as microglia have been shown to increase cell death in primary endothelial cells after oxygen-glucose deprivation, which can be reduced by inhibiting microglial activation with minocycline (Yenari et al., 2006).

How inflammation may contribute to neurodegeneration in AD is still largely unknown. As blood vessels from AD brains are directly toxic to neurons (Grammas et al., 2000), we asked if the compromised neurovasculature and inflammation in these experimental mice could promote neurodegeneration. Although we did not observe neuronal death, studies involving older TgCRND8 mice with enhanced inflammation and vascular damage may reveal detectable levels of neurodegeneration.

As fibrinogen is polymerized after activation by thrombin, it is important to note that thrombin injection into the rat cortex induces microgliosis (Lee da et al., 2006). Additionally, in human patients with advanced AD, plasma prothrombin can be found in the extravascular space (Zipser et al., 2006), which provides an environment where fibrin is likely to deposit.

Once polymerized in the parenchyma, fibrin is covalently cross-linked by tissue-resident transglutaminase factor XIII (Furie and Furie, 1988). Cross-linked fibrin is stabilized by covalent bonds between gamma chains. Because the capturing antibody used in the ELISA recognizes the gamma chain specifically (Jirouskova et al., 2001), crosslinked fibrin would not be detected and the ELISA results likely underestimate the total fibrin deposition. However, the

immunofluorescence uses a polyclonal antibody, which detects all forms of fibrin(ogen). Similarly, Triton-soluble Aβ levels likely underestimate the total Aβ burden. However, Aβ levels measured by ELISA correlate with plaque burdens observed with immunofluorescence. Both soluble and insoluble fibrin activates microglia via the CD11b receptor and contributes to the observed inflammation in AβPP transgenic mice and AD patients.

This study begins to outline a role for fibrin in the neuroinflammation seen in Alzheimer's disease. These results also indicate a role for fibrin deposition in accelerating the neurovascular damage observed in these mouse models and perhaps in reducing the brain's reparative capacity. Extravascular fibrin(ogen) functioning as a restraint to mechanisms of tissue repair has been shown in the peripheral nervous system (Akassoglou et al., 2002). The present study also demonstrates this effect on the progression of disease in mouse models of Alzheimer's disease. Therefore, fibrin and the mechanisms involved in its clearance may present novel therapeutic targets in slowing the progression of Alzheimer's disease.

5.4 Fibrin clot structure is altered

Fibrin, the major protein component of a blood clot, promotes inflammation and vascular damage in AD mouse models. Fibrin accumulates in AD brains due to influx through a damaged blood-brain barrier (Paul et al., 2007) and inhibition of tissue plasminogen activator (tPA)/plasmin fibrinolytic activity (Melchor et al., 2003). Normally, fibrinogen is excluded from the brain and circulates in the blood

at micromolar concentrations where Aβ peptides are nearly undetectable. This compartmentalization is lost in the AD brain, and damaged vasculature causes leakage of fibrinogen into the brain (Fiala et al., 2002; Finehout et al., 2007). As AD pathology progresses, concentrations of Aβ increase dramatically, which can affect the structure of fibrin (Merkle et al., 1996). We sought to study the consequences of the co-existence of Aβ peptide and fibrinogen on the formation and dissolution of fibrin.

Protein misfolding and aggregation is a hallmark of several neurodegenerative disorders. The common mechanism involves a misfolded protein serving as a template to influence the three-dimensional structure of other homologous proteins. Amyloid-induced alterations in clot structure represent an example of a misfolded protein disrupting the physical structure and mechanical properties of a different protein. Propagation of a metastable conformation from one protein to another homologous protein is defined as conformational autocatalysis. Here we introduce “conformational heterocatalysis” as the transmission of an abnormal structure from one protein to a different protein. The influence of misfolded Aβ on fibrin clots provides a simple model of this phenomenon.

Persistent fibrin in the brain could be contributing to cognitive decline intravascularly or extravascularly. The intravascular effects could be complicated as the balance between hemorrhage and thrombosis is delicate, and the abnormalities in the clots formed in the presence of Aβ could promote the occurrence of thrombosis or hemorrhage. Therefore, the physical and

mechanical properties of clots formed in the presence of Aβ are under investigation. Fibrin clots are viscoelastic materials, meaning they possess the physical and mechanical characteristics of viscous fluids and elastic materials simultaneously (Weisel, 2007). Determining the contribution of the viscous and elastic component to the material can lend some insight as to how the clot behaves when the stress of circulating blood is applied. Although the slowed fibrinolysis and heterogeneity of the Aβ-influenced clots could promote thrombosis, the weakened network dynamics could promote hemorrhage. The abnormalities may render the clots unstable and prone to bleeding when formed along the walls of blood vessels laden with amyloid (Van Broeckhoven et al., 1990; Winkler et al., 2002).

Mature solutions of Aβ42 promote formation of protease-resistant clumps of fibrin. This difference in clot structure could lead to more persistent fibrin aggregates in AD brains and could explain the tendency for plaques to accumulate fibrin and maintain high levels of inflammation in the brain parenchyma (Paul et al., 2007). Removal of fibrin with ancrod can reduce inflammation (Paul et al., 2007) and may improve learning and memory. It will also be important to determine if there are intravascular effects of Aβ42, resulting in an imbalance in hemostasis. Excess brain-derived Aβ is actively drained through the blood vessels (Shibata et al., 2000). As fibrillogenic mutations of Aβ40 slow its elimination from the brain through vascular drainage pathways (Monro et al., 2002), Aβ accumulates in and around blood vessels. These sites may be locally enriched for Aβ oligomers, which can lead to local thrombosis. To

support this, we found that amyloid-laden blood vessels in the brains of perfused AD mice contained fibrin.

In contrast to normal aging individuals, AD patients have elevated levels of fibrin degradation products in the blood, suggesting fibrin is formed and degraded more than under normal conditions (Gupta et al., 2005). Indeed, markers of thrombosis are independent predictors of dementia in the elderly (Barber et al., 2004), and cardiovascular disease is associated with more rapid cognitive decline in AD patients (Mielke et al., 2007). Also, fibrin clotting may slowly remove Aβ42 from the circulation as it is incorporated into clots (Matsubara et al., 2002), which is consistent with decreasing levels of plasma Aβ42 during progression of AD (Mayeux et al., 2003). It should be noted that thrombosis can produce areas of ischemia, which has been shown to induce tauopathy (Wen et al., 2004b; Wen et al., 2004a) and increase expression of β-amyloid cleaving enzyme, leading to production of more Aβ (Zhang et al., 2007) and therefore amplifying AD pathology.

However, the effects of amyloid deposits in the cerebral vasculature are not limited to thrombosis as amyloid-laden blood vessels are also at risk for hemorrhage (Van Broeckhoven et al., 1990; Winkler et al., 2002). Therefore, how fibrin behaves in circulation in the AD brain is likely multifaceted and the abnormalities in the clots formed in the presence of Aβ could predispose the AD brain to hemorrhagic or thrombotic events. The clots formed along the walls of blood vessels laden with amyloid are less stiff, which may account for the hemorrhagic events. Contrarily, the slowed fibrinolysis and heterogeneity may

produce thromboembolism. Alterations in cerebral blood flow have long been implicated in AD, this work provides a foundation for the biochemical processes underlying this disruption and therapeutic targets involved.

The delicate balance of free flowing blood to perfuse healthy tissue and clotted blood to stop bleeding in damaged tissue relies on many factors. The cerebral vasculature in mice transgenic for human AβPP is predisposed to both thrombosis and hemorrhage. These results are supported by the ability of Aβ to deform fibrin clots. However, there are several factors which could also explain defects both thrombosis and hemostasis. Blood vessels in AD mice hyperreactive and hyperconstrictive leading to reduced cerebral blood flow. Aβ is toxic to smooth muscle cells, which may render a vessel prone to rupture with even the slightest force.

5.5 Variable forms of Aβ and cerebral blood flow

Several characteristics of AβPP and Aβ peptide suggest it may be involved in blood flow and hemostasis (Hardy, 2007). The AßPP protein, is a type I integral membrane glycoprotein encoded by a gene on chromosome 21 (Kang et al., 1987; Tanzi et al., 1987). Full-length AβPP is translated from three alternatively spliced mRNA isoforms. The normal physiological function of AβPP protein is largely unknown although two of the three isoforms contain an insert, which is homologous to Kunitz-type protease inhibitors (KPI) (Van Nostrand et al., 1989), which may be relevant.

The 39-43 amino-acid long peptide fragments of AβPP are generated through several proteolytic cleavage pathways (Haass et al., 1992). Therefore, Aβ can exist in several different forms, the relative concentration of which changes depending on the stage of the disease (Wang et al., 1999). Some of the peptide fragments do not spontaneously form amyloid fibrils. But the amyloidogenic pathway involves two critical proteases. The β-site AβPP cleaving enzyme (BACE-1) cleaves Aβ at the amino-terminus of Aβ, while the presenilin protein complex is necessary for carboxy-terminal cleavage (Vassar et al., 1999; Kimberly et al., 2003).

Fragments of varying length and location within the Aβ peptide may be responsible for interaction with fibrinogen, ApoE (Aβ12-28) (Strittmatter et al., 1993), and another hemostasis-relevant molecules, heparin (Aβ12-17) (Brunden et al., 1993). Mutant forms of the Aβ peptides that are present in familial forms of AD which have dramatic aberrations in hemostasis including Gln22-Aβ(1-40)-Dutch (Levy et al., 1990), Asn23-Aβ(1-40)-Iowa (Grabowski et al., 2001), Lys22-Aβ(1-40)-Italian (Miravalle et al., 2000), and Gly22-Aβ(1-40)-Arctic (Nilsberth et al., 2001). These mutations often alter fibril formation kinetics and cause disease with earlier onset AD and vascular damage (Meinhardt et al., 2007).

5.6 Apo E

Apo E is a lipid carrying protein synthesized primarily by the liver and circulates in the blood. This protein is also expressed in the brain (Lefranc et al., 1996; Lindh et al., 1997; Skoog et al., 1997), and differences in ApoE genotype are the

strongest genetic link to sporadic forms of AD (Corder et al., 1993). Given the effects of Aβ on clot structure, we examined whether the various alleles of ApoE could influence the fibrin network organization in the presence of Aβ. ApoE2, ApoE3, and ApoE4 had similar effects when added to pure fibrin clots. Alone, each ApoE isoform increased the turbidity of pure fibrin clots, but had minimal effects on clot structure. However, when added in combination with Aβ42, clot structures showed isoform-specific differences. Aggregate formation was comparable between Aβ42-influenced clots formed with or without ApoE4 and the clots showed similar plasmin lysis where aggregates detached from the lysis front and were difficult to degrade. However, both ApoE2 and ApoE3 showed reduced CFA formation in the presence of Aβ.

Although the molecular differences are known, little is known about how these ApoE isoforms interact with other proteins to affect AD in the presence of Aβ. The ApoE molecule contains two distinct domains: the amino-terminal 22 kD receptor-binding region and the carboxy-terminal 10 kD lipid-binding region. The 22 kD amino-terminal fragment contains the allelic differences, and thrombin actively cleaves ApoE to release the 22 kD regions. Protein stability may play a role as the 22 kD region of ApoE4 fragment is less stable than the E2 and E3 forms (Morrow et al., 2002). It could be that this instability accounts for the inability of Apo E4 to normalize clot structure.

AD epidemiology suggests the ApoE2 is protective, while ApoE3 has no effect, and the less common ApoE4 has a gene-dosage effect to increase the risk of developing the disease earlier. In AD, ApoE4 affects amyloid deposition in

blood vessels as cerebral amyloid angiopathy (CAA) increases in frequency and severity with the E4 allele (Premkumar et al., 1996). ApoE4 has multiple neuropathological associations including impaired glucose metabolism (Small et al., 1995), head trauma severity (Teasdale et al., 1997; Friedman et al., 1999; Crawford et al., 2002), and dementia with stroke (Slooter et al., 1997). ApoE4 is known to bind Aβ and, by an unknown mechanism, promote deposition of fibrillar Aβ plaques in blood vessels (Holtzman et al., 2000; Fryer et al., 2005).

5.7 Plasmin cleaves fibrin and Aβ

Although deficiency in plasminogen alone is not enough to precipitate a defect in cerebral vasculature, plg-deficient mice crossed to hypercholesterolemic ApoE-deficient mice show aggravated blood vessel pathology and fibrin deposition in atherosclerotic plaques (Xiao et al., 1997). These atherosclerotic plaques are more prevalent and exaggerated over mutants bearing only the ApoE deficiency, suggesting that intact fibrinolysis is necessary to protect against vascular damage.

The senile plaques are thought to accumulate in the brains of AD patients because of an overproduction of Aβ and lack of its clearance. Aβ can be cleared through the blood vessels or degraded by proteolytic enzymes (Selkoe, 2001). Neprilysin is involved in the clearance of Aβ as treatment with inhibitors of the enzyme leads to reduced Aβ degradation (Iwata et al., 2000). Complementing this pharmacologic approach with targeted genetics, mice deficient for another implicated Aβ clearance factor, endothelin converting enzyme, accumulated

more Aβ than control mice (Eckman et al., 2003). Insulin degrading enzyme (IDE) also plays a role in this clearance (Vekrellis et al., 2000) and mice deficient for IDE likewise show more Aβ pathology (Miller et al., 2003). Conversely, mice overexpressing neprilysin or IDE show decreased Aβ levels (Leissring et al., 2003).

Although primarily known for its role in degradation of fibrin, the enzyme plasmin is also partly responsible for clearance of Aβ in the AD brain (Van Nostrand and Porter, 1999; Tucker et al., 2000b; Tucker et al., 2000a). Although Aβ increases tPA expression in neuronal cultures (Tucker et al., 2000b) and aggregated Aβ stimulates tPA activity (Kingston et al., 1995), the plasmin system is not effective at Aβ clearance in AD (Ledesma et al., 2000) because PAI-1 levels are elevated in AD brains (Sutton et al., 1994). These interactions are further complicated by another plasminogen activator, the urokinase plasminogen activator (uPA), which inhibits Aβ neurotoxicity (Tucker et al., 2002), and Aβ can stimulate the uPA and uPA receptor in cerebrovascular smooth muscle cells (Davis et al., 2003).

Plasminogen activators are serine proteases primarily known for their role to cleave plasminogen producing the active form plasmin, a broad-spectrum protease capable of degrading a variety of proteins and protein aggregates (Vassalli et al., 1991). The two major plasminogen activators are tissue-type plasminogen activator (tPA) and urokinase-type plasminogen activator (uPA). Each one compensates for the other as mice deficient for either one of these activators alone are viable and fertile with normal life spans (Carmeliet et al.,

1994), while elimination of both mechanisms results in a phenotype similar to plasminogen deficient animals marked by profound wasting, high mortality, spontaneous ulceration, rectal prolapse, and severe thrombosis (Bugge et al., 1995; Ploplis et al., 1995).

The brain expresses tPA in the hippocampus, amygdala, hypothalamus, and cerebellum. The role of this molecule is complex as there is evidence of necessary and deleterious functions (Carroll et al., 1993; Sappino et al., 1993; Seeds et al., 1999; Pawlak and Strickland, 2002; Salles and Strickland, 2002; Seeds et al., 2003; Yepes et al., 2003). As tPA expression in the hippocampus is critical for normal learning and memory (Qian et al., 1993). There is a link between tPA and neurodegeneration (Tsirka et al., 1995; Tsirka et al., 1996; Chen and Strickland, 1997), and dysfunction in tPA/plasmin fibrinolysis may contribute to this link in AD.

The tPA/plasmin system is tightly regulated by serine protease inhibitors (serpins). The protein plasminogen activator inhibitor-1 (PAI-1) and neuroserpin block tPA activity while plasmin is blocked by alpha-2 antiplasmin. Serpins like PAI-1 first form a reversible Michaelis complex which progresses to an irreversible inhibitory acyl-enzyme complex and cleavage of the reactive center loop of the serpin resulting in structural deformation of the protease (Lawrence et al., 1995; Ye et al., 2001). Fine tuning of plasmin's proteolytic activity is important in the delicate balance of hemostasis and thrombosis and it may be more important to determine if there are intravascular effects of Aβ42 resulting in an imbalance in this system (Breteler et al., 1998).

5.8 Toward a therapy for AD

The amyloid hypothesis does not explain the poor correlation between the number of Aβ plaques and the degree of cognitive impairment (Lue et al., 1999). However, these measures are often complicated by the classification of plaques and Aβ species present in the AD brain (Dickson, 1997). Plaques are quite variable in size and morphology and range from diffuse to fibrillar. Fibrillar plaques contain Aβ rich in β-sheet structure, which can be detected with dyes specific for this structure such as Congo Red. Fibrillar plaques are also more often described as "senile plaques" and are surrounded by inflammation and dystrophic neurites (Wilcock et al., 2006). This synaptic deformation likely contributes to the cognitive decline but other forms of Aβ have been shown to affect normal synapse function. Aβ Oligomers are soluble but can induce synaptic dysfunction (Haass and Selkoe, 2007). It could be that oligomers diffuse from plaques and damage in remote regions of the brain.

As AD is a neurodegenerative disorder, it is important to determine the mechanism behind cell death. Aβ is generally regarded as neurotoxic in its fibrillar amyloid form (Pike et al., 1993). The Aβ peptide is normally soluble but aggregates after the accumulation of β-pleated sheets in the peptide's secondary structure. Additionally, though the larger 10 nm fibrils are essentially confined to the plaques, smaller forms of aggregation such as the amyloid-β derived diffusible ligands (ADDLs) and other protofibrillar species are now known to be toxic to neurons as well (Lambert et al., 1998; Walsh et al., 2002; Gong et al., 2003).

The strongest pathological correlation to degree of dementia is synaptic changes associated with neurofibrillary tangles (NFTs) (Ballatore et al., 2007). However, unlike Aβ, NFTs are not specific to Alzheimer's disease and can be found in Frontotemporal dementia and Pick's dementia. Given that tangles are found in other dementias, it may be that Aβ and other processes contribute to the formation of NFTs, which are necessary to cause recognizable dementia (Hardy et al., 1998). Consistent with this, Aβ levels were found to be elevated before significant NFTs were detected (Naslund et al., 2000).

It should be noted that thrombosis can produce areas of ischemia, which has been shown to induce tauopathy (Wen et al., 2004b; Wen et al., 2004a) and increase expression of β-amyloid cleaving enzyme, leading to production of more Aβ (Zhang et al., 2007) and therefore amplifying AD pathology.

5.9 Implications and future research on Aβ and fibrin

Aβ associates with fibrinogen in vivo and in vitro, which alters the structure of the fibrin clot that is formed. Since this interaction may have implications for AD pathogenesis, it is critical to obtain a better understanding of the biochemical details. It will be important to which domains of fibrinogen are involved in this interaction by analyzing the binding of Aβ to fibrin degradation products and also regions of the Aβ peptide bind fibrinogen.

It will also be important to understand the basic aspects of the interaction, including binding strength and kinetics by SPR, immobilizing Aβ (Shuvaev and Siest, 1996) and fibrinogen (Geer et al., 2007).

Given the distribution of fibrin deposition in the mouse brain, it will be important to quantitatively asses the involvement of the Aβ/fibrinogen interaction as well as the distribution and extent of the interaction in different regions of human AD post-mortem brain tissue using rigorous morphometric imaging and analysis. This would provide a detailed explanation of where and how these proteins interact and may provide insight into how this interaction might be inhibited.

The formation of degradation-resistant fibrin clots in vitro in the presence of Aβ is specifically modified by the isoform of ApoE. ApoE2 and ApoE3 normalize the clot structure to resemble clot formation in the absence of Aβ, whereas ApoE4 has no effect.

Interestingly, when AD mice are deficient for the murine ApoE gene Aβ deposition is dramatically reduced and the disease onset is delayed. These results suggest that ApoE has an important role in Aβ pathology (reviewed in (Bales et al., 2002; Brendza et al., 2002)). Also, when replacing the mouse ApoE gene with the human gene, onset is delayed. (Holtzman et al., 2000; Brendza et al., 2002; Fagan et al., 2002; Fryer et al., 2005). The murine ApoE gene only differs by 30% to human ApoE gene, but *in vivo* they have different functional properties. Thus targeted replacement mice have been generated to study the human isoforms without the complication of the mouse ApoE genotype. Therefore, AD mice such as the TgCRND8 should be crossed with human ApoE2 (Sullivan et al., 1998), ApoE3 (Sullivan et al., 1997), and ApoE4 (Knouff et al., 1999) targeted replacement mice. Mice generated from this cross would

allow examination of the influence of each individual human ApoE isoform on the Aβ-fibrinogen interaction *in vivo*. The results from these experiments may shed light on how the interaction between Aβ and fibrinogen along with the ApoE genotype influences the susceptibility and severity of AD.

The most important therapeutic outcome in dementia is the improvement of cognition. It is possible that in the presence of Aβ, malformed fibrin clots result in blocked blood flow or hemorrhage, both of which would contribute to the cognitive decline. Given the ability of Apo E to modify this pathology, this work could form the basis for interventions targeting this abnormality.

References

Adams RA, Passino M, Sachs BD, Nuriel T, Akassoglou K (2004) Fibrin mechanisms and functions in nervous system pathology. Mol Interv 4:163-176.

Akassoglou K, Kombrinck KW, Degen JL, Strickland S (2000) Tissue plasminogen activator-mediated fibrinolysis protects against axonal degeneration and demyelination after sciatic nerve injury. J Cell Biol 149:1157-1166.

Akassoglou K, Yu WM, Akpinar P, Strickland S (2002) Fibrin inhibits peripheral nerve remyelination by regulating Schwann cell differentiation. Neuron 33:861-875.

Akiyama H, Barger S, Barnum S, Bradt B, Bauer J, Cole GM, Cooper NR, Eikelenboom P, Emmerling M, Fiebich BL, Finch CE, Frautschy S, Griffin WS, Hampel H, Hull M, Landreth G, Lue L, Mrak R, Mackenzie IR, McGeer PL, O'Banion MK, Pachter J, Pasinetti G, Plata-Salaman C, Rogers J, Rydel R, Shen Y, Streit W, Strohmeyer R, Tooyoma I, Van Muiswinkel FL, Veerhuis R, Walker D, Webster S, Wegrzyniak B, Wenk G, Wyss-Coray T (2000) Inflammation and Alzheimer's disease. Neurobiol Aging 21:383-421.

Aleshkov S, Abraham CR, Zannis VI (1997) Interaction of nascent ApoE2, ApoE3, and ApoE4 isoforms expressed in mammalian cells with amyloid peptide beta (1-40). Relevance to Alzheimer's disease. Biochemistry 36:10571-10580.

Altamura C, Squitti R, Pasqualetti P, Tibuzzi F, Silvestrini M, Ventriglia MC, Cassetta E, Rossini PM, Vernieri F (2007) What is the relationship among atherosclerosis markers, apolipoprotein E polymorphism and dementia? Eur J Neurol 14:679-682.

Baldwin HS, Shen HM, Yan HC, DeLisser HM, Chung A, Mickanin C, Trask T, Kirschbaum NE, Newman PJ, Albelda SM, et al. (1994) Platelet endothelial cell adhesion molecule-1 (PECAM-1/CD31): alternatively spliced, functionally distinct isoforms expressed during mammalian cardiovascular development. Development 120:2539-2553.

Bales KR, Dodart JC, DeMattos RB, Holtzman DM, Paul SM (2002) Apolipoprotein E, amyloid, and Alzheimer disease. Mol Interv 2:363-375, 339.

Ballatore C, Lee VM, Trojanowski JQ (2007) Tau-mediated neurodegeneration in Alzheimer's disease and related disorders. Nat Rev Neurosci 8:663-672.

Barber M, Tait RC, Scott J, Rumley A, Lowe GD, Stott DJ (2004) Dementia in subjects with atrial fibrillation: hemostatic function and the role of anticoagulation. J Thromb Haemost 2:1873-1878.

Bell WR, Shapiro SS, Martinez J, Nossel HL (1978) The effects of ancrod, the coagulating enzyme from the venom of Malayan pit viper (A. rhodostoma) on prothrombin and fibrinogen metabolism and fibrinopeptide A release in man. J Lab Clin Med 91:592-604.

Benchenane K, Berezowski V, Ali C, Fernandez-Monreal M, Lopez-Atalaya JP, Brillault J, Chuquet J, Nouvelot A, MacKenzie ET, Bu G, Cecchelli R, Touzani O, Vivien D (2005) Tissue-type plasminogen activator crosses the intact blood-brain barrier by low-density lipoprotein receptor-related protein-mediated transcytosis. Circulation 111:2241-2249.

Blanc EM, Toborek M, Mark RJ, Hennig B, Mattson MP (1997) Amyloid beta-peptide induces cell monolayer albumin permeability, impairs glucose transport, and induces apoptosis in vascular endothelial cells. J Neurochem 68:1870-1881.

Brendza RP, Bales KR, Paul SM, Holtzman DM (2002) Role of apoE/Abeta interactions in Alzheimer's disease: insights from transgenic mouse models. Mol Psychiatry 7:132-135.

Breteler MM (2000) Vascular involvement in cognitive decline and dementia. Epidemiologic evidence from the Rotterdam Study and the Rotterdam Scan Study. Ann N Y Acad Sci 903:457-465.

Breteler MM, Bots ML, Ott A, Hofman A (1998) Risk factors for vascular disease and dementia. Haemostasis 28:167-173.

Brun A, Englund E (1986) A white matter disorder in dementia of the Alzheimer type: a pathoanatomical study. Ann Neurol 19:253-262.

Brunden KR, Richter-Cook NJ, Chaturvedi N, Frederickson RC (1993) pH-dependent binding of synthetic beta-amyloid peptides to glycosaminoglycans. J Neurochem 61:2147-2154.

Bugge TH, Flick MJ, Daugherty CC, Degen JL (1995) Plasminogen deficiency causes severe thrombosis but is compatible with development and reproduction. Genes Dev 9:794-807.

Bugge TH, Kombrinck KW, Flick MJ, Daugherty CC, Danton MJ, Degen JL (1996) Loss of fibrinogen rescues mice from the pleiotropic effects of plasminogen deficiency. Cell 87:709-719.

Burkhart W, Smith GF, Su JL, Parikh I, LeVine H, 3rd (1992) Amino acid sequence determination of ancrod, the thrombin-like alpha-fibrinogenase from the venom of Akistrodon rhodostoma. FEBS Lett 297:297-301.

Busso N, Peclat V, Van Ness K, Kolodziesczyk E, Degen J, Bugge T, So A (1998) Exacerbation of antigen-induced arthritis in urokinase-deficient mice. J Clin Invest 102:41-50.

Carmeliet P, Schoonjans L, Kieckens L, Ream B, Degen J, Bronson R, De Vos R, van den Oord JJ, Collen D, Mulligan RC (1994) Physiological consequences of loss of plasminogen activator gene function in mice. Nature 368:419-424.

Carroll PM, Richards WG, Darrow AL, Wells JM, Strickland S (1993) Preimplantation mouse embryos express a cell surface receptor for tissue-plasminogen activator. Development 119:191-198.

Chalmers K, Wilcock GK, Love S (2003) APOE epsilon 4 influences the pathological phenotype of Alzheimer's disease by favouring cerebrovascular over parenchymal accumulation of A beta protein. Neuropathol Appl Neurobiol 29:231-238.

Chauhan VP, Chauhan A, Wegiel J (2001) Fibrillar amyloid beta-protein forms a membrane-like hydrophobic domain. Neuroreport 12:587-590.

Chen ZL, Strickland S (1997) Neuronal death in the hippocampus is promoted by plasmin-catalyzed degradation of laminin.PG - 917-25. Cell 91.

Chishti MA, Yang DS, Janus C, Phinney AL, Horne P, Pearson J, Strome R, Zuker N, Loukides J, French J, Turner S, Lozza G, Grilli M, Kunicki S, Morissette C, Paquette J, Gervais F, Bergeron C, Fraser PE, Carlson GA, George-Hyslop PS, Westaway D (2001) Early-onset amyloid deposition and cognitive deficits in transgenic mice expressing a double mutant form of amyloid precursor protein 695.PG. J Biol Chem 276.

Cleary JP, Walsh DM, Hofmeister JJ, Shankar GM, Kuskowski MA, Selkoe DJ, Ashe KH (2005) Natural oligomers of the amyloid-beta protein specifically disrupt cognitive function. Nat Neurosci 8:79-84.

Collet JP, Park D, Lesty C, Soria J, Soria C, Montalescot G, Weisel JW (2000) Influence of fibrin network conformation and fibrin fiber diameter on fibrinolysis speed: dynamic and structural approaches by confocal microscopy. Arterioscler Thromb Vasc Biol 20:1354-1361.

Corder EH, Saunders AM, Strittmatter WJ, Schmechel DE, Gaskell PC, Small GW, Roses AD, Haines JL, Pericak-Vance MA (1993) Gene dose of apolipoprotein E type 4 allele and the risk of Alzheimer's disease in late onset families. Science 261:921-923.

Corder EH, Saunders AM, Risch NJ, Strittmatter WJ, Schmechel DE, Gaskell PC, Jr., Rimmler JB, Locke PA, Conneally PM, Schmader KE, et al. (1994) Protective effect of apolipoprotein E type 2 allele for late onset Alzheimer disease. Nat Genet 7:180-184.

Crawford FC, Vanderploeg RD, Freeman MJ, Singh S, Waisman M, Michaels L, Abdullah L, Warden D, Lipsky R, Salazar A, Mullan MJ (2002) APOE genotype influences acquisition and recall following traumatic brain injury. Neurology 58:1115-1118.

Cummings JL, Cole G (2002) Alzheimer disease. JAMA 287:2335-2338.

Davis J, Wagner MR, Zhang W, Xu F, Van Nostrand WE (2003) Amyloid beta-protein stimulates the expression of urokinase-type plasminogen activator (uPA) and its receptor (uPAR) in human cerebrovascular smooth muscle cells. J Biol Chem 278:19054-19061.

de la Torre JC (2004) Is Alzheimer's disease a neurodegenerative or a vascular disorder? Data, dogma, and dialectics. Lancet Neurol 3:184-190.

Degen JL, Drew AF, Palumbo JS, Kombrinck KW, Bezerra JA, Danton MJ, Holmback K, Suh TT (2001) Genetic manipulation of fibrinogen and fibrinolysis in mice. Ann N Y Acad Sci 936:276-290.

DeMattos RB, Bales KR, Cummins DJ, Dodart JC, Paul SM, Holtzman DM (2001) Peripheral anti-A beta antibody alters CNS and plasma A beta clearance and decreases brain A beta burden in a mouse model of Alzheimer's disease. Proc Natl Acad Sci U S A 98:8850-8855.

Dickson DW (1997) The pathogenesis of senile plaques. J Neuropathol Exp Neurol 56:321-339.

Dickstein DL, Biron KE, Ujiie M, Pfeifer CG, Jeffries AR, Jefferies WA (2006) Abeta peptide immunization restores blood-brain barrier integrity in Alzheimer disease. Faseb J 20:426-433.

Dodart JC, Bales KR, Gannon KS, Greene SJ, DeMattos RB, Mathis C, DeLong CA, Wu S, Wu X, Holtzman DM, Paul SM (2002) Immunization reverses memory deficits without reducing brain Abeta burden in Alzheimer's disease model. Nat Neurosci 5:452-457.

Donahue JE, Johanson CE (2008) Apolipoprotein E, Amyloid-beta, and Blood-Brain Barrier Permeability in Alzheimer Disease. J Neuropathol Exp Neurol 67:261-270.

Doraiswamy PaX, GL (2006) Pharmacological strategies for the prevention of Alzheimer's disease. Expert Opin Pharmacother 7:1-10.

Dudal S, Krzywkowski P, Paquette J, Morissette C, Lacombe D, Tremblay P, Gervais F (2004) Inflammation occurs early during the Abeta deposition process in TgCRND8 mice. Neurobiol Aging 25:861-871.

Duff K, Eckman C, Zehr C, Yu X, Prada CM, Perez-tur J, Hutton M, Buee L, Harigaya Y, Yager D, Morgan D, Gordon MN, Holcomb L, Refolo L, Zenk B, Hardy J, Younkin S (1996) Increased amyloid-beta42(43) in brains of mice expressing mutant presenilin 1. Nature 383:710-713.

Eckman EA, Watson M, Marlow L, Sambamurti K, Eckman CB (2003) Alzheimer's disease beta-amyloid peptide is increased in mice deficient in endothelin-converting enzyme. J Biol Chem 278:2081-2084.

Ellis RJ, Olichney JM, Thal LJ, Mirra SS, Morris JC, Beekly D, Heyman A (1996) Cerebral amyloid angiopathy in the brains of patients with Alzheimer's disease: the CERAD experience, Part XV. Neurology 46:1592-1596.

Fagan AM, Watson M, Parsadanian M, Bales KR, Paul SM, Holtzman DM (2002) Human and murine ApoE markedly alters A beta metabolism before and after plaque formation in a mouse model of Alzheimer's disease. Neurobiol Dis 9:305-318.

Farkas E, Luiten PG (2001) Cerebral microvascular pathology in aging and Alzheimer's disease. Prog Neurobiol 64:575-611.

Fiala M, Liu QN, Sayre J, Pop V, Brahmandam V, Graves MC, Vinters HV (2002) Cyclooxygenase-2-positive macrophages infiltrate the Alzheimer's disease brain and damage the blood-brain barrier. Eur J Clin Invest 32:360-371.

Finehout EJ, Franck Z, Choe LH, Relkin N, Lee KH (2007) Cerebrospinal fluid proteomic biomarkers for Alzheimer's disease. Ann Neurol 61:120-129.

Finkel SI (2003) Behavioral and psychologic symptoms of dementia. Clin Geriatr Med 19:799-824.

Fischer VW, Siddiqi A, Yusufaly Y (1990) Altered angioarchitecture in selected areas of brains with Alzheimer's disease. Acta Neuropathol (Berl) 79:672-679.

Flick MJ, Du X, Witte DP, Jirouskova M, Soloviev DA, Busuttil SJ, Plow EF, Degen JL (2004) Leukocyte engagement of fibrin(ogen) via the integrin receptor alphaMbeta2/Mac-1 is critical for host inflammatory response in vivo. J Clin Invest 113:1596-1606.

Friedman G, Froom P, Sazbon L, Grinblatt I, Shochina M, Tsenter J, Babaey S, Yehuda B, Groswasser Z (1999) Apolipoprotein E-epsilon4 genotype predicts a poor outcome in survivors of traumatic brain injury. Neurology 52:244-248.

Fryer JD, Simmons K, Parsadanian M, Bales KR, Paul SM, Sullivan PM, Holtzman DM (2005) Human apolipoprotein E4 alters the amyloid-beta 40:42 ratio and promotes the formation of cerebral amyloid angiopathy in an amyloid precursor protein transgenic model. J Neurosci 25:2803-2810.

Furie B, Furie BC (1988) The molecular basis of blood coagulation. Cell 53:505-518.

Games D, Adams D, Alessandrini R, Barbour R, Berthelette P, Blackwell C, Carr T, Clemens J, Donaldson T, Gillespie F, et al. (1995) Alzheimer-type neuropathology in transgenic mice overexpressing V717F beta-amyloid precursor protein. Nature 373:523-527.

Geer CB, Tripathy A, Schoenfisch MH, Lord ST, Gorkun OV (2007) Role of 'B-b' knob-hole interactions in fibrin binding to adsorbed fibrinogen. J Thromb Haemost 5:2344-2351.

Glenner GG, Wong CW (1984) Alzheimer's disease: initial report of the purification and characterization of a novel cerebrovascular amyloid protein.PG - 885-90. Biochem Biophys Res Commun 120.

Gong Y, Chang L, Viola KL, Lacor PN, Lambert MP, Finch CE, Krafft GA, Klein WL (2003) Alzheimer's disease-affected brain: presence of oligomeric A beta ligands (ADDLs) suggests a molecular basis for reversible memory loss. Proc Natl Acad Sci U S A 100:10417-10422.

Grabowski TJ, Cho HS, Vonsattel JP, Rebeck GW, Greenberg SM (2001) Novel amyloid precursor protein mutation in an Iowa family with dementia and severe cerebral amyloid angiopathy. Ann Neurol 49:697-705.

Grammas P, Reimann-Philipp U, Weigel PH (2000) Cerebrovasculature-mediated neuronal cell death. Ann N Y Acad Sci 903:55-60.

Gupta A, Watkins A, Thomas P, Majer R, Habubi N, Morris G, Pansari K (2005) Coagulation and inflammatory markers in Alzheimer's and vascular dementia. Int J Clin Pract 59:52-57.

Haass C, Selkoe DJ (2007) Soluble protein oligomers in neurodegeneration: lessons from the Alzheimer's amyloid beta-peptide. Nat Rev Mol Cell Biol 8:101-112.

Haass C, Koo EH, Mellon A, Hung AY, Selkoe DJ (1992) Targeting of cell-surface beta-amyloid precursor protein to lysosomes: alternative processing into amyloid-bearing fragments.PG - 500-3. Nature 357.

Hardy J (2007) Does Abeta 42 have a function related to blood homeostasis? Neurochem Res 32:833-835.

Hardy J, Selkoe DJ (2002) The amyloid hypothesis of Alzheimer's disease: progress and problems on the road to therapeutics. Science 297:353-356.

Hardy J, Duff K, Hardy KG, Perez-Tur J, Hutton M (1998) Genetic dissection of Alzheimer's disease and related dementias: amyloid and its relationship to tau. Nat Neurosci 1:355-358.

Hase M, Araki S, Hayashi H (1997) Fragments of amyloid beta induce apoptosis in vascular endothelial cells. Endothelium 5:221-229.

Hatters DM, Peters-Libeu CA, Weisgraber KH (2006) Apolipoprotein E structure: insights into function. Trends Biochem Sci 31:445-454.

Hebert LE, Scherr PA, Bienias JL, Bennett DA, Evans DA (2003) Alzheimer disease in the US population: prevalence estimates using the 2000 census. Arch Neurol 60:1119-1122.

Holtzman DM, Fagan AM (1998) Potential role of apoE in structural plasticity in the nervous system; implications for disorders of the central nervous system. Trends Cardiovasc Med 8:250-255.

Holtzman DM, Bales KR, Tenkova T, Fagan AM, Parsadanian M, Sartorius LJ, Mackey B, Olney J, McKeel D, Wozniak D, Paul SM (2000) Apolipoprotein E isoform-dependent amyloid deposition and neuritic degeneration in a mouse model of Alzheimer's disease. Proc Natl Acad Sci U S A 97:2892-2897.

Honig LS, Tang MX, Albert S, Costa R, Luchsinger J, Manly J, Stern Y, Mayeux R (2003) Stroke and the risk of Alzheimer disease. Arch Neurol 60:1707-1712.

Hoylaerts M, Rijken DC, Lijnen HR, Collen D (1982) Kinetics of the activation of plasminogen by human tissue plasminogen activator. Role of fibrin. J Biol Chem 257:2912-2919.

Hsiao K, Chapman P, Nilsen S, Eckman C, Harigaya Y, Younkin S, Yang F, Cole G (1996) Correlative memory deficits, Abeta elevation, and amyloid plaques in transgenic mice.PG - 99-102. Science 274.

Iadecola C, Gorelick PB (2003) Converging pathogenic mechanisms in vascular and neurodegenerative dementia. Stroke 34:335-337.

Iwata N, Tsubuki S, Takaki Y, Watanabe K, Sekiguchi M, Hosoki E, Kawashima-Morishima M, Lee HJ, Hama E, Sekine-Aizawa Y, Saido TC (2000) Identification of the major Abeta1-42-degrading catabolic pathway in brain parenchyma: suppression leads to biochemical and pathological deposition. Nat Med 6:143-150.

Janus C, Pearson J, McLaurin J, Mathews PM, Jiang Y, Schmidt SD, Chishti MA, Horne P, Heslin D, French J, Mount HT, Nixon RA, Mercken M, Bergeron C, Fraser PE, St George-Hyslop P, Westaway D (2000) A beta peptide immunization reduces behavioural impairment and plaques in a model of Alzheimer's disease. Nature 408:979-982.

Jarrett JT, Berger EP, Lansbury PT, Jr. (1993) The carboxy terminus of the beta amyloid protein is critical for the seeding of amyloid formation: implications for the pathogenesis of Alzheimer's disease. Biochemistry 32:4693-4697.

Jirouskova M, Smyth SS, Kudryk B, Coller BS (2001) A hamster antibody to the mouse fibrinogen gamma chain inhibits platelet-fibrinogen interactions and FXIIIa-mediated fibrin cross-linking, and facilitates thrombolysis. Thromb Haemost 86:1047-1056.

Kang J, Lemaire HG, Unterbeck A, Salbaum JM, Masters CL, Grzeschik KH, Multhaup G, Beyreuther K, Muller-Hill B (1987) The precursor of Alzheimer's disease amyloid A4 protein resembles a cell-surface receptor. Nature 325:733-736.

Kimberly WT, LaVoie MJ, Ostaszewski BL, Ye W, Wolfe MS, Selkoe DJ (2003) Gamma-secretase is a membrane protein complex comprised of presenilin, nicastrin, Aph-1, and Pen-2. Proc Natl Acad Sci U S A 100:6382-6387.

Kingston IB, Castro MJ, Anderson S (1995) In vitro stimulation of tissue-type plasminogen activator by Alzheimer amyloid beta-peptide analogues. Nat Med 1:138-142.

Klunk WE, Jacob RF, Mason RP (1999) Quantifying amyloid beta-peptide (Abeta) aggregation using the Congo red-Abeta (CR-abeta) spectrophotometric assay. Anal Biochem 266:66-76.

Knouff C, Hinsdale ME, Mezdour H, Altenburg MK, Watanabe M, Quarfordt SH, Sullivan PM, Maeda N (1999) Apo E structure determines VLDL clearance and atherosclerosis risk in mice. J Clin Invest 103:1579-1586.

Koistinaho M, Koistinaho J (2005) Interactions between Alzheimer's disease and cerebral ischemia--focus on inflammation. Brain Res Brain Res Rev 48:240-250.

Kouznetsova E, Klingner M, Sorger D, Sabri O, Grossmann U, Steinbach J, Scheunemann M, Schliebs R (2006) Developmental and amyloid plaque-related changes in cerebral cortical capillaries in transgenic Tg2576 Alzheimer mice. Int J Dev Neurosci 24:187-193.

Kowalska MA, Badellino K (1994) beta-Amyloid protein induces platelet aggregation and supports platelet adhesion. Biochem Biophys Res Commun 205:1829-1835.

Kranenburg O, Bouma B, Kroon-Batenburg LM, Reijerkerk A, Wu YP, Voest EE, Gebbink MF (2002) Tissue-type plasminogen activator is a multiligand cross-beta structure receptor. Curr Biol 12:1833-1839.

Kumar-Singh S, Pirici D, McGowan E, Serneels S, Ceuterick C, Hardy J, Duff K, Dickson D, Van Broeckhoven C (2005) Dense-core plaques in Tg2576 and PSAPP mouse models of Alzheimer's disease are centered on vessel walls. Am J Pathol 167:527-543.

LaDu MJ, Falduto MT, Manelli AM, Reardon CA, Getz GS, Frail DE (1994) Isoform-specific binding of apolipoprotein E to beta-amyloid. J Biol Chem 269:23403-23406.

Lambert MP, Barlow AK, Chromy BA, Edwards C, Freed R, Liosatos M, Morgan TE, Rozovsky I, Trommer B, Viola KL, Wals P, Zhang C, Finch CE, Krafft GA, Klein WL (1998) Diffusible, nonfibrillar ligands derived from Abeta1-42 are potent central nervous system neurotoxins. Proc Natl Acad Sci U S A 95:6448-6453.

Lawrence DA, Ginsburg D, Day DE, Berkenpas MB, Verhamme IM, Kvassman JO, Shore JD (1995) Serpin-protease complexes are trapped as stable acyl-enzyme intermediates. J Biol Chem 270:25309-25312.

Ledesma MD, Da Silva JS, Crassaerts K, Delacourte A, De Strooper B, Dotti CG (2000) Brain plasmin enhances APP alpha-cleavage and Abeta degradation and is reduced in Alzheimer's disease brains. EMBO Rep 1:530-535.

Lee da Y, Park KW, Jin BK (2006) Thrombin induces neurodegeneration and microglial activation in the cortex in vivo and in vitro: Proteolytic and non-proteolytic actions. Biochem Biophys Res Commun 346:727-738.

Lefranc D, Vermersch P, Dallongeville J, Daems-Monpeurt C, Petit H, Delacourte A (1996) Relevance of the quantification of apolipoprotein E in the cerebrospinal fluid in Alzheimer's disease. Neurosci Lett 212:91-94.

Leissring MA, Farris W, Chang AY, Walsh DM, Wu X, Sun X, Frosch MP, Selkoe DJ (2003) Enhanced proteolysis of beta-amyloid in APP transgenic mice prevents plaque formation, secondary pathology, and premature death. Neuron 40:1087-1093.

Levy E, Carman MD, Fernandez-Madrid IJ, Power MD, Lieberburg I, van Duinen SG, Bots GT, Luyendijk W, Frangione B (1990) Mutation of the Alzheimer's disease amyloid gene in hereditary cerebral hemorrhage, Dutch type. Science 248:1124-1126.

Lim GP, Yang F, Chu T, Chen P, Beech W, Teter B, Tran T, Ubeda O, Ashe KH, Frautschy SA, Cole GM (2000) Ibuprofen suppresses plaque pathology and inflammation in a mouse model for Alzheimer's disease. J Neurosci 20:5709-5714.

Lindh M, Blomberg M, Jensen M, Basun H, Lannfelt L, Engvall B, Scharnagel H, Marz W, Wahlund LO, Cowburn RF (1997) Cerebrospinal fluid apolipoprotein E (apoE) levels in Alzheimer's disease patients are increased at follow up and show a correlation with levels of tau protein. Neurosci Lett 229:85-88.

Lue LF, Kuo YM, Roher AE, Brachova L, Shen Y, Sue L, Beach T, Kurth JH, Rydel RE, Rogers J (1999) Soluble amyloid beta peptide concentration as

a predictor of synaptic change in Alzheimer's disease. Am J Pathol 155:853-862.

Mari D, Parnetti L, Coppola R, Bottasso B, Reboldi GP, Senin U, Mannucci PM (1996) Hemostasis abnormalities in patients with vascular dementia and Alzheimer's disease. Thromb Haemost 75:216-218.

Matsubara E, Shoji M, Murakami T, Abe K, Frangione B, Ghiso J (2002) Platelet microparticles as carriers of soluble Alzheimer's amyloid beta (sAbeta). Ann N Y Acad Sci 977:340-348.

Mattila KM, Pirttila T, Blennow K, Wallin A, Viitanen M, Frey H (1994) Altered blood-brain-barrier function in Alzheimer's disease? Acta Neurol Scand 89:192-198.

Mauch DH, Nagler K, Schumacher S, Goritz C, Muller EC, Otto A, Pfrieger FW (2001) CNS synaptogenesis promoted by glia-derived cholesterol. Science 294:1354-1357.

Mayeux R, Honig LS, Tang MX, Manly J, Stern Y, Schupf N, Mehta PD (2003) Plasma A[beta]40 and A[beta]42 and Alzheimer's disease: relation to age, mortality, and risk. Neurology 61:1185-1190.

McCarron MO, Nicoll JA (2004) Cerebral amyloid angiopathy and thrombolysis-related intracerebral haemorrhage. Lancet Neurol 3:484-492.

McGeer PL, Schulzer M, McGeer EG (1996) Arthritis and anti-inflammatory agents as possible protective factors for Alzheimer's disease: a review of 17 epidemiologic studies. Neurology 47:425-432.

Meinhardt J, Tartaglia GG, Pawar A, Christopeit T, Hortschansky P, Schroeckh V, Dobson CM, Vendruscolo M, Fandrich M (2007) Similarities in the thermodynamics and kinetics of aggregation of disease-related Abeta(1-40) peptides. Protein Sci 16:1214-1222.

Melchor JP, Van Nostrand WE (2000) Fibrillar amyloid beta-protein mediates the pathologic accumulation of its secreted precursor in human cerebrovascular smooth muscle cells. J Biol Chem 275:9782-9791.

Melchor JP, Pawlak R, Strickland S (2003) The tissue plasminogen activator-plasminogen proteolytic cascade accelerates amyloid-beta (Abeta) degradation and inhibits Abeta-induced neurodegeneration. J Neurosci 23:8867-8871.

Merkle DL, Cheng CH, Castellino FJ, Chibber BA (1996) Modulation of fibrin assembly and polymerization by the beta-amyloid of Alzheimer's disease. Blood Coagul Fibrinolysis 7:650-658.

Mielke MM, Rosenberg PB, Tschanz J, Cook L, Corcoran C, Hayden KM, Norton M, Rabins PV, Green RC, Welsh-Bohmer KA, Breitner JC, Munger R, Lyketsos CG (2007) Vascular factors predict rate of progression in Alzheimer disease. Neurology 69:1850-1858.

Miller BC, Eckman EA, Sambamurti K, Dobbs N, Chow KM, Eckman CB, Hersh LB, Thiele DL (2003) Amyloid-beta peptide levels in brain are inversely correlated with insulysin activity levels in vivo. Proc Natl Acad Sci U S A 100:6221-6226.

Miravalle L, Tokuda T, Chiarle R, Giaccone G, Bugiani O, Tagliavini F, Frangione B, Ghiso J (2000) Substitutions at codon 22 of Alzheimer's abeta peptide induce diverse conformational changes and apoptotic effects in human cerebral endothelial cells. J Biol Chem 275:27110-27116.

Monro OR, Mackic JB, Yamada S, Segal MB, Ghiso J, Maurer C, Calero M, Frangione B, Zlokovic BV (2002) Substitution at codon 22 reduces clearance of Alzheimer's amyloid-beta peptide from the cerebrospinal fluid and prevents its transport from the central nervous system into blood. Neurobiol Aging 23:405-412.

Morris DC, Zhang Z, Davies K, Fenstermacher J, Chopp M (1999) High resolution quantitation of microvascular plasma perfusion in non-ischemic and ischemic rat brain by laser-scanning confocal microscopy. Brain Res Brain Res Protoc 4:185-191.

Morrison RS, Siu AL (2000) Survival in end-stage dementia following acute illness. JAMA 284:47-52.

Morrow JA, Hatters DM, Lu B, Hochtl P, Oberg KA, Rupp B, Weisgraber KH (2002) Apolipoprotein E4 forms a molten globule. A potential basis for its association with disease. J Biol Chem 277:50380-50385.

Munson GW, Roher AE, Kuo YM, Gilligan SM, Reardon CA, Getz GS, LaDu MJ (2000) SDS-stable complex formation between native apolipoprotein E3 and beta-amyloid peptides. Biochemistry 39:16119-16124.

Naslund J, Haroutunian V, Mohs R, Davis KL, Davies P, Greengard P, Buxbaum JD (2000) Correlation between elevated levels of amyloid beta-peptide in the brain and cognitive decline. JAMA 283:1571-1577.

Naslund J, Thyberg J, Tjernberg LO, Wernstedt C, Karlstrom AR, Bogdanovic N, Gandy SE, Lannfelt L, Terenius L, Nordstedt C (1995) Characterization of stable complexes involving apolipoprotein E and the amyloid beta peptide in Alzheimer's disease brain. Neuron 15:219-228.

Navarro A, Del Valle E, Astudillo A, Gonzalez del Rey C, Tolivia J (2003) Immunohistochemical study of distribution of apolipoproteins E and D in human cerebral beta amyloid deposits. Exp Neurol 184:697-704.

Nilsberth C, Westlind-Danielsson A, Eckman CB, Condron MM, Axelman K, Forsell C, Stenh C, Luthman J, Teplow DB, Younkin SG, Naslund J, Lannfelt L (2001) The 'Arctic' APP mutation (E693G) causes Alzheimer's disease by enhanced Abeta protofibril formation. Nat Neurosci 4:887-893.

Niwa K, Kazama K, Younkin SG, Carlson GA, Iadecola C (2002a) Alterations in cerebral blood flow and glucose utilization in mice overexpressing the amyloid precursor protein. Neurobiol Dis 9:61-68.

Niwa K, Kazama K, Younkin L, Younkin SG, Carlson GA, Iadecola C (2002b) Cerebrovascular autoregulation is profoundly impaired in mice overexpressing amyloid precursor protein. Am J Physiol Heart Circ Physiol 283:H315-323.

Ohno M, Sametsky EA, Younkin LH, Oakley H, Younkin SG, Citron M, Vassar R, Disterhoft JF (2004) BACE1 Deficiency Rescues Memory Deficits and Cholinergic Dysfunction in a Mouse Model of Alzheimer's Disease. Neuron 41:27-33.

Passer B, Pellegrini L, Russo C, Siegel RM, Lenardo MJ, Schettini G, Bachmann M, Tabaton M, D'Adamio L (2000) Generation of an apoptotic intracellular peptide by gamma-secretase cleavage of Alzheimer's amyloid beta protein precursor. J Alzheimers Dis 2:289-301.

Paul J, Strickland S, Melchor JP (2007) Fibrin deposition accelerates neurovascular damage and neuroinflammation in mouse models of Alzheimer's disease. J Exp Med 204:1999-2008.

Pawlak R, Strickland S (2002) Tissue plasminogen activator and seizures: a clot-buster's secret life. J Clin Invest 109:1529-1531.

Pendlebury WW, Iole ED, Tracy RP, Dill BA (1991) Intracerebral hemorrhage related to cerebral amyloid angiopathy and t-PA treatment. Ann Neurol 29:210-213.

Perez RL, Ritzenthaler JD, Roman J (1999) Transcriptional regulation of the interleukin-1beta promoter via fibrinogen engagement of the CD18 integrin receptor. Am J Respir Cell Mol Biol 20:1059-1066.

Pike CJ, Burdick D, Walencewicz AJ, Glabe CG, Cotman CW (1993) Neurodegeneration induced by beta-amyloid peptides in vitro: the role of peptide assembly state.PG - 1676-87. J Neurosci 13.

Ploplis VA, Carmeliet P, Vazirzadeh S, Van Vlaenderen I, Moons L, Plow EF, Collen D (1995) Effects of disruption of the plasminogen gene on thrombosis, growth, and health in mice. Circulation 92:2585-2593.

Premkumar DR, Cohen DL, Hedera P, Friedland RP, Kalaria RN (1996) Apolipoprotein E-epsilon4 alleles in cerebral amyloid angiopathy and cerebrovascular pathology associated with Alzheimer's disease. Am J Pathol 148:2083-2095.

Qian Z, Gilbert ME, Colicos MA, Kandel ER, Kuhl D (1993) Tissue-plasminogen activator is induced as an immediate-early gene during seizure, kindling and long-term potentiation. Nature 361:453-457.

Ramsay DA, Penswick JL, Robertson DM (1990) Fatal streptokinase-induced intracerebral haemorrhage in cerebral amyloid angiopathy. Can J Neurol Sci 17:336-341.

Roher AE, Esh C, Kokjohn TA, Kalback W, Luehrs DC, Seward JD, Sue LI, Beach TG (2003) Circle of willis atherosclerosis is a risk factor for sporadic Alzheimer's disease. Arterioscler Thromb Vasc Biol 23:2055-2062.

Salles FJ, Strickland S (2002) Localization and regulation of the tissue plasminogen activator-plasmin system in the hippocampus. J Neurosci 22:2125-2134.

Sappino AP, Madani R, Huarte J, Belin D, Kiss JZ, Wohlwend A, Vassalli JD (1993) Extracellular proteolysis in the adult murine brain. J Clin Invest 92:679-685.

Schenk D, Barbour R, Dunn W, Gordon G, Grajeda H, Guido T, Hu K, Huang J, Johnson-Wood K, Khan K, Kholodenko D, Lee M, Liao Z, Lieberburg I, Motter R, Mutter L, Soriano F, Shopp G, Vasquez N, Vandevert C, Walker S, Wogulis M, Yednock T, Games D, Seubert P (1999) Immunization with amyloid-beta attenuates Alzheimer-disease-like pathology in the PDAPP mouse.PG - 173-7. Nature 400.

Schmued LC, Hopkins KJ (2000) Fluoro-Jade B: a high affinity fluorescent marker for the localization of neuronal degeneration. Brain Res 874:123-130.

Seeds NW, Basham ME, Haffke SP (1999) Neuronal migration is retarded in mice lacking the tissue plasminogen activator gene. Proc Natl Acad Sci U S A 96:14118-14123.

Seeds NW, Basham ME, Ferguson JE (2003) Absence of tissue plasminogen activator gene or activity impairs mouse cerebellar motor learning. J Neurosci 23:7368-7375.

Selkoe DJ (1998) The cell biology of beta-amyloid precursor protein and presenilin in Alzheimer's disease. Trends Cell Biol 8:447-453.

Selkoe DJ (2001) Clearing the brain's amyloid cobwebs. Neuron 32:177-180.

Shibata M, Yamada S, Kumar SR, Calero M, Bading J, Frangione B, Holtzman DM, Miller CA, Strickland DK, Ghiso J, Zlokovic BV (2000) Clearance of Alzheimer's amyloid-ss(1-40) peptide from brain by LDL receptor-related protein-1 at the blood-brain barrier. J Clin Invest 106:1489-1499.

Shuvaev VV, Siest G (1996) Interaction between human amphipathic apolipoproteins and amyloid beta-peptide: surface plasmon resonance studies. FEBS Lett 383:9-12.

Skoog I, Hesse C, Fredman P, Andreasson LA, Palmertz B, Blennow K (1997) Apolipoprotein E in cerebrospinal fluid in 85-year-old subjects. Relation to dementia, apolipoprotein E polymorphism, cerebral atrophy, and white matter lesions. Arch Neurol 54:267-272.

Slooter AJ, Tang MX, van Duijn CM, Stern Y, Ott A, Bell K, Breteler MM, Van Broeckhoven C, Tatemichi TK, Tycko B, Hofman A, Mayeux R (1997) Apolipoprotein E epsilon4 and the risk of dementia with stroke. A population-based investigation. Jama 277:818-821.

Small GW, Mazziotta JC, Collins MT, Baxter LR, Phelps ME, Mandelkern MA, Kaplan A, La Rue A, Adamson CF, Chang L, et al. (1995) Apolipoprotein E type 4 allele and cerebral glucose metabolism in relatives at risk for familial Alzheimer disease. Jama 273:942-947.

Strittmatter WJ, Roses AD (1995) Apolipoprotein E and Alzheimer disease. Proc Natl Acad Sci U S A 92:4725-4727.

Strittmatter WJ, Bova Hill C (2002) Molecular biology of apolipoprotein E. Curr Opin Lipidol 13:119-123.

Strittmatter WJ, Saunders AM, Schmechel D, Pericak-Vance M, Enghild J, Salvesen GS, Roses AD (1993) Apolipoprotein E: high-avidity binding to beta-amyloid and increased frequency of type 4 allele in late-onset familial Alzheimer disease. Proc Natl Acad Sci U S A 90:1977-1981.

Sugo T, Endo H, Matsuda M, Ohmori T, Madoiwa S, Mimuro J, Sakata Y (2006) A classification of the fibrin network structures formed from the hereditary dysfibrinogens. J Thromb Haemost 4:1738-1746.

Suh TT, Holmback K, Jensen NJ, Daugherty CC, Small K, Simon DI, Potter S, Degen JL (1995) Resolution of spontaneous bleeding events but failure of pregnancy in fibrinogen-deficient mice. Genes Dev 9:2020-2033.

Sullivan PM, Mezdour H, Quarfordt SH, Maeda N (1998) Type III hyperlipoproteinemia and spontaneous atherosclerosis in mice resulting from gene replacement of mouse Apoe with human Apoe*2. J Clin Invest 102:130-135.

Sullivan PM, Mezdour H, Aratani Y, Knouff C, Najib J, Reddick RL, Quarfordt SH, Maeda N (1997) Targeted replacement of the mouse apolipoprotein E gene with the common human APOE3 allele enhances diet-induced hypercholesterolemia and atherosclerosis. J Biol Chem 272:17972-17980.

Sutton ET, Hellermann GR, Thomas T (1997) beta-amyloid-induced endothelial necrosis and inhibition of nitric oxide production. Exp Cell Res 230:368-376.

Sutton R, Keohane ME, VanderBerg SR, Gonias SL (1994) Plasminogen activator inhibitor-1 in the cerebrospinal fluid as an index of neurological disease. Blood Coagul Fibrinolysis 5:167-171.

Tabrizi P, Wang L, Seeds N, McComb JG, Yamada S, Griffin JH, Carmeliet P, Weiss MH, Zlokovic BV (1999) Tissue plasminogen activator (tPA) deficiency exacerbates cerebrovascular fibrin deposition and brain injury in a murine stroke model: studies in tPA-deficient mice and wild-type mice on a matched genetic background. Arterioscler Thromb Vasc Biol 19:2801-2806.

Tanzi RE, Kovacs DM, Kim TW, Moir RD, Guenette SY, Wasco W (1996) The gene defects responsible for familial Alzheimer's disease. Neurobiol Dis 3:159-168.

Tanzi RE, Gusella JF, Watkins PC, Bruns GA, St George-Hyslop P, Van Keuren ML, Patterson D, Pagan S, Kurnit DM, Neve RL (1987) Amyloid beta protein gene: cDNA, mRNA distribution, and genetic linkage near the Alzheimer locus.PG - 880-4. Science 235.

Teasdale GM, Nicoll JA, Murray G, Fiddes M (1997) Association of apolipoprotein E polymorphism with outcome after head injury. Lancet 350:1069-1071.

Thomas T, McLendon C, Sutton ET, Thomas G (1997) beta-Amyloid-induced cerebrovascular endothelial dysfunction. Ann N Y Acad Sci 826:447-451.

Thomas T, Thomas G, McLendon C, Sutton T, Mullan M (1996) beta-Amyloid-mediated vasoactivity and vascular endothelial damage. Nature 380:168-171.

Tsirka SE, Rogove AD, Strickland S (1996) Neuronal cell death and tPA. Nature 384:123-124.

Tsirka SE, Gualandris A, Amaral DG, Strickland S (1995) Excitotoxin-induced neuronal degeneration and seizure are mediated by tissue plasminogen activator.PG - 340-4. Nature 377.

Tucker HM, Kihiko-Ehmann M, Estus S (2002) Urokinase-type plasminogen activator inhibits amyloid-beta neurotoxicity and fibrillogenesis via plasminogen. J Neurosci Res 70:249-255.

Tucker HM, Kihiko-Ehmann M, Wright S, Rydel RE, Estus S (2000a) Tissue plasminogen activator requires plasminogen to modulate amyloid-beta neurotoxicity and deposition. J Neurochem 75:2172-2177.

Tucker HM, Kihiko M, Caldwell JN, Wright S, Kawarabayashi T, Price D, Walker D, Scheff S, McGillis JP, Rydel RE, Estus S (2000b) The plasmin system is induced by and degrades amyloid-beta aggregates. J Neurosci 20:3937-3946.

Ugarova TP, Yakubenko VP (2001) Recognition of fibrinogen by leukocyte integrins. Ann N Y Acad Sci 936:368-385.

Ujiie M, Dickstein DL, Carlow DA, Jefferies WA (2003) Blood-brain barrier permeability precedes senile plaque formation in an Alzheimer disease model. Microcirculation 10:463-470.

Van Broeckhoven C, Haan J, Bakker E, Hardy JA, Van Hul W, Wehnert A, Vegter-Van der Vlis M, Roos RA (1990) Amyloid beta protein precursor gene and hereditary cerebral hemorrhage with amyloidosis (Dutch). Science 248:1120-1122.

Van Nostrand WE, Porter M (1999) Plasmin cleavage of the amyloid beta-protein: alteration of secondary structure and stimulation of tissue plasminogen activator activity.PG. Biochemistry 38.

Van Nostrand WE, Wagner SL, Suzuki M, Choi BH, Farrow JS, Geddes JW, Cotman CW, Cunningham DD (1989) Protease nexin-II, a potent antichymotrypsin, shows identity to amyloid beta-protein precursor.PG - 546-9. Nature 341.

Vassalli JD, Sappino AP, Belin D (1991) The plasminogen activator/plasmin system. J Clin Invest 88:1067-1072.

Vassar R, Bennett BD, Babu-Khan S, Kahn S, Mendiaz EA, Denis P, Teplow DB, Ross S, Amarante P, Loeloff R, Luo Y, Fisher S, Fuller J, Edenson S, Lile J, Jarosinski MA, Biere AL, Curran E, Burgess T, Louis JC, Collins F, Treanor J, Rogers G, Citron M (1999) Beta-secretase cleavage of Alzheimer's amyloid precursor protein by the transmembrane aspartic protease BACE.PG - 735-41. Science 286.

Vekrellis K, Ye Z, Qiu WQ, Walsh D, Hartley D, Chesneau V, Rosner MR, Selkoe DJ (2000) Neurons regulate extracellular levels of amyloid beta-protein via proteolysis by insulin-degrading enzyme. J Neurosci 20:1657-1665.

Vinters HV (1987) Cerebral amyloid angiopathy. A critical review. Stroke 18:311-324.

Vinters HV, Wang ZZ, Secor DL (1996) Brain parenchymal and microvascular amyloid in Alzheimer's disease. Brain Pathol 6:179-195.

Walsh DM, Selkoe DJ (2004) Oligomers on the brain: the emerging role of soluble protein aggregates in neurodegeneration. Protein Pept Lett 11:213-228.

Walsh DM, Klyubin I, Fadeeva JV, Cullen WK, Anwyl R, Wolfe MS, Rowan MJ, Selkoe DJ (2002) Naturally secreted oligomers of amyloid beta protein potently inhibit hippocampal long-term potentiation in vivo. Nature 416:535-539.

Wang J, Dickson DW, Trojanowski JQ, Lee VM (1999) The levels of soluble versus insoluble brain Abeta distinguish Alzheimer's disease from normal and pathologic aging. Exp Neurol 158:328-337.

Weisel JW (2007) Structure of fibrin: impact on clot stability. J Thromb Haemost 5 Suppl 1:116-124.

Weller RO, Yow HY, Preston SD, Mazanti I, Nicoll JA (2002) Cerebrovascular disease is a major factor in the failure of elimination of Abeta from the aging human brain: implications for therapy of Alzheimer's disease. Ann N Y Acad Sci 977:162-168.

Weller RO, Subash M, Preston SD, Mazanti I, Carare RO (2008) Perivascular drainage of amyloid-beta peptides from the brain and its failure in cerebral amyloid angiopathy and Alzheimer's disease. Brain Pathol 18:253-266.

Wen Y, Yang S, Liu R, Simpkins JW (2004a) Transient cerebral ischemia induces site-specific hyperphosphorylation of tau protein. Brain Res 1022:30-38.

Wen Y, Yang S, Liu R, Brun-Zinkernagel AM, Koulen P, Simpkins JW (2004b) Transient cerebral ischemia induces aberrant neuronal cell cycle re-entry and Alzheimer's disease-like tauopathy in female rats. J Biol Chem 279:22684-22692.

Wilcock DM, Gordon MN, Morgan D (2006) Quantification of cerebral amyloid angiopathy and parenchymal amyloid plaques with Congo red histochemical stain. Nat Protoc 1:1591-1595.

Winkler DT, Biedermann L, Tolnay M, Allegrini PR, Staufenbiel M, Wiessner C, Jucker M (2002) Thrombolysis induces cerebral hemorrhage in a mouse model of cerebral amyloid angiopathy. Ann Neurol 51:790-793.

Wisniewski T, Ghiso J, Frangione B (1997) Biology of A beta amyloid in Alzheimer's disease. Neurobiol Dis 4:313-328.

Wolozin B, Maheshwari S, Jones C, Dukoff R, Wallace W, Racchi M, Nagula S, Shulman NR, Sunderland T, Bush A (1998) Beta-amyloid augments platelet aggregation: reduced activity of familial angiopathy-associated mutants. Mol Psychiatry 3:500-507.

Xiao Q, Danton MJ, Witte DP, Kowala MC, Valentine MT, Bugge TH, Degen JL (1997) Plasminogen deficiency accelerates vessel wall disease in mice predisposed to atherosclerosis. Proc Natl Acad Sci U S A 94:10335-10340.

Ye S, Cech AL, Belmares R, Bergstrom RC, Tong Y, Corey DR, Kanost MR, Goldsmith EJ (2001) The structure of a Michaelis serpin-protease complex. Nat Struct Biol 8:979-983.

Yenari MA, Xu L, Tang XN, Qiao Y, Giffard RG (2006) Microglia potentiate damage to blood-brain barrier constituents: improvement by minocycline in vivo and in vitro. Stroke 37:1087-1093.

Yepes M, Sandkvist M, Moore EG, Bugge TH, Strickland DK, Lawrence DA (2003) Tissue-type plasminogen activator induces opening of the blood-brain barrier via the LDL receptor-related protein. J Clin Invest 112:1533-1540.

Zhang F, Eckman C, Younkin S, Hsiao KK, Iadecola C (1997) Increased susceptibility to ischemic brain damage in transgenic mice overexpressing the amyloid precursor protein. J Neurosci 17:7655-7661.

Zhang X, Zhou K, Wang R, Cui J, Lipton SA, Liao FF, Xu H, Zhang YW (2007) Hypoxia-inducible factor 1alpha (HIF-1alpha)-mediated hypoxia increases BACE1 expression and beta-amyloid generation. J Biol Chem 282:10873-10880.

Zhou Y, Su Y, Li B, Liu F, Ryder JW, Wu X, Gonzalez-DeWhitt PA, Gelfanova V, Hale JE, May PC, Paul SM, Ni B (2003) Nonsteroidal anti-inflammatory drugs can lower amyloidogenic Abeta42 by inhibiting Rho. Science 302:1215-1217.

Zipser BD, Johanson CE, Gonzalez L, Berzin TM, Tavares R, Hulette CM, Vitek MP, Hovanesian V, Stopa EG (2006) Microvascular injury and blood-brain barrier leakage in Alzheimer's disease. Neurobiol Aging.

Zlokovic BV (2008) The blood-brain barrier in health and chronic neurodegenerative disorders. Neuron 57:178-201.